RSC Advances

ROYAL SOCIETY OF CHEMISTRY

www.rsc.org/advances

Selectively sensing first-row transition metal ions through fluorescence enhancement

Sanchari Pal, Nabanita Chatterjee and Parimal K. Bharadwaj*
Department of Chemistry, Indian Institute of Technology Kanpur, Kanpur 208016, India.

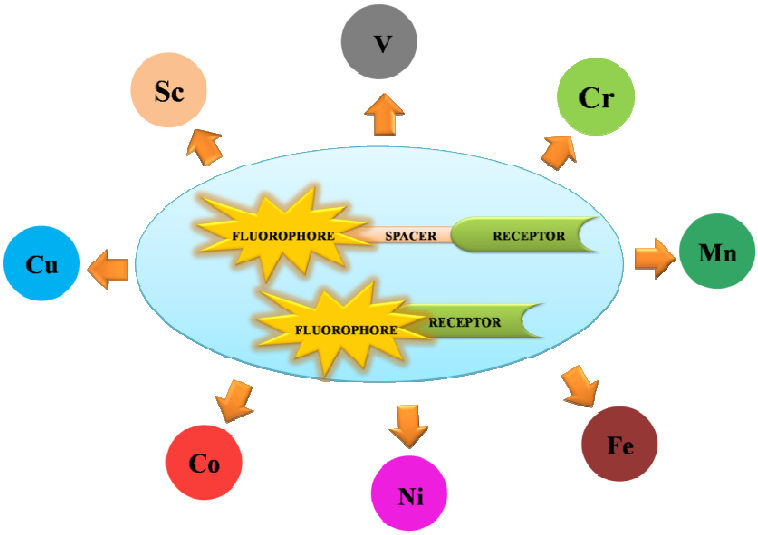

Fluorescence signaling systems that give enhancement in presence of first-row transition metal ions are discussed.

Selectively sensing first-row transition metal ions through fluorescence enhancement

Sanchari Pal, Nabanita Chatterjee and Parimal K. Bharadwaj*
Department of Chemistry, Indian Institute of Technology Kanpur, Kanpur 208016, India.
E-mail:pkb@iitk.ac.in

Abstract: Transition metal ions, especially the first-row ones are ubiquitous in nature and they perform many biological functions. However, high accumulation of these ions can be quite detrimental to health. Their spatial distribution with high fidelity inside as well as outside cells is, therefore, of paramount importance. In addition to biological sensing, fluorescence enhancement by transition metal ions can be potentially useful in other areas of science. However, most of the transition metal ions are paramagnetic and they very effectively quench fluorescence. Surmounting this problem of fluorescence quenching, a number of systems have been reported which is the topic of the present review.

Key words: Turn-on fluorescence signaling, First-row transition metal ions, Fluorophores, Receptors, Fluorescence reversibility

1. Introduction

Many transition metal ions are ubiquitous in nature and they perform[1] several biological functions while at the same time, excess accumulation of these ions in biosystems can lead to diseases[2] and ultimately to fatal consequences. Their spatial as well as temporal distribution inside and outside the cells is, therefore, of paramount importance to understand physiological conditions. Fluorescence spectroscopy[3] is a sensitive tool to detect and measure concentration of

an analyte with high fidelity. The basic design of the signaling system is, however, consists of a signaling (fluorophore) and a guest-binding (receptor) moieties that may be integrated or covalently attached through a spacer (Scheme 1). Out of these two designs, the one with a spacer

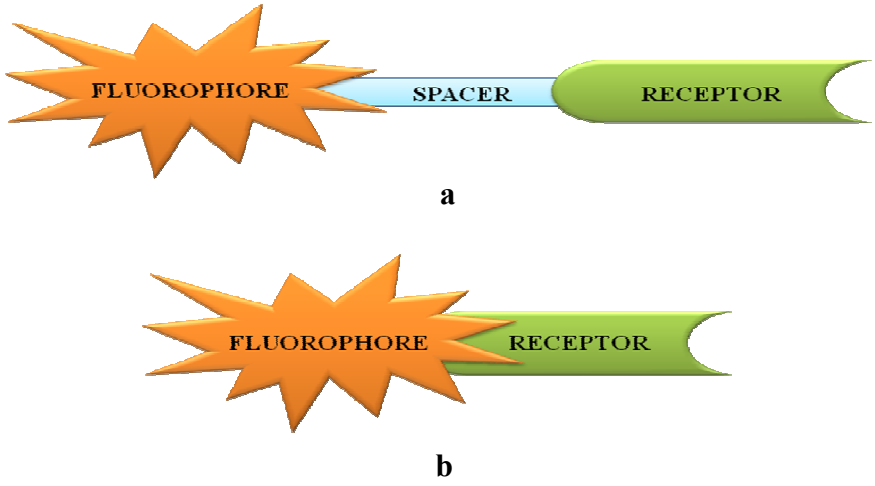

Scheme 1 Two common designs used in fluorescence signaling unit (a) through spacer signaling unit and (b) integrated signaling unit.

is preferable as either the fluorophore or the receptor or simultaneously both units can be varied at will. An ideal chemosensor will be the one that can recognize a particular metal ion in presence of many other competing ones. It should be designed with new recognition principles or fine tuning the existing ones, both of which are formidable challenges to chemists. The right donor atoms should be placed at strategic positions to match the coordination preferences of the metal ion. Biologically relevant paramagnetic transition metal ions quench emission quite effectively and in many cases, emission quenching has been adopted[4] as a signaling mode to detect the presence of an analyte. However, for practical as well as sensitivity reasons, fluorescence enhancement and not quenching should be the preferred mechanism in fabricating a sensor. In simple terms, blocking of the fluorescence quenching by a paramagnetic transition

metal ion requires that metal ion–receptor (M–R) interaction should be greater than the metal ion–fluorophore (M–F) communication. This idea can be incorporated in designing the overall architecture of the signaling system. Choice of the fluorophore should be made based on its excitation/emission characteristics, photochemical as well as thermal stability, magnitude of the Stokes shift, solubility properties and so on. In cases where a spacer is used, the nature of the later is also important[5] in the signal transduction process. Although most of the emission techniques and uses revolve around small organic molecules as receptors, recent years have witnessed a large number of supramolecular systems with interesting photochemical as well as photophysical properties. In addition to the sensory roles, it can also be used for information processing[6] that opens up a whole new window of opportunities. Finally, accessing a signal *via* remote control with waveguides and fiber-optics technology has led to widespread use of the fluorescence techniques in chemistry related sensing and switching applications. In the present review, only first-row transition metal ions are covered without Zn^{2+} ion as several excellent review articles[7] on Zn^{2+} ion sensing are available. Generally, literature from 2005 onwards has been covered. Of course, in some cases chemosensors reported prior to 2005 are included especially for those metal ions for which not many examples are known. However, the literature coverage is not exhaustive and at the outset, we apologize if we have not covered any important work in the present review. There are several reviews available in the literature[8] on transition metal ion chemosensors using fluorescence.

2. Sensing of Metal Ions

2.1. Scandium Chemosensors

Pure organic stereoisomers are much sought after synthetic compounds in pharmaceutical, agrochemical, and other industries. These aspects have spurred research in asymmetric synthesis and the development of analytical techniques for determining their stereochemical purity. Fluorescence enhancement upon binding of Sc^{3+} with stereoisomers has been used as a high throughput technique for determining the purity of stereoisomers. Thus, chemosensor 1,8-bis(3-*tert*-butyl-9-acridyl)naphthalene *N,N′*-dioxide (**1**), has been synthesized from 3-*tert*-butylaniline and 2-chlorobenzoic acid.[9] Free **1** does not show any significant emission upon excitation. However, with Sc^{3+} ion, it forms a 2:1 complex showing high chelation-enhanced fluorescence (CHEF) enhancement while other competing metal ions like Cu^{2+}, Zn^{2+}, Yb^{3+}, Sn^{2+} and In^{3+} do not exhibit such enhancement. Compound **1** thus serves as a selective fluorescence-on chemosensor for the Sc^{3+} ion. Stereoselective displacement of Sc^{3+} from the complex with concomitant loss of fluorescence output can be used to determine the presence of a particular enantiomer.

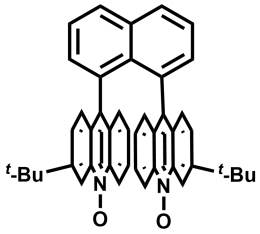

1

The compound 2,3,5,6-tetrakis(2-pyridyl)pyrazine (TPPZ) (**2**) itself shows negligible fluorescence but in presence of 1 equivalent of Sc^{3+} ion in MeCN affords a strong fluorescence

due to the formation of a 1:1 complex[10] (scheme 2) albeit with a low association constant of (1.4 ± 0.1) × 10^2. Since Zn^{2+} ion strongly interferes, it must be absent for sensing of Sc^{3+} ion.

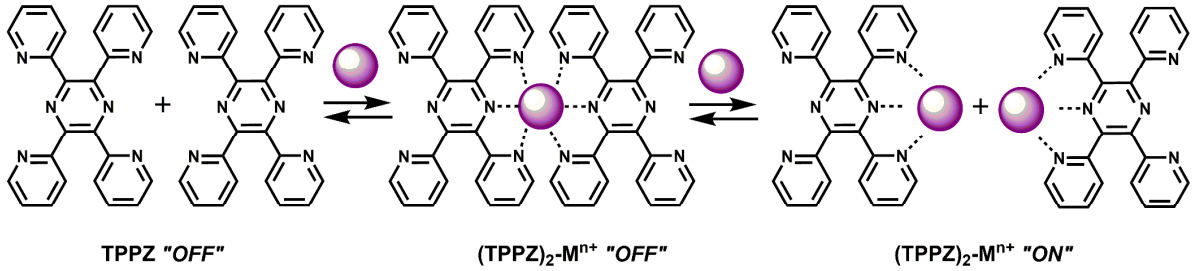

2

Scheme 2 Binding mode of **2** with metal ion.

2.2. Vanadium Chemosensors

Vanadium is an essential trace element due to its significant roles in various enzyme systems.[11] Vanadate ion (VO_4^{3-}) is a structural analogue of phosphate; it is also a transition state analogue of phosphate in the penta-coordinated form. So, vanadate interacts with a broad range of phosphate-metabolizing enzymes.[12] Besides, vanadate is also found as the cofactor of vanadium haloperoxidases (V-HPOs),[13] which are important enzymes that catalyze halogenation of natural compounds.[14] In aqueous medium, however, vanadate ion undergoes complicated hydrolysis and oligomerization reactions that can make it a difficult one to trace. Epidemiological evidences suggest that vanadium may also play a beneficial role in the prevention of heart-disease.[15] However, it is quite toxic and at high concentration level, vanadium is a potentially dangerous chemical pollutant that can play havoc with the agricultural system. It is thus quite important to have a method available for quantitative detection of the metal ion in aqueous medium.

The rhodamine-derived chemosensor **3** has been synthesized by reacting rhodamine hydrazide with 5-chlorosalicylaldehyde in ethanol[16] to provide a N_2O donor set. Metal free **3** does not show any emission when excited at 530 nm in aqueous MeOH (1:1, v/v, pH 7.2) as the spirolactam ring remains intact. However, in presence of 10^{-9} M VO^{2+} at pH 7-8, a 40-fold enhancement of emission is observed at 583 nm due to spiro-bond cleavage (scheme 3). On the other hand, Cu^{2+} affords only 3.6 fold enhancement. Other competing metal ions (Bi^{3+}, Tb^{3+}, Pb^{2+},Cr^{3+}, Al^{3+}, Eu^{3+}, Ru^{3+}, Sm^{3+}, Sn^{4+}, Ni^{2+}, Co^{2+}, Yb^{3+}, Hg^{2+}, Ga^{3+}, Zr^{4+}, Er^{3+}, Ho^{3+}, Fe^{3+}, Zn^{2+}, Mg^{2+}, Mn^{2+}, La^{3+}, Nd^{3+}) including heavy metal ions do not give any emission. The VO^{2+} ion which has a preference for O donors, forms a square pyramidal complex with the chemosensor. ESI-MS data supports the formation of a 1:1 complex although no stability constant value for the complexation is available.

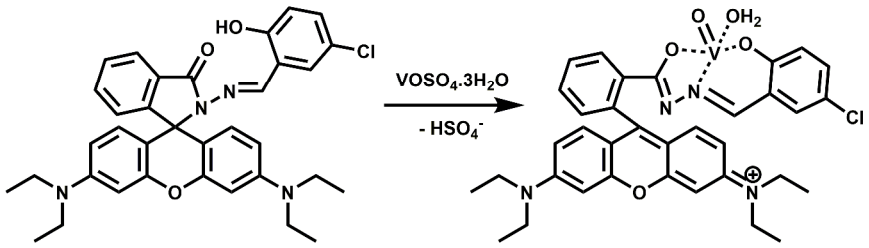

3

Scheme 3 Proposed sensing mechanism of **3** to VO^{2+}.

A flow method has been developed for the determination of pentavalent V in different media. In this method, continuous fluorescence measurement is done on the complex formed between V^{5+} and 1,2-dihydroxyanthraquinone-3-sulfonate (**4**) sorbed on anionic resin beads.[17] Although no association constant data are available, it is found that the dye shows increased sensitivity by about 4×10^3 times higher compared to the same system without immobilizing beads. Besides, immobilization of the reagent in the solid support[18] makes possible the

production of a more rigid environment which closes deactivation pathway. Both these factors allow nM amounts of V^{5+} to be detected in different kinds of samples, *viz.,*water from various sources, urine and serum, as well as mussel tissues.

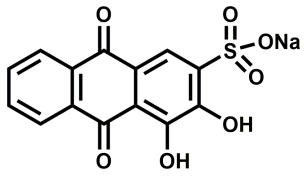

4

The receptor **5** has been designed for sensing vanadates and its oligomers.[19] The pyrene groups in **5** with their strong stacking tendency, can make the receptor pre-organized[20] and this can open up to accommodate dimer and trimers of vanadate. The chemosensor is found to bind preferentially the vanadate VO_4^{3-} ion in DMSO (scheme 4). The fluorescence spectrum of **5** in DMSO exhibits pyrene monomer emission bands at 390, 410 and 437 nm as well as a small peak at 607 nm. Upon addition of VO_4^{3-}, the monomer emissions along with the emission at 607 nm are quenched while a peak at 508 nm, assigned to the emission of the pyrene excimer[21] and a shoulder at 564 nm appear, confirming stacking of the pyrene units. With the addition of 7 equivalents of VO_4^{3-}, the intensity of the major peak at 513 nm, with a 5 nm red-shift, increased significantly with a 30-fold enhancement. After about 8 h, the peak at 513 nm disappears and a new peak at 564 nm appears showing a 50-fold enhancement due to binding of the oligomers that are in equilibrium with the monomer. This sensor, therefore, represents a design to tackle complicated hydrolysis and oligomerization of the vanadate ion in aqueous medium.

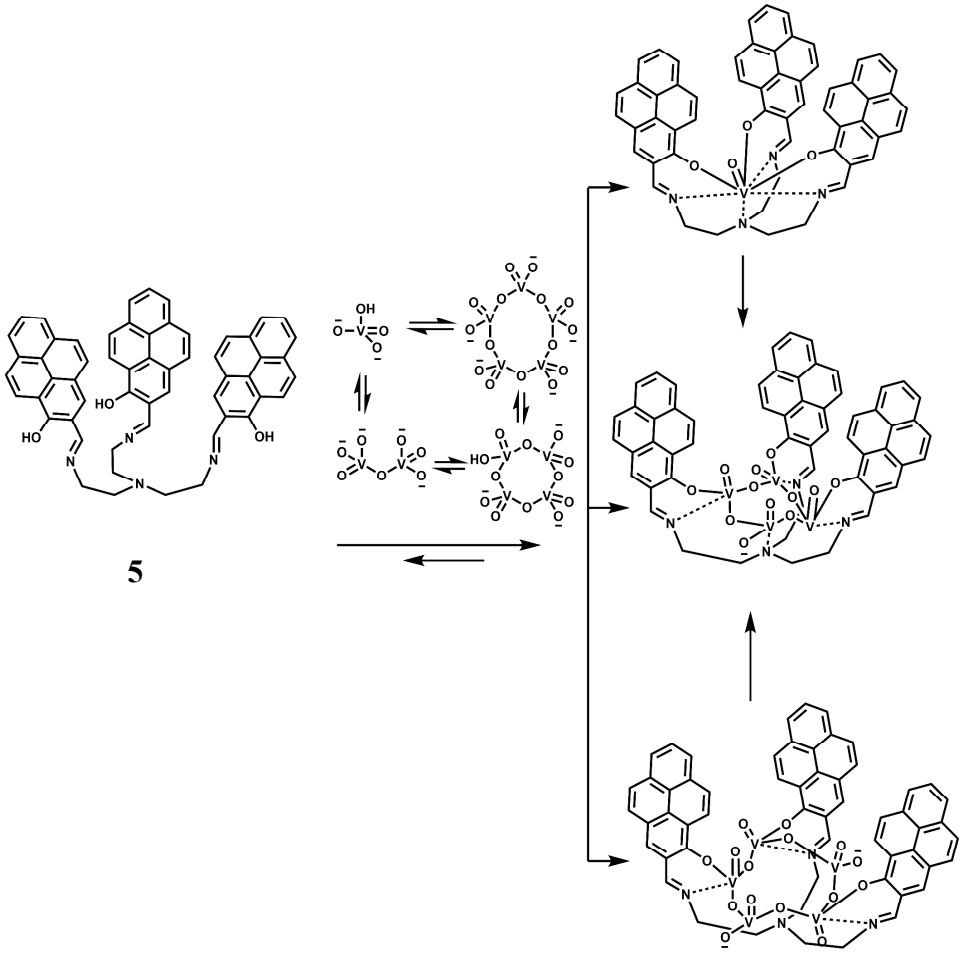

Scheme 4 Proposed binding mechanism of **5** with different vanadate species.

2.3. Chromium Chemosensors

Cr^{3+} is an essential trace element in human nutrition. It exerts great impacts on the metabolism of carbohydrates, fats, proteins and nucleic acids by activating certain enzymes and stabilizing proteins and nucleic acids.[22] Insufficient dietary intake of Cr^{3+} leads to increased risk factors associated with diabetes and cardiovascular diseases, including elevated levels of circulating insulin, glucose, triglycerides and total cholesterol and impaired immune function.[23] As a contaminant, chromium is found mostly in Cr(VI) form and its bacterial reduction to Cr^{3+} is considered as one of the promising strategies for bioremediation. However, exposure to high

levels of Cr^{3+} can negatively affect cellular structures. The environmental protection agency (USA) has set the maximum permissible level of total chromium at 100 ppb. Fluorescence turn-on reagents for monitoring intracellular Cr^{3+} concentration remain underdeveloped especially in aqueous media. In earlier reports on Cr^{3+} sensors, several divalent and trivalent metal ions like Cu^{2+}, Zn^{2+}, Cd^{2+}, Ni^{2+} , Cd^{2+} or Al^{3+} were found[24] to interfere with the detection processes. Amongst different designs, spirolactam ring opening in presence of the metal ion has been a popular method of detection of the Cr^{3+} ion.[25]

The chemosensor **6** is based on rhodamine B where 8-hydroxyquinoline moiety has been attached along with a ferrocene substituent.[26] This is found to be highly selective for the Cr^{3+} ion in presence of a host of other biologically relevant metal ions. The association constant for Cr^{3+} is estimated to be 7.5×10^3 M^{-1} in the aqueous ethanol (1:1, v/v, pH 7.4) solution. On excitation at 530 nm in 50% aqueous ethanol, metal-free **6** shows very low fluorescence at 580 nm since the spirocyclic form of rhodamine prevail. Upon addition of Cr^{3+} ion in the pH range of 5-10 in aqueous ethanol, a 15-fold increase in fluorescence is observed within 1 min, with a peak at 587 nm due to opening of the spirolactam ring. Under similar experimental conditions, only Hg^{2+} exhibits slight enhancement. However, other metal ions do not show any discernible change compared to the metal-free chemosensor. The most likely donor atoms for Cr^{3+} are the conjugated moiety including carbonyl O, imino N, and quinoline N and O atoms (scheme 5). Due to its instantaneous response and solubility in aqueous ethanol, **6** is used in cell imaging studies. When the HeLa cells are stained with a 20 μM solution in ethanol/PBS buffer (1:99, v/v) for 30 min at 25 °C a very faint intracellular fluorescence is observed. Addition of Cr^{3+} at 37 °C, affords a significant fluorescence in the intracellular domain in 2.5 h. Bright-field measurements after the Cr^{3+} treatment indicates that the cells remain viable throughout the period. Moreover,

differential pulse voltammetric studies in ethanol gives a significant shift of the ferrocenium/ferrocene potential in absence/presence of Cr^{3+} ion indicating that **6** can be used as a redox chemosensor of Cr^{3+}.

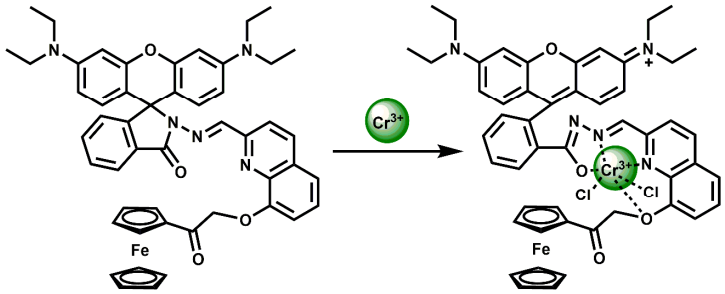

6

Scheme 5 Probable complexation mechanism of **6** with Cr^{3+}.

The rhodamine 6G based chemosensor **7** has been designed incorporating a diethylene triamine moiety as the binding site for Cr^{3+} ion at pH 7.2 in aqueous medium.[27] The association constant (K_a) with Cr^{3+} is found to be 4.16×10^4 M^{-1}. This sensor gives about 60-fold enhancement upon addition of 5 equivalents of Cr^{3+} due to spiro-ring opening (scheme 6) while other ions including Cd^{2+}, Co^{2+}, Cu^{2+}, Ni^{2+}, Zn^{2+}, Mg^{2+}, Ba^{2+}, Pb^{2+}, Na^+ and K^+ afford no distinct response. Only Fe^{3+} also forms a 1:1 complex giving a stability constant of 4.73×10^3 M^{-1} and shows a 17-fold enhancement upon addition of 5 equivalents of Fe^{3+} ion. Iron being much more biologically abundant than chromium, this chemosensor can only be useful in absence of Fe^{3+} ion which seriously limits its utility. This also suggests that cell imaging studies for temporal distribution of Cr^{3+} cannot be made with **7**.

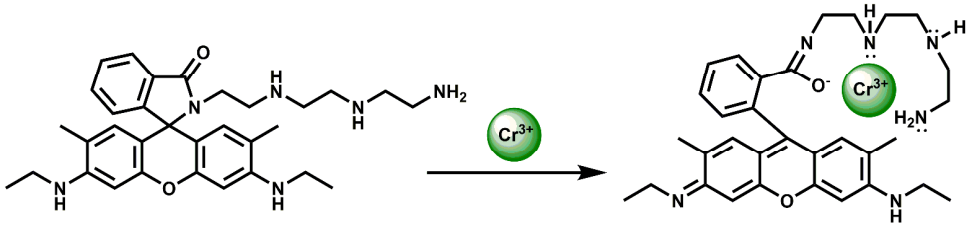

7

Scheme 6 Proposed mechanism for fluorescence enhancement of **7** upon the addition of Cr^{3+}.

The rhodamine B derived chemosensor **8** forms a 2:1 complex with Cr^{3+} and exhibits appreciable response due to spiro-bond opening in the range, 0–10 μM with a detection limit of 1 ppm. The system is functional within a wide range of pH (4.0-8.0) in 20% aqueous methanolic medium.[28] Other competing metal ions that include alkali/alkaline earth, first row transition and heavy metal ions, do not give any significant response. The response towards Cr^{3+} is found to be independent of the nature of anion used. Although response time for enhancement is found to be sluggish (~10 min), no interference from competing metal ions makes it an excellent sensor for the Cr^{3+} ion. Its usability in aqueous alcohol allows for imaging of living MGC803 cell lines demonstrating its potential applications in biological systems.

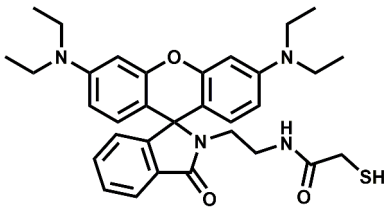

8

For sensing of Cr^{3+} ion in aqueous medium with low detection limit, the rhodamine B derivative **9** has been synthesized.[29] This chemosensor gives Cr^{3+} ion induced spiro-bond opened turn-on fluorescence in aqueous ethanol within a wide pH (5-9) range. The detection limit is found to be quite low at 0.023 μM. Besides, the Cr^{3+} ion can be removed using EDTA making the system reversible. However, the metal:chemosensor stoichiometry of 1:1 proposed by the authors is not consistent with the strong preference of hexacoordintion for the Cr^{3+} ion (scheme 7). No association constant value for complexation is available. However, since other competing

metal ions do not show any significant emission, this system has been used for intracellular imaging in live cells and determination of the ion in tap water and river water.

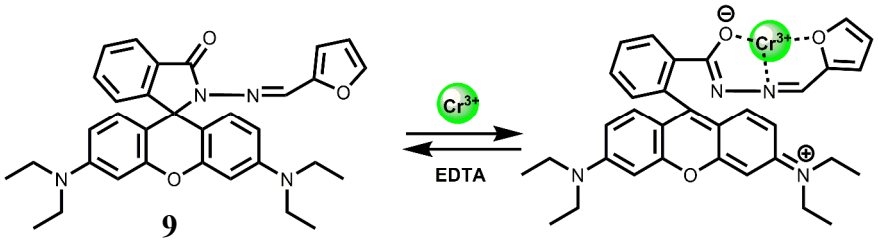

9

Scheme 7 Proposed mechanism for fluorescence enhancement of **8** upon the addition of Cr^{3+}.

The chemosensor **10** is structurally quite similar to **9** except that a thiophene moiety has been used in place of a furan to bind a metal ion through the carbonyl O, inamine N and thiophene S donors.[30] The sensor forms a 1:1 complex with Cr^{3+} giving a moderately high association constant of 2.0×10^4 M^{-1}. Complexing with Cr^{3+} triggers the formation of the highly fluorescent ring-opened form which is pink in colour. It affords an emission centering at 583 nm with about 1200-fold enhancement. However, Hg^{2+} also gives significant emission at 576 nm with this fluorescent probe.

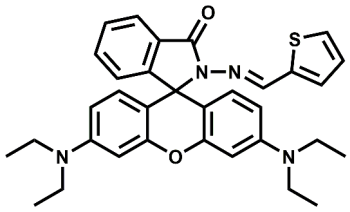

10

Rhodamine 6G derived chemosensors **11** and **12** are found to bind specifically to Hg^{2+} or Cr^{3+} in presence of large excess of other competing ions with associated changes in their optical and fluorescence spectral properties.[31] For **11**, the detection limit is lower than the permissible [Cr^{3+}] or [Hg^{2+}] in drinking water as per standard U.S. EPA norms. The chemosensor **12** can be

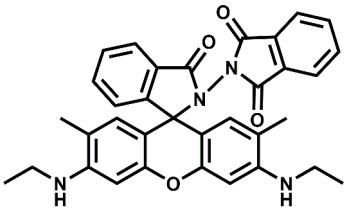

11

used as a ratiometric sensor for detection of Cr^{3+} and Hg^{2+} based on the Förster resonance energy transfer (FRET) process involving the donor naphthalimide and the acceptor Cr^{3+}/Hg^{2+}-bound xanthene fragment (scheme 8). Studies reveal that **12** can be used for recognition and sensing of Hg^{2+}/Cr^{3+}. Further, confocal microscopic studies confirm that **12** can also be used as an imaging probe for detection of these ions in A431 cells.

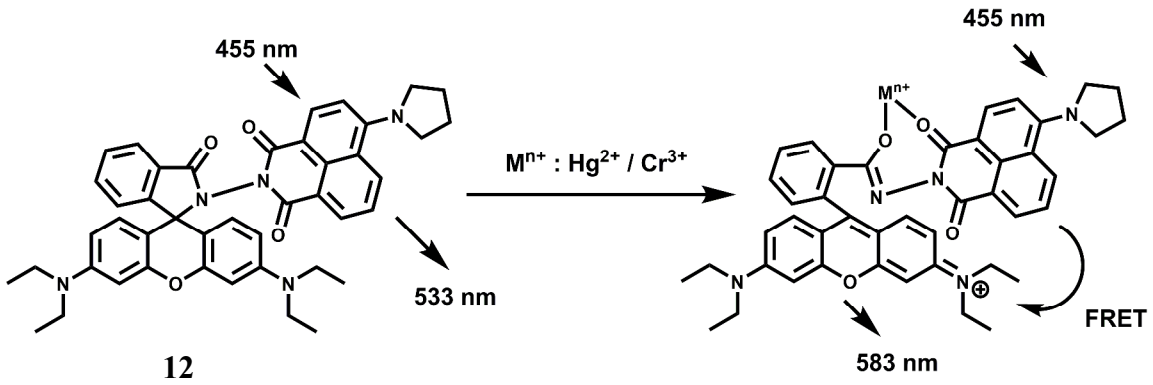

12

Scheme 8 Probable metal ion binding mode of **12**.

On the basis of FRET from 1,8-naphthalimide to rhodamine, the dyad **13** has been synthesized as a Cr^{3+} selective fluorescent probe for monitoring Cr^{3+} ion concentration in living cells with ratiometric fluorescence methods.[32] When excited at 405 nm in aqueous ethanol (1:2 v/v), a yellow fluorescence centered at 536 nm is observed attributable to an intramolecular charge transfer (ICT) band involving the 1,8-naphthalimide chromophore. Addition of 10 equivalents of Cr^{3+} ion causes the appearance of a strong absorption band centered at 568 nm

changing the colour of the solution to red-orange from yellow. The Cr^{3+}-complex on excitation at 515 nm, shows a 15-fold enhancement of fluorescence at 590 nm due to spirolactam ring opening (scheme 9). Further, when excited at 405 nm, the ICT band intensity at 536 nm is reduced drastically with a concomitant increase of the intensity at 594 nm due to an efficient FRET from the naphthalimide to the ring-opened spirolactam. This fluorescent probe exhibits excellent selectivity over other metal ions. Competition experiments for Cr^{3+} mixed with excess of competing metal ions does not show any change in the emission band intensity, although Mn^{2+}, Ag^{+} and Al^{3+} ions induces slight quenching or increasing of the ratio, F_{594}/F_{536}. Confocal microscopic studies confirm that **13** can be used for monitoring intracellular Cr^{3+} levels in living cells with general fluorescence and FRET methods. Such systems will be of help in studying the bioactivity of Cr^{3+} in biological systems.

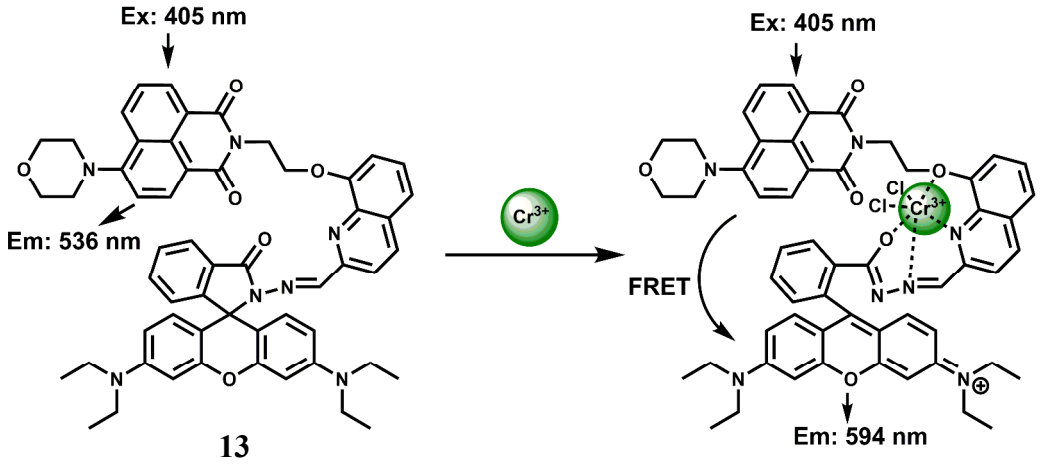

Scheme 9 Probable sensing mechanism of **13**.

The absorption maximum of a rhodamine derivative normally appears around 550 nm and typically gives a 25 nm Stokes shift of the emission band. This can limit its application as an effective chemosensor in many biological applications.[33,34] To circumvent this, the chemosensor

14 capable of showing two-photon excited fluorescence (TPEF) upon Cr^{3+} binding has been synthesized.[35] In presence of Cr^{3+} ion, **14** changes to the open-ring form giving remarkable fluorescence enhancement both in one and two-photon excitations. The broad excitation wavelength, on/off fluorescence and high selectivity to Cr^{3+} ($K_S = 9.4 \times 10^3\ M^{-1}$) enable **14** to be a powerful Cr^{3+} cation sensor with potential applications in biological systems.

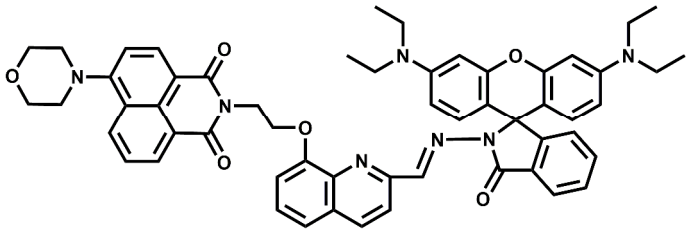

14

The photoinduced electron transfer (PET) chemosensor **15** represents one of the few fluorescence chemosensor for Cr^{3+} where a rhodamine is not used.[36] The signaling and the receptor moieties are covalently attached. In THF, it exhibits 17-fold chelation enhanced fluorescence (CHEF) in presence of Cr^{3+}. The receptor is found to be highly selective for Cr^{3+} ion against the background of environmentally and biologically relevant metal ions forming a 1:1 complex with a high association constant of $11.3 \times 10^4\ M^{-1}$.

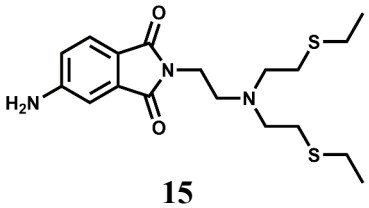

15

The highly selective luminescent chemosensor **16** in aqueous solution has been assembled by a low-selectivity luminogenic receptor with Cu^{2+} as a metal quencher.[37] Three

tetranitrogen chelating sites are integrated into the multichannel receptor with a tris(1,10-phenanthroline)ruthenium(II) luminophore at the core. This receptor exhibits chelating affinity

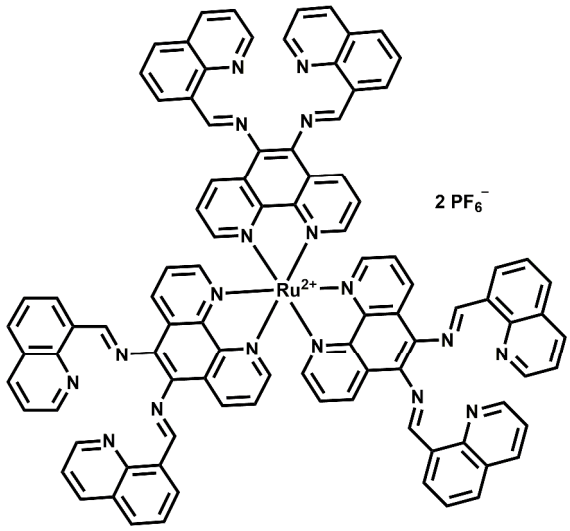

16

towards several transition metal cations, among which Cu^{2+} efficiently quenches the emission. Addition of Cr^{3+} into the Cu^{2+}-complex of **16** results in a metal-exchange reaction with concomitant recovery of fluorescence. Other transition metal ions do not take part in the metal-exchange reaction. The quencher displacement sensing strategy in this design can be a simple but efficient approach for OFF−ON luminescent sensing of metal cations that inherently lack selective ligands. This strategy of fluorescence sensing is, however, not that useful for biological imaging studies as many side reactions might interfere with the determination of a particular ion.

Two PET chemosensors **17** and **18**, incorporating dansyl dye as a fluorophore and various carboxhydrazones as receptors, have been reported.[38] Sensor **17** contains a pyridine-carboxhydrazone tridentate coordination site, forming a 2:1 complex with Cr^{3+} ($K_{as} = 6.07 \pm 0.10 \times 10^7$ M^{-2}). Metal-free **17** gives a weak dansyl based emission at 545 nm when excited at 350 nm in DMF-water (9:1, v/v). Upon addition of Cr^{3+} it affords a 5-fold enhancement in the pH range,

5-9. No emission is observed in presence of alkali, alkaline earth or competing first-row transition metal ions. Likewise, **18** offers a 4-fold enhancement of dansyl based emission selectively in presence of Cr^{3+} under similar experimental conditions (scheme 10). The metal ion forms a 1:1 complex with **18** giving an association constant value of $K_{as} = 9.59 \pm 0.03 \times 10^3$ M^{-1}.

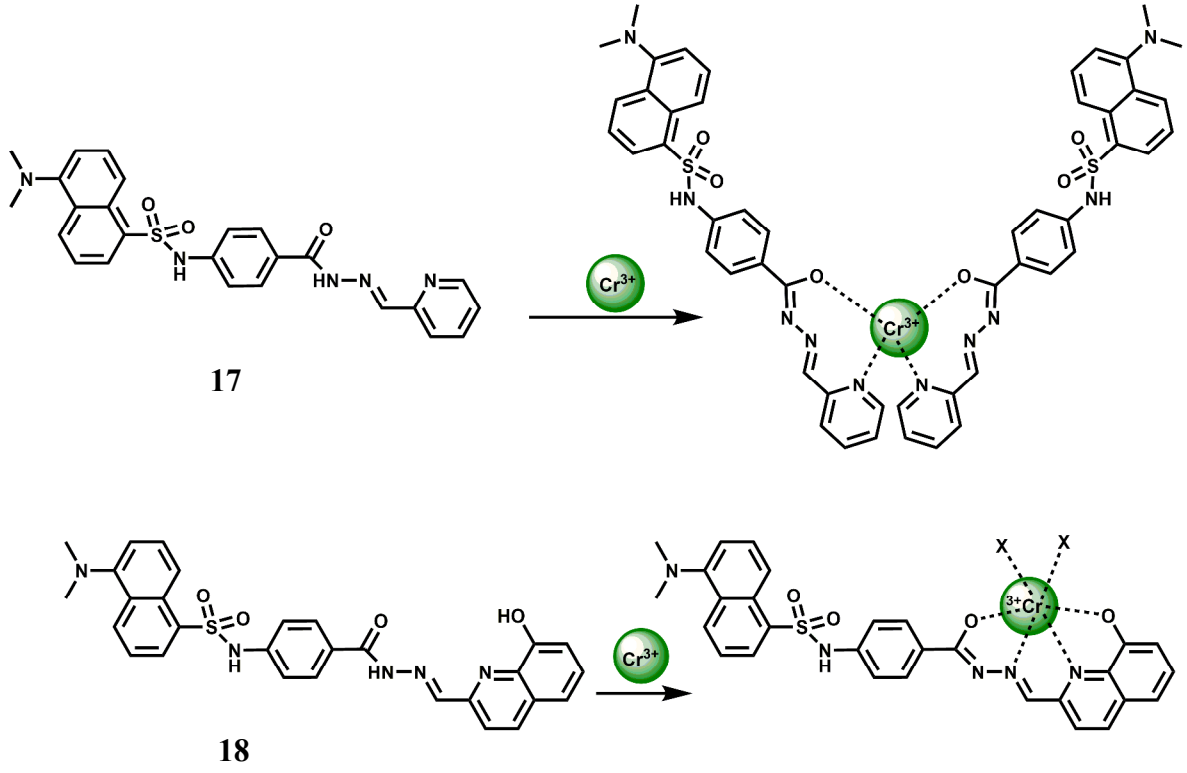

Scheme 10 Possible binding mode of **17** and **18** with Cr^{3+} (X is the coordinating anion or solvent).

Biaryl borondipyrromethene (BODIPY) fluorophore has high photostability with high fluorescence quantum yields. Besides, it is excitable with visible light, has narrow absorption and emission bands and is amenable to easy structural modification that can lead to spectral shifts in the absorption and emission bands to longer wavelengths. In **19**, a BODIPY group is covalently

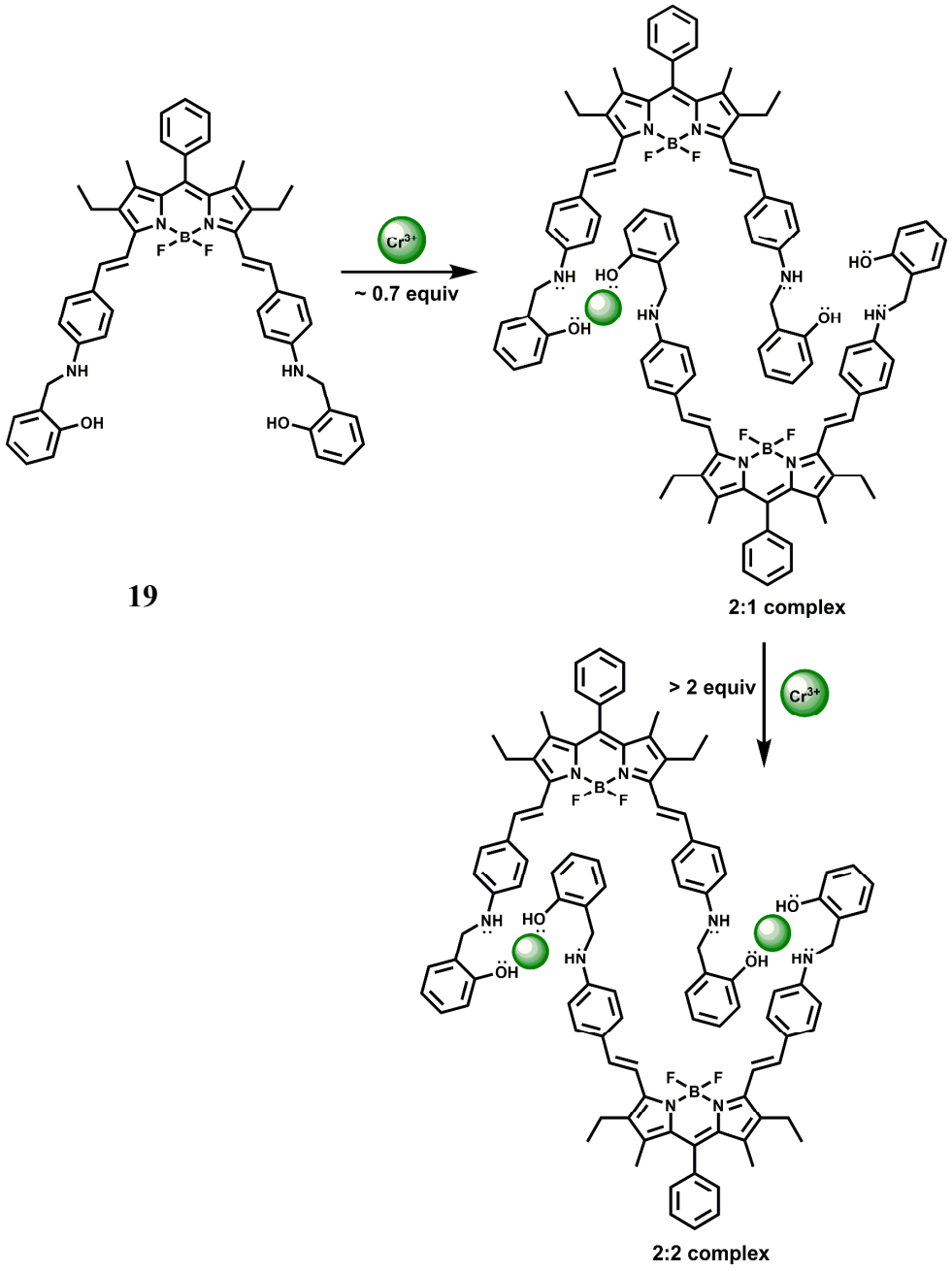

Scheme 11 Possible sequence for coordination between **19** and Cr^{3+}.

connected to a receptor incorporating NO donors. In acetonitrile, metal-free **19** gives almost no fluorescence when excited at 560 nm due to efficient PET from the amino N to the BODIPY.[39]

Upon addition of Cr^{3+} ion, initially it forms a 2:1 complex (scheme 11) giving weak fluorescence because the uncoordinated amine nitrogens can take part in the PET process to the photoexcited BODIPY moieties. With gradual increase of Cr^{3+} ion concentration, it forms a 2:2 complex (scheme 11) engaging all the N lone-pairs that blocks PET to the BODIPY group. As a result, a strong BODIPY based emission with nearly 2800-fold enhancement factor is observed around 640 nm. The enhancement is observed within 10 s indicating that **19** can detect Cr^{3+} very rapidly. Other competing metal ions do not interfere with Cr^{3+} sensing. However, in presence of more than 1% water in MeCN, Fe^{3+}, Cu^{2+} and Hg^{2+} strongly quenches fluorescence and thus seriously limits the use of **19** as a probe. Besides, the detailed coordination mode of Cr^{3+} with **19** requires further studies.

For ratiometric fluorescence sensing of Cr^{3+} in aqueous medium, a rhodamine derivative (RG1) and a coumarin derivative (CG1) have been used.[40] Together, they constitute the chemosensor **20** as shown in scheme 12. Upon addition of Cr^{3+} to a buffered solution (pH = 6) containing equimolar amounts of CG1 and RG1, the metal ion binds to both the components as shown (scheme 12). When the coumarin derivative is excited at 450 nm, the metal ion acts as a conduit for efficient FRET from the coumarin moiety to the ring-opened rhodamine moiety.[41] Fluorescence measurements also show an excellent selectivity toward Cr^{3+} over metal ions such as alkali, alkaline earth and other first-row transition metal ions. Even the presence of heavy metal ions cannot bring any obvious fluorescence change. Confocal fluorescence microscopic investigation on HeLa cells are found to be capable of detecting subcellular concentration of Cr^{3+} ion.

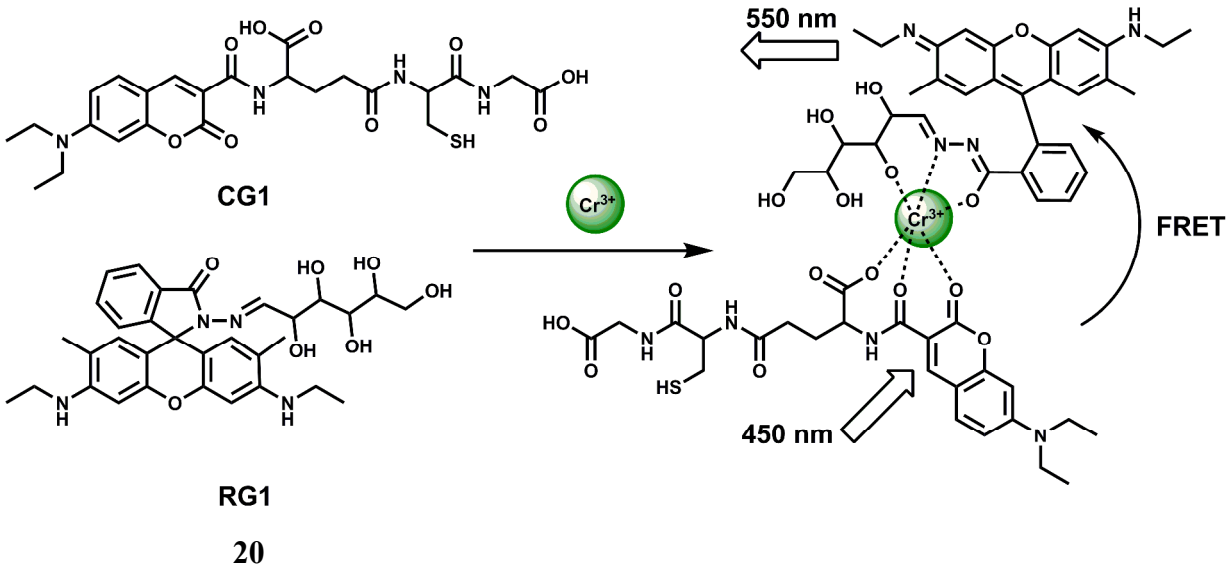

20

Scheme 12 Possible sensing mechanism of **20**.

The fluorescent probes **21(a-d)** having N, O/S/Se donors show donor specific 'turn-on' recognition property[42] towards Cr^{3+}, Fe^{2+} and Cu^{2+}. Here, the fluorescence signals are controlled by the conformational change of the ligand framework upon binding with the metal ion (scheme 13). Theoretical studies at the B3LYP/6-31G* level supports the mode of binding. However, they suffer from poor selectivity and only provide the starting point for the development of chemosensors with better selectivity and sensitivity.

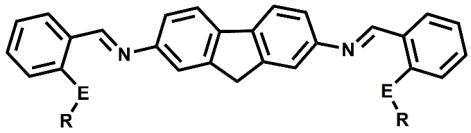

a E = O, R = Me
b E = S, R = Me
c E = Se, R = Me
d E = Se, R = *n*-$C_{12}H_{25}$

21

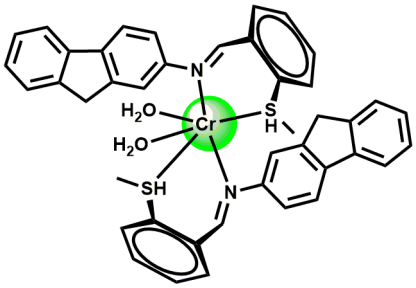

Scheme 13 The binding mode of Cr^{3+} ion with the fluorescent probe **21**.

The bis-dioxime chemosensor **22** upon excitation at 417 nm gives an emission at 515 nm that shows about 60% CHEF enhancement in presence of Cr^{3+} while quenching in presence of Fe^{3+}.[43] Therefore, in absence of Fe^{3+}, this sensor can be used for detecting Cr^{3+} ion.

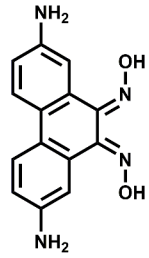

22

The chemosensor **23** with the naphthalimide based fluorophore connected to a BINOL framework shows low emission in THF-H_2O (85/15, v/v) due to an efficient PET from the receptor.[44] It forms a 1:1 complex (scheme 14) with Cr^{3+} ion with a moderately high association constant of 2.4×10^4 M^{-1} in THF/H_2O (85/15, v/v). Once a Cr^{3+} ion binds at the receptor it gives a 600-fold emission enhancement with the band centering at 498 nm. Other competing metal ions gives slight quenching although in the competition experiments they do not interfere. The detection limit is calculated to be 0.20 μM and response time is found to be about 10 s making it a fast responsive and highly sensitive probe for Cr^{3+}.

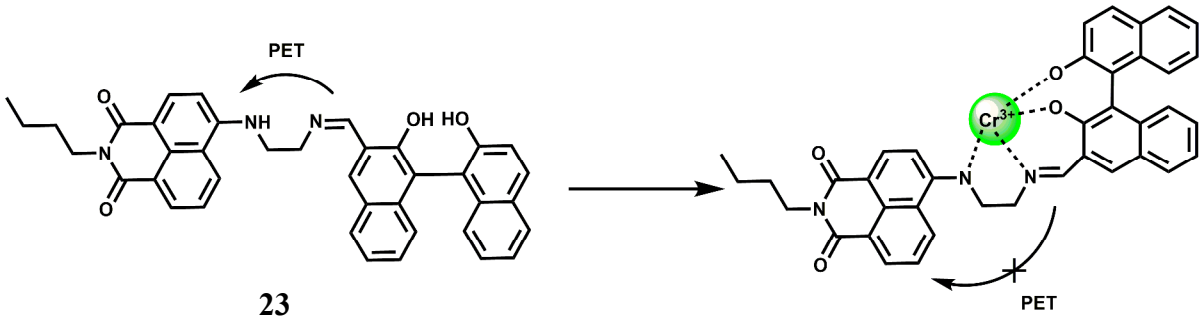

23

Scheme 14 The binding mode of Cr^{3+} ion with the fluorescent probe **23**.

A dansyl fluorophore is covalently attached to asparagine to have the fluorescent probe **24**.[45] The probe shows a fluorescence "turn-on" and can detect Cr^{3+} at trace levels (5.2 ppb) in aqueous solution under acidic pH (5.9). When a Cr^{3+} ion binds at the sulphonamide group, the ICT from the sulfonamide to the dansyl is inhibited giving a 1.6-fold fluorescence enhancement. However, first row transition metal ions and few heavy metal ions also exhibit enhancement to a lesser degree and hence **24** should be regarded as a signaling system with poor chemoselectivity.

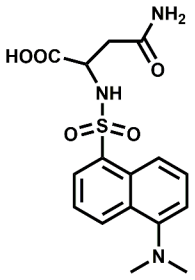

24

A spirobenzopyran derivative **25** with an amide moiety as the binding site for Cr^{3+} has been designed for use in MeCN.[46] The spiro-bond breaking in presence of Cr^{3+} (scheme 15) gives 25-fold enhancement of fluorescence at 675 nm. The metal ion forms a 1:1 complex with

the association constant (K_a) of 7.5 × 10^4 M^{-1}. This is one of the few probes that gives emission in the NIR region although it is workable in organic media and cannot be used in imaging studies. Efforts should be made to modify the system at sites away from the receptor for enhanced water solubility.

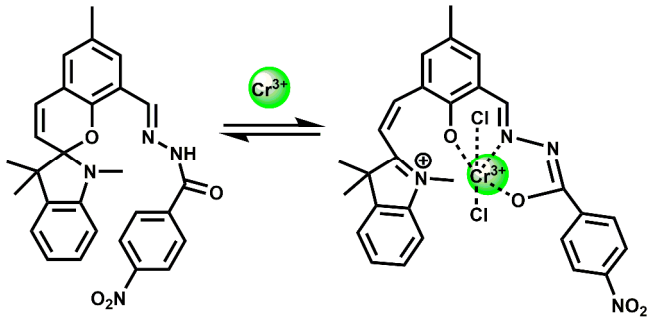

25

Scheme 15 Possible sensing mechanism of **25**.

A fairly strong interaction between Cr^{3+} and the PET probe **26** is found in aqueous MeCN at pH 7.4 with 1:1 stoichiometry and a binding constant value of 8 × 10^4 M^{-1}.[47] The metal-free fluorescent probe does not emit significantly when excited at 409 nm. Upon addition of Cr^{3+}, a 50-fold enhancement at 550 nm is observed due to snapping of the PET (scheme 16). Competition experiments with other biologically relevant metal ions show that none of the metal ions interfere. Cell viability tests for the fluorescent probe is encouraging but use of organic solvent limits its use in live cell imaging studies.

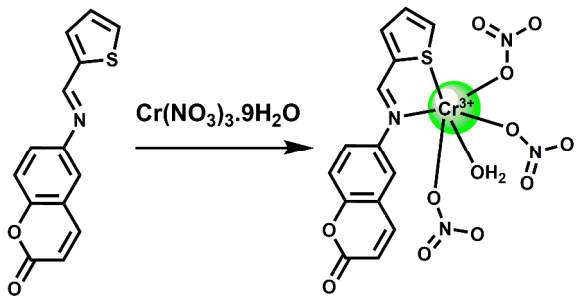

26

Scheme 16 Possible sensing mechanism of **26**.

2.4. Manganese Chemosensors

Manganese is an essential metal in all forms of life.[48] The manganese enzymes that have attracted considerable attention are the O_2 evolving complex of photosystem II and superoxide dismutase of prokaryotes and of the organelles of eukaryotes. This metal is also used widely as a versatile tool for biological studies. For example, high-spin Mn^{2+} is an excellent MRI relaxation agent that has been used in clinical diagnosis and is of widespread interest as a tool in neurobiological research.[49] Chronic overexposure to manganese can result in movement disorders, mental disturbances and other brain-related toxicities.[50] Fluorescent probes for detection and quantification of Mn^{2+} in biological systems will be of tremendous importance. However, development of an effective fluorescent probe for Mn^{2+} faces several challenges such as its paramagnetic nature, selectivity over abundant cellular metal ions especially Ca^{2+}, aqueous solubility for cell imaging and so on. Overcoming these hurdles, presently there are few Mn^{2+} specific fluorescence signaling systems available. One such system (**27**) is a conjugate of 1,2-bis-(2-pyren-1-ylmethylamino-ethoxy)ethane (NPEY) and graphene nanosheets (GNs) via π-π stacking that can be synthesized by simply mixing the diluted aqueous solutions of both components.[51] The conjugate itself does not show any significant emission due to an efficient PET from NPEY to GN. Upon addition of Mn^{2+} ion that binds to the NPEY blocking the PET to give enhancement of fluorescence. The NPEY-GN combination (**27**) not only shows good selectivity toward Mn^{2+} with the detection limit as low as 4.6×10^{-5} M, but also shows "turn-on" response both *in vitro* and in living cells (scheme 17). These sensing capabilities of NPEY-GNs

in living cells make it a robust candidate for many biological fields, such as intracellular tracking, intracellular imaging, etc.

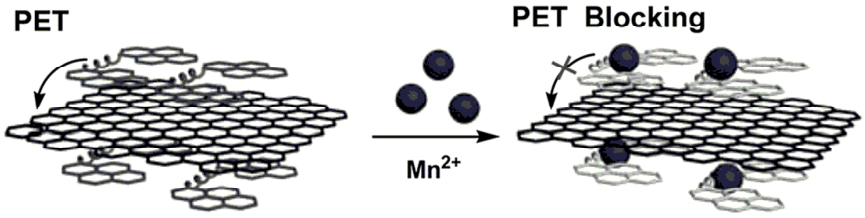

27

Scheme 17 Schematic demonstration of fluorescence "Turn-On" mechanism for Mn^{2+} detection by **27**.

The receptor (*O,O′*-bis-(2-aminophenyl)ethyleneglycol-*N,N,N′,N′*-tetraacetic acid popularly known as BAPTA, is an excellent receptor for Ca^{2+} ion and several Ca^{2+} sensors are built around this moiety. Chemosensors **28** and **29** have been designed to differentiate binding affinities of Mn^{2+} over Ca^{2+} by partially replacing hard carboxylate oxygens of BAPTA by softer pyridines.[52] Both Mn^{2+} and Ca^{2+} are classified as "hard" metals and, therefore, prefer to bind hard donors. However, Mn^{2+} appears to be more tolerant toward softer donors compared to Ca^{2+}.[53,54]

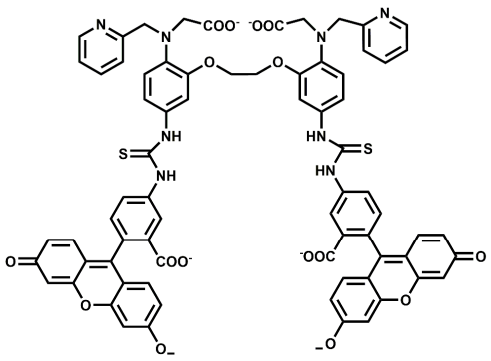

28

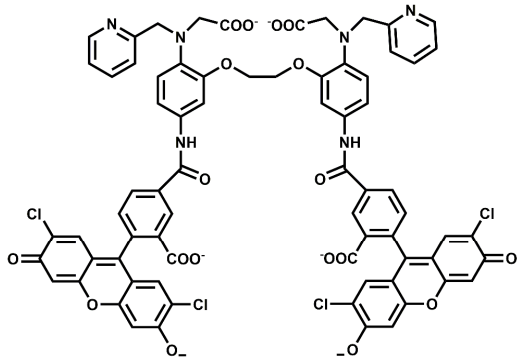

29

The association constant ratio ($logK_{Mn}/logK_{Ca}$) is found to be 2.368 for **28** while it is 2.402 for **29**. When excited at 493 nm, metal-free **28** shows a low intensity emission centering at 519 nm in aqueous medium. Upon addition of Mn^{2+}, a 4-fold enhancement is observed until saturation after 1 equivalent. On the other hand, metal-free **29** can be excited at 505 nm to obtain an emission maximum at 530 nm. It also affords almost a 4-fold enhancement in presence of 1 equivalent of Mn^{2+} ion. Both the probes have been used for intracellular Mn^{2+} with HeLa cell lines. However, it is to be noted that biological concentration of Ca^{2+} is about thousand times that of Mn^{2+} and hence cell imaging studies for Mn^{2+} will not be suitable especially when it is present in trace quantities.

The two-metal two-dye displacement assay has been adopted for detection of Mn^{2+} ion in **30(a,b)** where two commercially available dyes, *viz*., calcein blue (CB) and fluozin-1 (Fz1) have been used.[55] It works due to differential binding abilities of the two dyes. Initially, Cd^{2+} is chelated by the stronger ligand CB and the resulting complex is highly fluorescent. The other ligand, Fz1remain uncomplexed and gives a weak fluorescence. Upon addition of Mn^{2+} to the mixture, the Cd^{2+} is displaced from CB by Mn^{2+} resulting in quenching of fluorescence (scheme 18). However, Cd^{2+} presently available in the solution, forms a complex with Fz1 accompanied

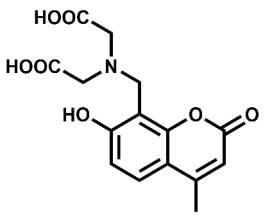

Calcein Blue

30a

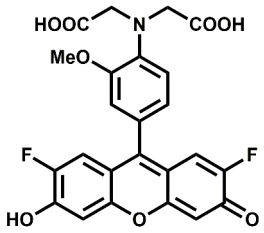

FluoZin-I

30b

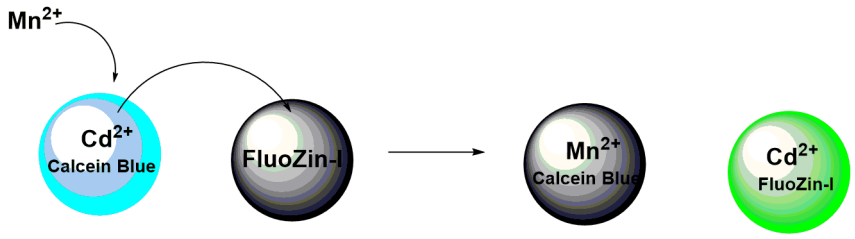

Scheme 18 Possible metal ion binding mode of **30(a, b)**.

by a strong fluorescence. The Cd^{2+}-complex of CB gives a green fluorescence with the emission band at 493 nm upon excitation at 350 nm. On the other hand, Cd^{2+}-complex of Fz1 gives an emission with maximum at 518 nm. Thus, it allows indirect detection of Mn^{2+} and also cell imaging studies.

The PET chemosensor **31** forms a 1:1 complex with Mn^{2+} with log $\beta \approx 3.0$.[56] On excitation at 310 nm in aqueous MeCN (1:1, v/v, pH 4.0) a 4-fold enhancement of fluorescence peaking at 360 nm is observed upon addition of Mn^{2+} ion due snapping of PET. However, alkaline earth metal ions also show enhancement albeit to lesser degrees.

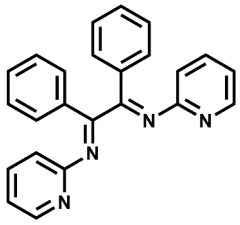

31

2.5. Iron Chemosensors

Iron is an essential element for many biological processes. But it is also detrimental to health as it causes the generation of highly destructive oxygen species. Accumulated data on iron metabolism suggest that alterations in the intracellular pool of 'redox-active' iron (also called

'chelatable iron') can contribute substantially to a variety of injurious processes such as ischemia-reperfusion injury, ethanol toxicity and oxidative injury after nutrient deprivation[57] and so on. On the other hand, chelatable iron is increasingly found to be decisively involved in several intracellular signalling pathways.[58] Most studies have been focused on detecting the cytosolic pool of chelatable, redox-active iron which is generally regarded as the cellular chelatable iron pool.[59] However, a 'transit' pool of chelatable iron must also be assumed to exist within the mitochondria during haem synthesis. Iron is incorporated into protoporphyrin IX within the mitochondrial matrix. In addition, there is now increasing list of evidences that suggest a definite role of mitochondrial chelatable iron in the pathogenesis of various human diseases.[60] It follows, therefore, that quantitative knowledge of spatial distribution of different forms of iron is of extreme importance.

Like many first-row transition metal ions, fabrication of iron sensors has been dependent heavily on the spirolactam ring opening in presence of the metal ion. One or two rhodamine derivatives have been used in sensing the metal ion in +2 and +3 oxidation states. Thus, chemosensor **32** gives a spirolactam ring-opening fluorescence enhancement at 583 nm by a factor of 112 in aqueous MeCN in presence of Fe^{3+} while an enhancement of 18-fold is observed with Cu^{2+}.[61] Other biologically relevant alkali, alkaline earth and transition and heavy metal ions show very weak response. With Fe^{3+}, **32** forms a 1:1 complex with the stability constant value of 2.3×10^4 M^{-1}. This fluorescent probe has been used for live cell imaging studies although authors are silent about the solvent system used in imaging studies and possible interference from Cu^{2+} ion. It is important that cell imaging as well as cell viability studies are made in pure aqueous or aqueous ethanolic medium.

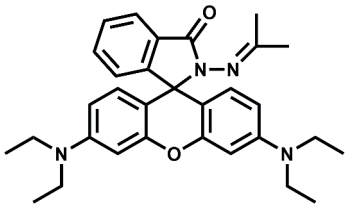

32

The rhodamine B hydroxamate fluorescent probe **33** having a biomimetic hydroxamate binding unit is prepared in two steps from rhodamine B.[62] It binds Fe^{3+} in 1:1 stoichiometry in MeOH:MeCN (1:1, v/v) mixed solvent with the association constant of 2.3×10^4 M^{-1}. Upon addition of Fe^{3+} to the probe solution, a 112-fold enhancement is observed due to spirolactam ring opening (scheme 19). Other biologically relevant metal ions do not show any significant response or fluorescence response of Fe^{3+} is not affected by the presence of any other metal ion. The reversible binding of Fe^{3+} with **33** is demonstrated by observing immediate disappearance of fluorescence (and colour) upon the addition of excess of EDTA into the solution of **33** and Fe^{3+}.

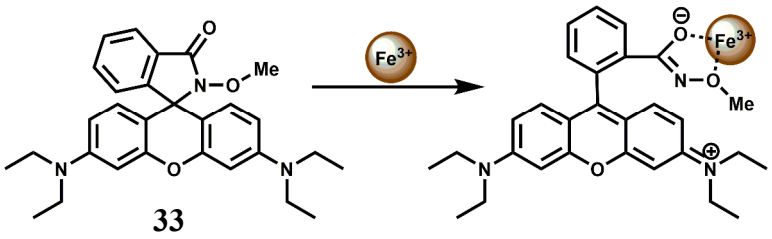

33

Scheme 19 Possible binding mode of chemosensor **33**

The imine linkage in the rhodamine 6G based chemosensor **34** is broken in presence of Fe^{3+} ion in aqueous medium and in the process, the spirolactam ring is also broken (scheme 20).[63] As a result, a strong emission band at 551 nm is observed. This Fe^{3+}-catalyzed hydrolysis reaction of **34** is not influenced by excess amounts of other biologically active metal ions such as K^+, Na^+, Fe^{2+}, Ca^{2+}, Mg^{2+} or Mn^{2+} ion. Besides, heavy and transition-metals that are potential pollutants do not interfere in the binding of Fe^{3+} and subsequent emission enhancement. The

high selectivity of this chemosensor for Fe^{3+} has been used to determine excess, free Fe^{3+} ions deposited into live cells using a ferric citrate-overloaded cell line. The greater concentration of

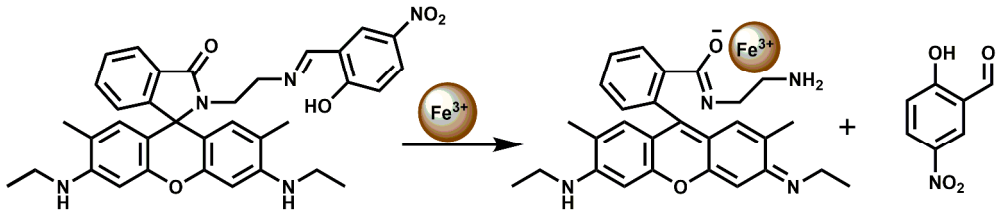

34

Scheme 20 Possible mechanism of Fe^{3+}-induced Schiff base hydrolysis and the spirolactam ring opening of **34**.

fluorescent cells and the stronger intensities are found to be much more evident for the iron-overloaded cells compared to the normal untreated cells. Thus, this chemosensor can be used for determination of free Fe^{3+} in live liver cells without any detrimental effect on the Fe^{3+}-based enzymes.

The rhodamine 6G–phenylurea conjugate **35** gives a strong fluorescence in the presence of Fe^{3+} in H_2O:CH_3CN (1:1, v/v) due to spirolactam ring opening.[64] In presence of acetate ion, the metal ion is extracted with the formation of spirolactam bond once again thus offering a reversible fluorescence (scheme 21). In response to acetate ions, the system not only provides remarkable fluorescence quenching but also exhibits a clear colour change from pink to colourless for naked eye observation. The background anions show small or no interference with the detection of acetate ions. This is the first chemosensor based on metal ion complexes that can selectively detect acetate ions over fluoride and dihydrophosphate ions in an aqueous environment. Such systems are expected to find a lot of practical applications.

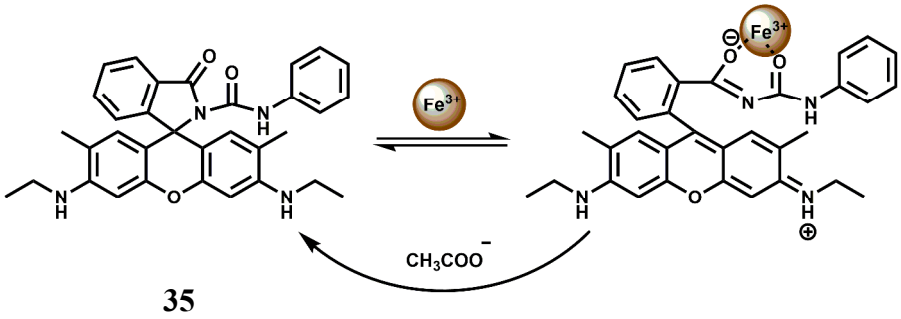

Scheme 21 Possible binding mode of chemosensor **35**

The chemosensor **36** containing quinoline moiety as the binding site for Fe^{3+} ion has been synthesized.[65] Upon addition of Fe^{3+} in aqueous ethanol medium, the spirolactam bond is broken (scheme 22) affording an approximately 190-fold enhancement of fluorescence with a peak at 559 nm following excitation at 505 nm. Fe^{3+} forms a 1:1 complex with **36** as shown in Scheme 22 with a high association constant of 1.1×10^6 M^{-1}. While other transition, alkali and alkaline earth or heavy metal ions do not interfere, Cr^{3+} and Al^{3+} gives mild enhancement of fluorescence. However, none of these metal ions are essential and hence the probe can be used in imaging studies. Structural studies of **36** indicate that the phthalimide side chain plays an important role in the ion selectivity due to its steric bulk. Upon addition of excess EDTA, Fe^{3+} is removed changing the solution to colourless with 98% quenching of fluorescence. Thus **36** can be classified as a reversible chemosensor for Fe^{3+} ion. Bioimaging studies of EJ cells with **36** shows that it can act as a Fe^{3+} sensor in living cells.

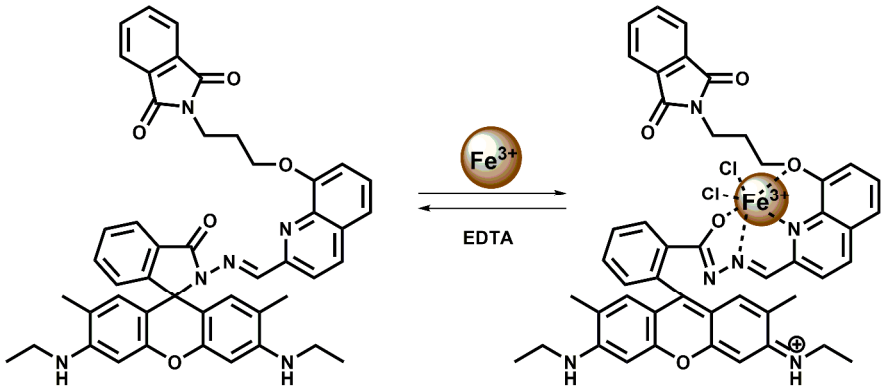

36

Scheme 22 Possible binding mode of chemosensor **36**.

The rhodamine 6G derived chemosensor **37** has been synthesized that provides a definite binding site for Fe^{3+} (scheme 23).[66] The chemosensor forms a 1:1 complex with Fe^{3+} and the association constant is moderately high at 1.04×10^{4} M^{-1}. The free **37** gives only a weak emission at 550 nm when excited at 505 nm. A 23-fold enhanced green-yellow fluorescence is observed with the peak at 550 nm upon addition of Fe^{3+}in aqueous MeCN (1:1) at pH = 7.2. No interference from other competing ions is observed. The detection limit is found to be in the 10^{-8} M range. Gradual addition of Na_2-EDTA to the Fe^{3+}-complex causes decrease in fluorescence intensity and upon addition of 10 equivalents of $EDTA^{2-}$ ion, Fe^{3+} is totally removed with complete quenching of the fluorescence making it a reversible chemosensor for Fe^{3+} ion. However, its lack of solubility in aqueous ethanolic medium does not allow its use in live cell imaging studies.

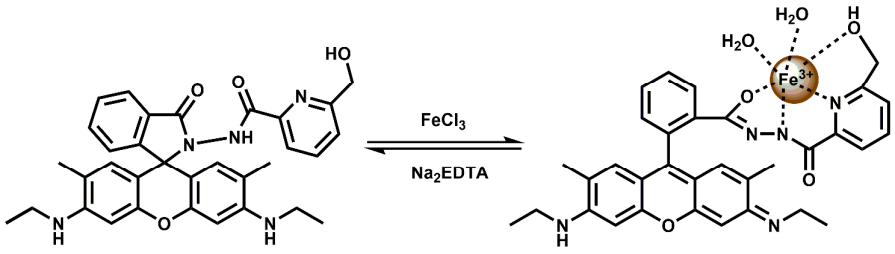

37

Scheme 23 Possible binding mode of chemosensor **37**.

For increasing water solubility, rhodamine B hydrazide derived chemosensor **38** has been synthesized. This binds Fe^{3+} with 1:1 stoichiometry (scheme 24) with the association constant K_a showing 7.52×10^4 M^{-1}.[67] The fluorescent probe gives spiro-bond opened 10-fold enhancement of fluorescence in presence of Fe^{3+} in water containing less than 1% organic co-solvent. Other biologically relevant metal ions exerted negligible effect even when present in excess. However, Cr^{3+} also gives enhancement to a lesser extent although that may not be a problem as compared to chromium, iron is present in large amount in biosystems. This probe is also found to be cell permeable and suitable for monitoring intracellular Fe^{3+} with low cytotoxicity in living cells by confocal microscopy.

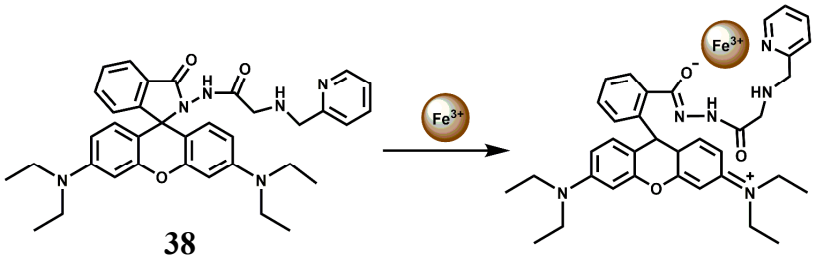

38

Scheme 24 Possible sensing mechanism of **38**.

To improve selectivity towards Fe^{3+}, a different coordination moiety has been added to rhodamine B to have **39**.[68] Indeed, this probe offers a spiro-ring opened (scheme 25) 23-fold enhancement with Fe^{3+} at 586 nm when excited at 530 nm in aqueous buffer solution. No other competing metal ions show any enhancement. The dissociation constant (K_d) of Fe^{3+} complex is found to be 1.87×10^{-5} M. The fluorescent probe is found to be safe for long hours at low

concentration; it is cell permeable and suitable for the real-time imaging of Fe^{3+} in living MGC803 cells.

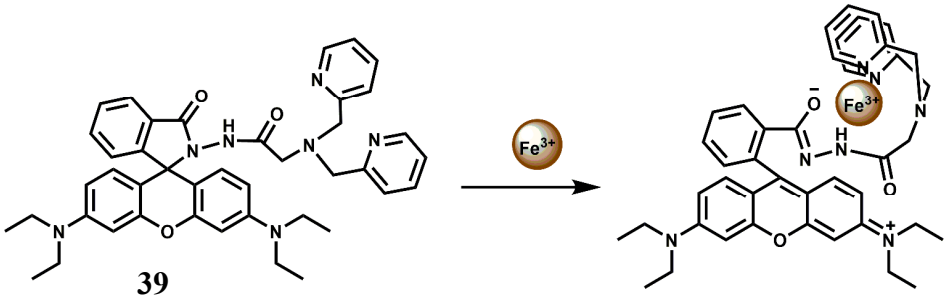

39

Scheme 25 Possible metal ion binding mode of **39**.

The rhodamine 6G derived chemosensors **40** and **41** are found to show excellent selectivity towards Fe^{3+} with the binding constant values of 6.74×10^4 M^{-1} and 3.946×10^4 M^{-1} respectively with **40** and **41** in aqueous DMSO at pH 7.4.[69] Upon excitation at 480 nm both the probes show substantial spiro-ring opened enhancement at 553 nm in presence of Fe^{3+}. None of the other coexisting metal or heavy metal ions shows any enhancement. Live cell imaging experiments with each probe demonstrated its value of practical applications in biological systems.

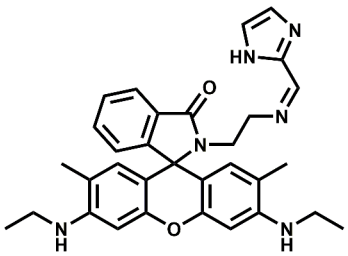

40

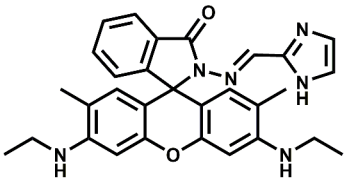

41

Although several rhodamine based chemosensors for Fe^{3+} are available as mentioned above, in most cases either a pure organic organic solvent or an organic co-solvent will be required to guarantee a high affinity of Fe^{3+} towards a chemosensor. However, in some cases, it

is required that the probe be highly soluble in water for detecting Fe^{3+} ions in natural water samples. For increased solubility in water the N-stabilized rhodamine hydrazide fluorescent probe **42** has been synthesized. The N-stablization of rhodamine increases its rigidity resulting in larger Stokes shift and higher intensity of fluorescence.[70] This chemosensor itself does not show any fluorescence but in presence of Fe^{3+} in aqueous medium (pH 5-8) gives about 164-fold enhancement in less than a minute (scheme 26).[71] Under similar conditions other biologically relevant metal ions do not show any fluorescence except Cr^{3+} ion which also gives substantial enhancement. This probe forms a 1:1 complex with Fe^{3+} and although no association constant data are available, this binding is found to be reversible. Upon addition of 20 equiv. of K_3PO_4 to the **42**-Fe^{3+} complex in water, the fluorescence is completely quenched. Further addition of 20 equiv. of Fe^{3+} restores the fluorescence to its original value. This chemosensor is found to be useful in imaging MGC803 cells for monitoring Fe^{3+} ion.

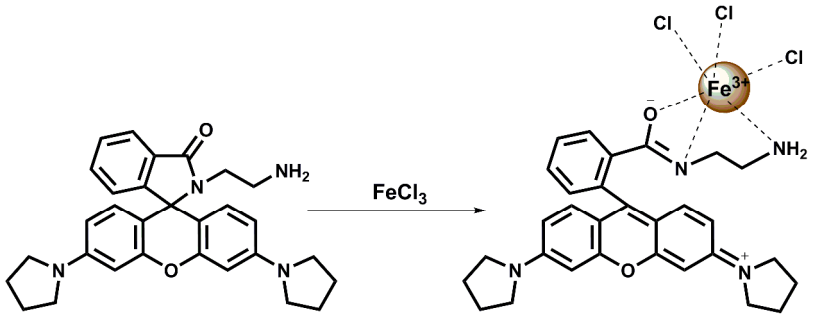

42

Scheme 26 Possible sensing mechanism of **42**.

The fluorescent probe **43** has two fluorophores: a dansyl unit as a donor and a rhodamine 101 as an acceptor for FRET based signaling.[72] In FRET based sensing, the pseudo-Stokes shifts are larger than the Stokes shift of either fluorophore. This avoids self-quenching as well as fluorescence detection errors due to backscattering effects from the excited source.[73] The probe

forms a complex of 1:1 stoichiometry with Fe^{3+} showing a moderately high association constant (K_a) of 1.74 × 10^4 M^{-1}. The Fe^{3+} induced spirolactam ring-opening of the rhodamine moiety transforms it as a FRET acceptor (scheme 27). When the dansyl group is excited at 380 nm, the FRET acceptor emits at 605 nm. The probe displayed a linear response to Fe^{3+} in the range of 5.5–25 μM with a detection limit of 0.64 μM. Other competing metal ions do not give any fluorescence and their presencedo not change the fluorescence profile of the Fe^{3+} complex. Thus, this novel rhodamine-dansyl conjugate can selectively sense Fe^{3+} ion in presence of a host of other ions.

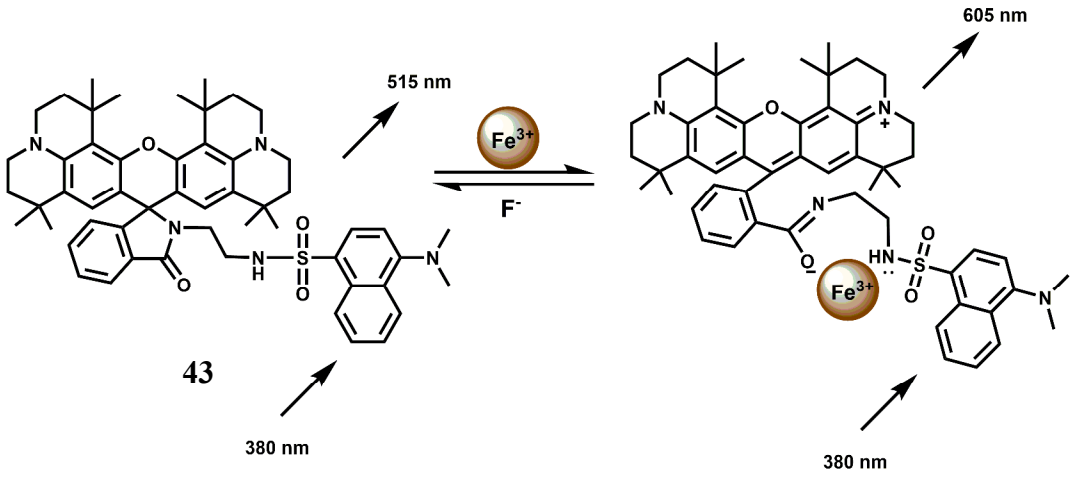

Scheme 27 Possible sensing mechanism of **43**.

Another FRET based chemosensor on the rhodamine platform for Fe^{3+} is provided by the system **44** has been shown below. A quinoline fluorescent group is covalently linked[74] to a rhodamine moiety. Metal free **44** exhibits a weak emission at 482 nm which changes upon addition of Fe^{3+} ion, due to an efficient FRET from the conjugated quinoline to rhodamine. Thus, the excitation interference of the new rhodamine based probe is eliminated as a result of efficient FRET (scheme 28). Binding of the metal ion also causes opening of the spiro-bond of the rhodamine moiety resulting in an enhancement by a factor of 186 times indicating that the new sensor can be used as a highly

sensitive Fe^{3+} probe especially when other competing metal ions taken in excess, do not interfere with the Fe^{3+} determination. Its aqueous solubility makes it an useful probe for live cell imaging studies.

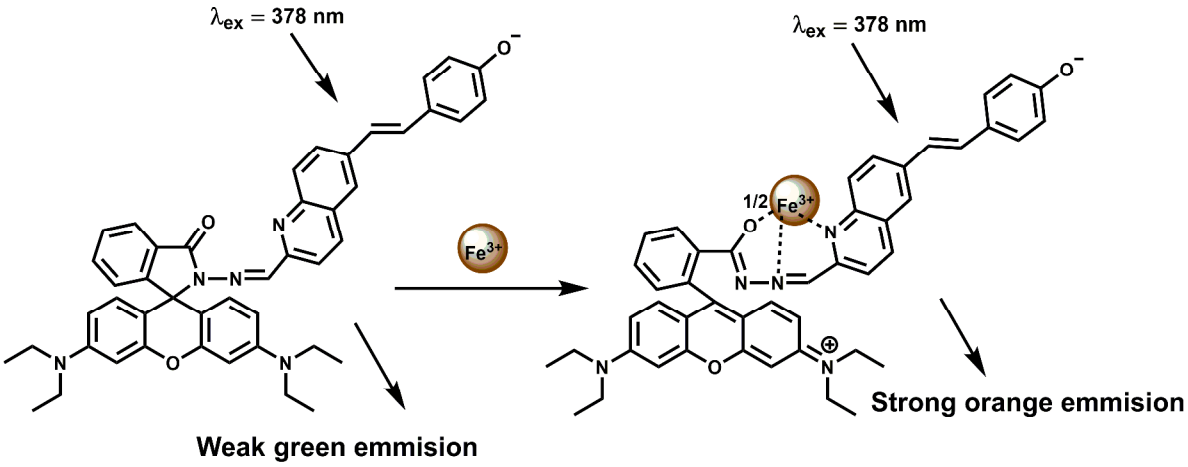

44

Scheme 28 Possible mechanism of Fe^{3+} induced FRET

A rhodamine B and a coumarin are connected to have the ratiometric fluorescent probe **45** for Fe^{3+} with high sensitivity and selectivity.[75] Upon addition of Fe^{3+} it binds to both the moiety in aqueous medium with the appearance of spiro-ring opened fluorescence peak at 580 nm and PET suppressed fluorescence from the coumarin moiety at 460 nm (scheme 29). The association constant for Fe^{3+} (K_a) is found to be $1.172 \times 10^4\ M^{-1}$ which is quite significant. But a host of other competing metal ions also give enhancement at 460 nm belong to the coumarin moiety. Thus, the design principle is not at all clear in this case.

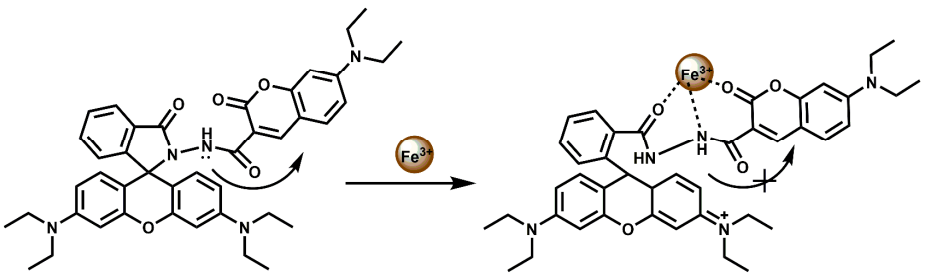

45

Scheme 29 Possible sensing mechanism of **45**.

In a novel approach, NP conjugate of Fe_3O_4-Rh6G has been synthesized as the chemosensor **46** and found to be sensitive and selective in detecting Fe^{3+} ion.[76] It forms a 1:1 complex with Fe^{3+} with high stability constant (5.0×10^6 M^{-1}). A ~60-fold enhancement due to spirolactam ring opening is observed for Fe^{3+} with the detection limit reaching as low as 2 ppb (scheme 30). Amongst other metal ions, only Cr^{3+} shows some enhancement. Since the system can work in aqueous medium, confocal microscopic studies have been made on HeLa cells. The chemosensor **46** is more sensitive compared to the system where no NP is used due to its low solubility.

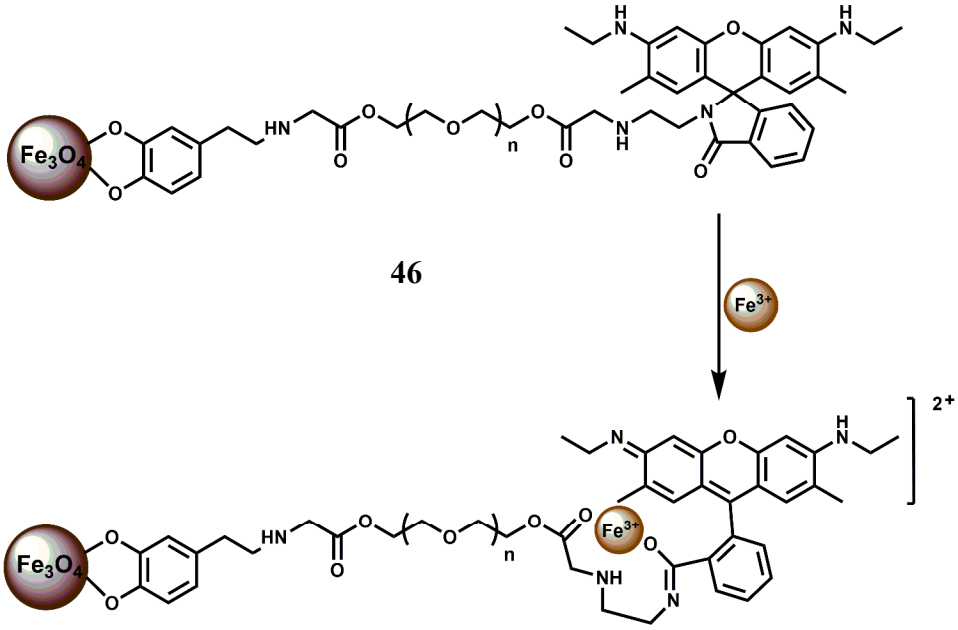

Scheme 30 Binding of Fe^{3+} to the chemosensor **46**.

In addition to mono-rhodamine derived systems, a number of bis-rhodamine derivatives have been designed for detection of iron in different oxidation states. One such bis-rhodamine based chemosensor **47** is easily synthesized from rhodamine B and diethylenetriamine.[77] The free sensor is colourless in absolute ethanol or in water in the pH range, 5.0-9.0 and does not show any significant emission suggesting that the spirolactam bonds are intact. Upon addition of Fe^{3+}, colour of the solution changes immediately to purple both in ethanol and water giving an orange fluorescence while other competing metal ions do not show any change. However, in ethanol medium, Cr^{3+}, Fe^{2+} and Cu^{2+} show emission to a small extent. Addition of Fe^{3+} causes both the spirocyclic rings to the open form with a ~110 and ~40-fold enhancement at 580 nm in ethanol and water respectively when excited at 510 nm (scheme 31).

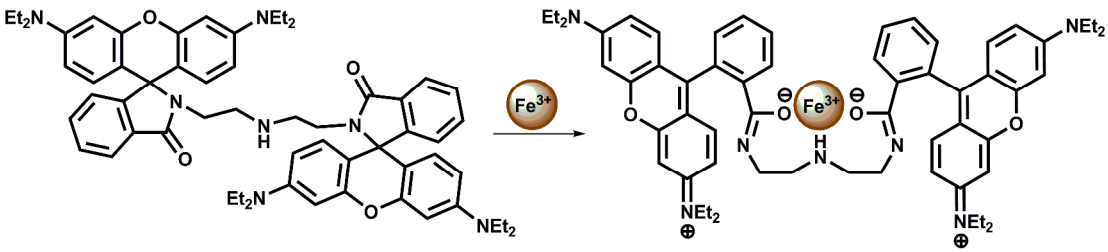

47

Scheme 31 Binding of Fe^{3+} to the chemosensor **47**.

The bis-rhodamine-based dual sensor **48** upon complexation with Fe^{3+} triggers the formation of a highly fluorescent ring-opened form.[78] This sensing mechanism is reversible, as indicated by disappearance of the emission with the addition of excess EDTA. However, Cu^{2+} interferes and Fe^{3+} cannot be detected in presence of Cu^{2+} ion (scheme 32).

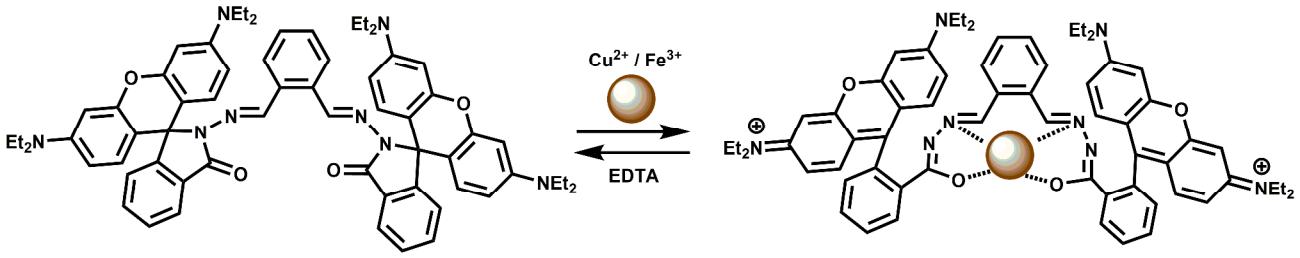

48

Scheme 32 Reversible binding of Fe^{3+}/Cu^{2+} to the chemosensor **48**.

Another bis(rhodamine)-based chemosensor **49** exhibits high selectivity for Fe^{3+} over other transition metal ions in 50% aqueous ethanol.[79] The spirocyclic rings are opened and a 115-fold enhancement of fluorescence at 575 nm is observed. However, Cr^{3+} also gives enhancement of emission albeit to a lesser degree.

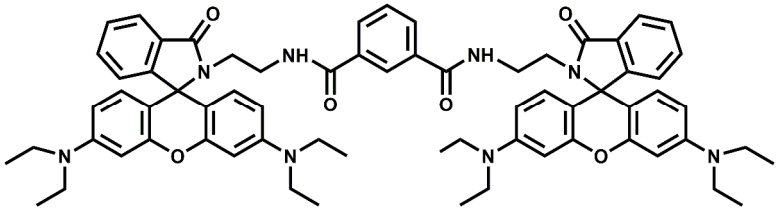

49

When two rhodamine moieties are connected through a disulfide linkage to have chemosensor **50**, it gives about 60-fold enhancement in presence of Fe^{3+} in aqueous ethanol within a wide pH range.[80] However, as is found for most of the rhodamine derivatives, Cr^{3+} ion also affords enhancement to a less amount. The association constant (K_a) with Fe^{3+} is found to be 7.4×10^4 M^{-1}. Since cytotoxic measurements are found to be negative, the probe has been used for live cell imaging studies.

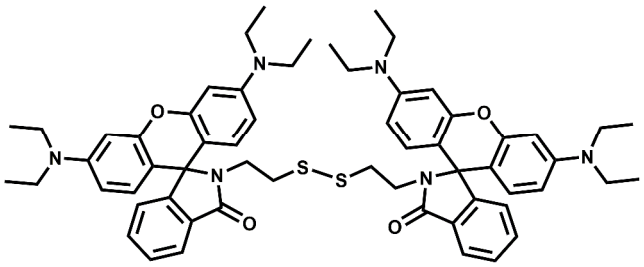

50

In an elegant approach**,** a 12-membered dithia-aza-oxa macrocycle is attached to two different fluorophores through *para*-substituted benzene to have the chemosensors **51** and **52**.[81] In this design, the fluorophores are well-separated from the receptor to minimize metal-fluorophore interaction and possible quenching. The response of Fe^{3+} in presence of potentially interfering metal ions are studied in solvents of different polarity. In organic solvents, fluorescence of metal-free sensors are quenched due to ICT/PET when excited. Addition of Fe^{3+} leads to recovery of the fluorescence without pronounced spectral shifts. Also, metal-free **52** shows dual emissions in water and can be employed for the selective ratiometric signaling of Fe^{3+} in buffered aqueous solution.

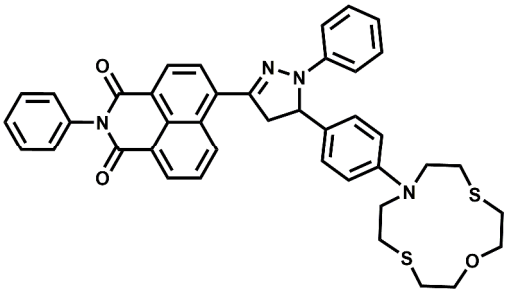

51

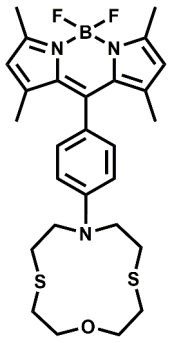

52

The fluorophore **53** has two di-(2-picolyl)-amine (DPA) groups as the metal binding sites attached to a perylene tetracarboxylic diimide fluorophore via benzene as the spacer.[82] Perylene tetracarboxylic diimides have excellent thermal and photo-stability, high luminescence efficiency and novel optoelectronic properties.[83] The receptor and the fluorophore moieties being separated through the rigid spacer, gives low M-F interactions when a metal ion is bound at the receptor. Upon addition of Fe^{3+}, PET from the dipicolyl moiety to the fluorophore is blocked leading to recovery of fluorescence. An enhancement factor of 138 in presence of Fe^{3+} is observed although metal ions such as Co^{2+}, Zn^{2+} and Cu^{2+} also give emission to a small extent. The Zn^{2+} ion although diamagnetic shows low enhancement and hence it appears that binding strength of the metal ion at the receptor decides the extent of enhancement.

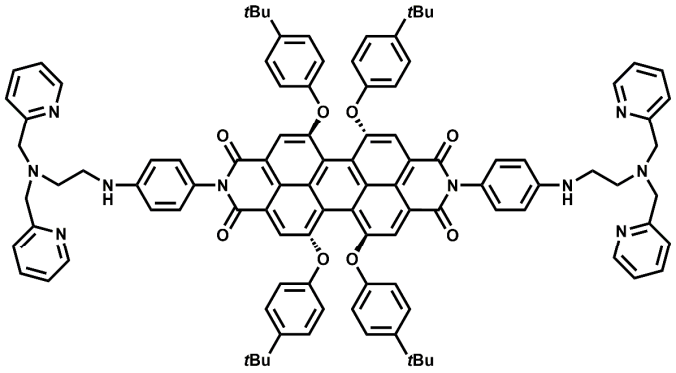

53

The bis(coumarinyl) Schiff base **54** does not show any significant emission in MeOH:H_2O (98:2,v/v) medium.[84] This low-fluorescence character of free **54** is attributed to a photoinduced charge transfer (PCT) process from the electron donating C=N moiety to the coumarin ring leading to quenching of the excited state of coumarin. Upon addition of Fe^{3+} to **54** which catalyzes the hydrolysis of the imine linkage that releases strongly fluorescent coumarin

derivative offering about a 140-fold enhancement in fluorescence (scheme 33). Other first-row transition metal ions do not catalyze the hydrolysis and hence does not interfere.

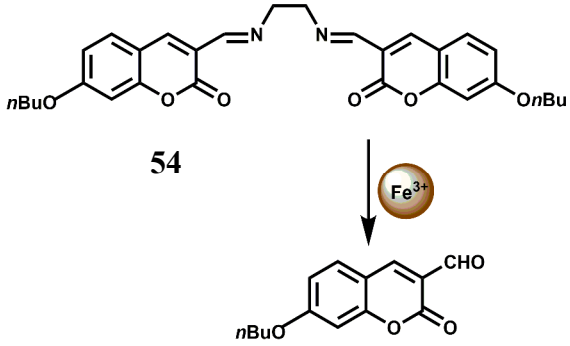

54

Scheme 33 Probable Fe^{3+} induced sensing mechanism of **54**.

It is known that Fe^{3+} has a strong binding affinity with imidazole N atom.[85] The association constant K_a of **55** for Fe^{3+} ion is found to be (2.9 ± 0.2) x 10^3 M^{-1} with the metal ion engaging four N donors equatorially while the axial sites are occupied by counter anions as proven by different spectroscopic techniques. When excited at 288 nm in MeCN-H_2O (95:5, v/v) the metal-free **55** gives an emission at 412 nm.[86] Addition of Fe^{3+} to the solution causes the emission at 412 nm to decrease in intensity with the appearance of a new band at 475 nm. Thus, this chemosensor can be used as a ratiometric probe for Fe^{3+}. Other competing metal ions do not afford any ratiometric response neither they interfere with the response obtained with Fe^{3+} ion.

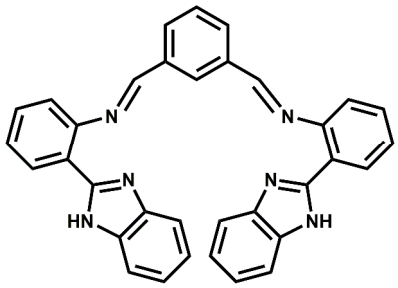

55

The PET chemosensor **56** has a squarate hydroxamate and a coumarin signaling units linked through a spacer. The squarate dianion itself does not bind first- and second-row transition-metal ions in a chelating fashion because the bite angle imposed by the cyclobutene framework is too large to sustain such coordination. That is why, the squarate hydroxamate has been used which is known to bind Fe^{3+} effectively.[87] The amine linking the squaramide moiety and the fluorophore is likely to cause a PET-type quenching of the chromophore. The linker moiety is designed to be rigid to prevent a bound metal to have any significant communication with the fluorophore and to lessen the effects of the paramagnetic quenching.[88]

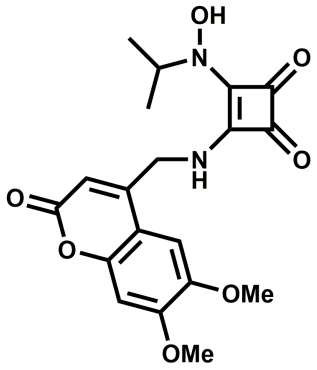

56

The metal-free sensor shows low emission suggestive of an efficient PET quenching of the coumarin chromophore. Upon addition of Fe^{3+} to an aqueous buffered (pH, 4.4) solution of **56** a 9-fold enhancement of fluorescence is observed due to blocking of the PET (scheme 34). At a 150 μM concentration of **56** in the presence of 1 equiv of Fe^{3+} at ambient temperature, equilibration of the emission intensity is reached only after 15 min suggesting its slow response. However, the signal does not degrade over the course of 48 h. Although no stability constant

value is given, the fluorescence signal does not diminish even in presence of 1000-fold excess of EDTA.

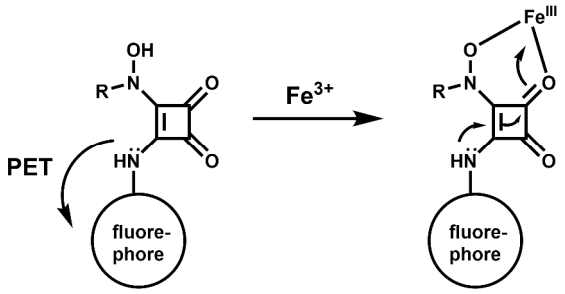

Scheme 34 Possible binding mode of chemosensor **56**.

The chemosensor **57** has been built with two fluorophores *viz.,* a coumarin and a naphthalimide for sensing Fe^{3+} (scheme 35).[89] The metal free sensor shows very weak emission when excited at 456 nm. In presence of Fe^{3+} ion, however, it gives an enhancement at 504 nm with high selectivity over other biologically relevant metal ions in aqueous THF solution. The association constant K_a value is, however, found to be moderate at 2.589±0.206 × 10^3 M^{-1}. Utility of using two fluorophores is not clear from the studies and also possible interference from Cr^{3+} ion has not been probed for this chemosensor.

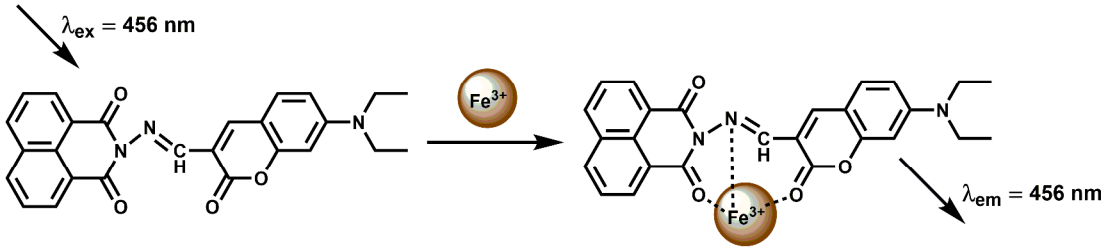

57

Scheme 35 Possible sensing mechanism of **57**.

Two 1-naphthylamine derived ICT probes **58** and **59** are found to act as fluorescence turn-on sensors selectively for Fe^{3+} ion in methanol.[90] Other competing metal ions shows

quenching of fluorescence like the metal-free probes. However, it is necessary to study the efficiency of enhancement when other metal ions are added in presence of Fe^{3+} ion for its effective use.

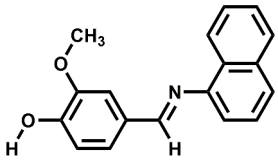

58

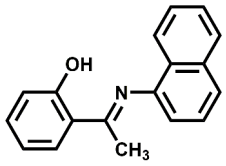

59

Two pyrene moieties are present at the two ends of a linear chain incorporating O and N donors to have the fluorescent probe **60**.[91] In the metal-free state, the two pyrene groups are far apart for any possible excimer emission. Besides, no monomer emission is observed due to an efficient PET from the imine N to the excited pyrene. Selectively in presence of Fe^{3+} ion, the probe folds around the metal ion that brings the two pyrene moieties close to one another to give an excimer band at 507 nm when excited at 330 nm. However, no monomer emission is mentioned arising out of the blocked of PET upon Fe^{3+} binding. The association constant of the Fe^{3+} complex is found to be moderately high at $1.27 \times 10^4\ M^{-1}$.

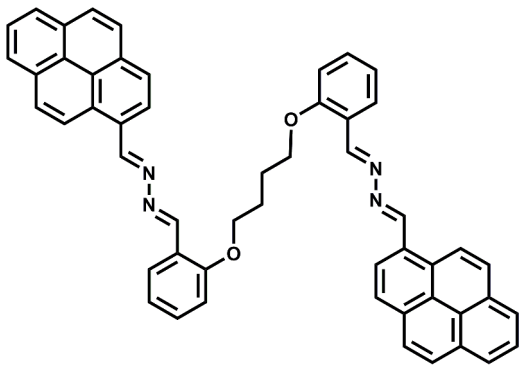

60

A BODIPY covalently linked with 8-hydroxyquinoline has been attached to a benzoate linked porphyrin to have the dyad **61**.[92] The 8-hydroxulquinoline benzoate moiety not only facilitates the energy transfer process but also provides binding sites for Hg^{2+} and Fe^{2+} ions. On irradiation at 470 nm where the BODIPY unit absorbs most of the light, **61** gives not only the BODIPY emission at 516 nm but also the porphyrin emission at 650 nm. Addition of Hg^{2+} leads to a significant decrease in the BODIPY emission (almost 90% in comparison with that of the metal-free **61**) and a slight increase in the porphyrin emission decreasing the F516/F650 ratio from 16.4 to 1.24. In presence of Fe^{2+}, however, an opposite change in the corresponding emission intensities are observed. The emission from BODIPY is remarkably enhanced (83.62% relative to that of metal-free **61**) and porphyrin emission, simultaneously diminished slightly, with the F516/F650 ratio increasing from 16.4 to 26.67. It is believed that binding of either metal ion at the 8-hydroxyquinoline site leads to twisting of the dyad bringing the two fluorophores closer. This facilitates FRET from BODIPY to porphyrin. Presence of Fe^{2+} induces partial restraint in the FRET due to non-radiative quenching in the excited states associated with the unpaired electrons in Fe^{2+}. This system represents a rare example of Fe^{2+} detection.

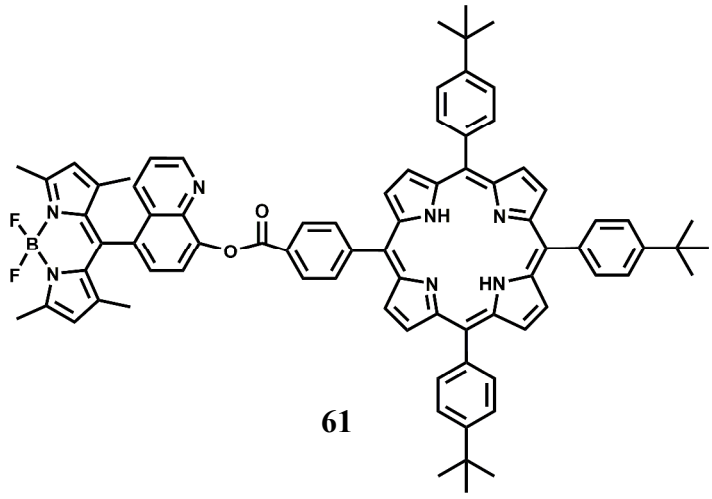

61

2.6 Cobalt Chemosensors

Cobalt is an essential trace element in human body and found in cobalamin and also in a few metalloproteins.[93] Apart from its biological roles, exposure to high levels of cobalt can lead to health hazards like decreased cardiac output, cardiac and thyroid enlargements, heart disease, elevated red blood cells accompanied by increased cells in the bone marrow, increased blood volume, vasodilation, flushing and so on.[94] Monitoring its concentration in human is, therefore, of crucial importance. However, there is hardly any fluorescence signaling systems available for Co^{2+} that can be utilized for tracking this transition metal in living cells or other biological specimens. Two principal challenges of Co^{2+} detection in biosystems are its paramagnetic nature and its biologically relevant divalent metal ion competitors like Ni^{2+}, Cu^{2+} and Zn^{2+} that typically bind more tightly to common ligands compared to Co^{2+} owing to Irving-Williams series considerations.[95] In spite of these difficulties, there are several chemosensors available for detecting the Co^{2+} ion.

The chemosensor **62** has been synthesized by connecting a Tokyo Green (TG) dye derivative with a tetradentate N_3O chelator ligand through a cleavable ether linkage.[96] In presence of O_2, the Co^{2+} ion can break the C–O bond releasing TG free which does not contain a bound, quenching paramagnetic metal center (scheme 36). This transforms a weakly fluorescent probe into a highly fluorescent dye, that gives about 18-fold fluorescence enhancement in aqueous medium. Cellular concentrations of other competing and biologically relevant s- and d-block metal ions do not elicit any significant fluorescence enhancement. This sensor can also detect changes in exchangeable Co^{2+} pools in living cells as found in case of lung carcinoma A549 cell line.

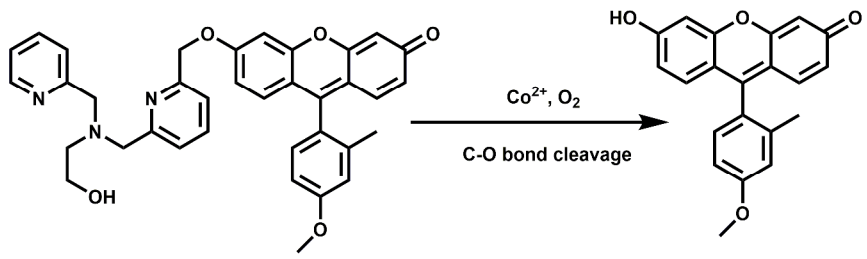

62

Scheme 36 Possible sensing mechanism of chemosensor **62**.

Two 8-sulfonamidoquinoline derivatives **63** and **64** were designed for the determination of Co^{2+} in presence of H_2O_2.[97] It has been observed that under basic medium it forms a chelate with the sulphonamide group resulting in intense emission in the ultraviolet region where a range of metal ions, including Cr^{3+}, Cu^{2+} and Ni^{2+} do not interfere with the exception of Fe^{3+}. This makes these probes useful for the determination of trace amount of Co^{2+} in food and hair samples. While speciation of the complex is not clear, it is likely that Co^{2+} is oxidized to the kinetically inert Co^{3+} complex. Interestingly, no emission is observed in absence of H_2O_2.

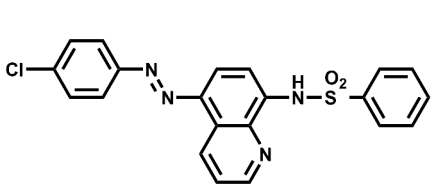

63

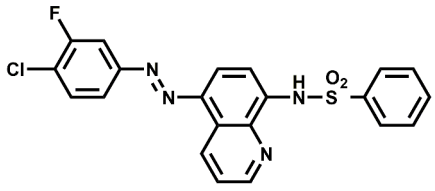

64

Cyanide anions are extremely poisonous as they inhibit the process of cellular respiration in mammals by interacting strongly with a heme unit in the active site of cytochrome a_3.[98] Also, the high level of intracellular Ca^{2+} concentration is caused by the uptake of CN^- and triggers a cascade of enzymatic reactions to increase the level of reactive oxygen species that finally inhibits the antioxidant defense system.[99] It is thus crucially important to have a sensor to

monitor the CN^- concentration in biosystems. The coumarinylsalen fluorescence chemosensor **65** binds a Co^{2+} ion at the salen moiety as shown in scheme 37.[100] While the metal-free ligand shows emission, when it is bound to Co^{2+} no emission is observed due to an efficient PET from the coumarin moieties to the metal center. Upon addition of CN^- anion which occupies the two axial sites (association constant, $K_1 \geq 10^7$ M^{-1} and $K_2 = 4.0 \times 10^5$ M^{-1}) the LUMO of the cobalt complex is raised above the HOMO of the fluorophore. This blocks the donor excited PET to give a strong fluorescence recovery.

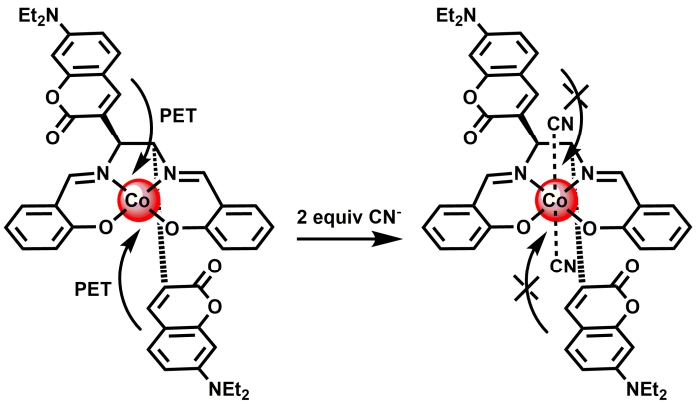

65

Scheme 37 Complexation of the cyanide ion with **65**·Co.

An efficient and selective fluorescent optode membrane based on the chemosensor **66** has been fabricated in the plasticized PVC membrane containing sodium tetraphenylborate as a liphophilic anionic additive.[101] The metal-free sensor upon excitation at 345 nm gives a strong emission at 520 nm at pH 5.0. Upon addition of Co^{2+} ion, this emission is quenched with the appearance of two new bands in the region, 385-420 nm. Quenching of the 520 nm band and appearance of the 420 nm band ratio can be used for quantitative estimation of Co^{2+} up to the concentration range of 5.0×10^{-7} to 2.0×10^{-2} M with a relatively fast response time of less than

5 min. The proposed fluorescence optode has been successfully applied to find out cobalt content of vitamin B12 ampoule, cobalt cake, cobalt alloy and tap water samples.

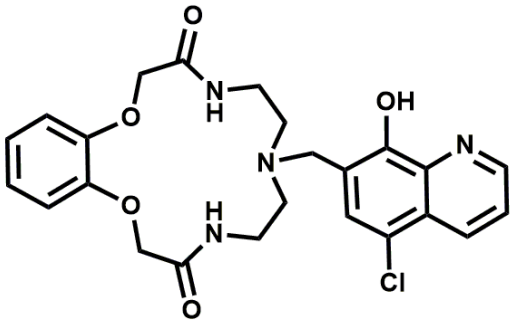

66

The chemosensor **67** based on ICT mechanism has been reported.[102] The free probe on excitation at 404 nm gives a weak, structureless emission band at 428 nm in buffered MeOH-H_2O (1:1 v/v) at pH 7.4. Upon addition of Co^{2+}, the metal ion binds at the site shown that results in the colour modulation as well as increases the ICT transition by a 37-fold enhancement in the fluorescence output. The selectivity of Co^{2+} arises as it fits well in the pseudo-cavity with N_2O donor set (scheme 38). Other biologically relevant metal ions give negligible enhancement. A slight modification of the receptor can make this system highly sensitive and selective for Co^{2+} ion.

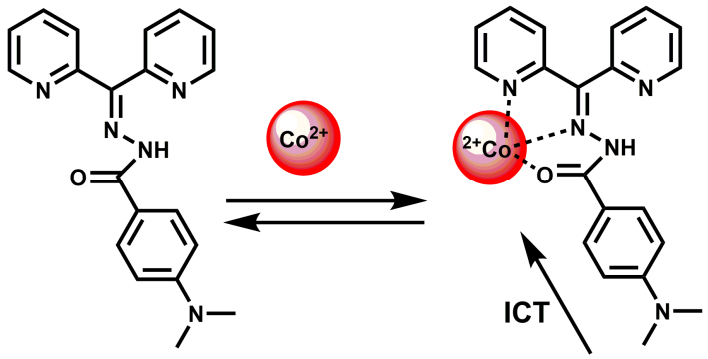

67

Scheme 38 Possible Co^{2+} binding mode of **67**.

Chemosensor **68** based on 9,10-anthraquinone has been introduced to show that binding of Co^{2+} changes the colour from yellow to pale green.[103] It also affords a 100-fold CHEF with green fluorescence in 20% aqueous methanol at pH 7 with the Co^{2+} ion. However, metal ions like Cu^{2+} and Ni^{2+} interfere by completely quenching the fluorescence (in presence of Cu^{2+}) or significantly reduce the emission (in presence of Ni^{2+}). This fluorescent probe is, therefore, not suitable for use in biological samples.

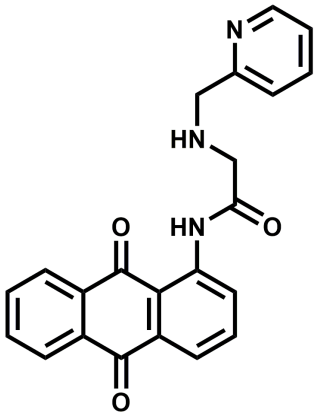

68

The fluorescent probe **69** with a benzyl ether linker on excitation at 350 nm emits at 380 nm in aqueous solution at pH 7.2.[104] Addition of Co^{2+} to the solution leads to quenching of this emission band and appearance of a new band at 460 nm. The rapid fluorescence quenching of the 380 nm band is due to binding of the paramagnetic Co^{2+}. However, Co^{2+} mediated cleavage of the benzyl ether bond releases highly fluorescent 2-(2'-hydroxyphenyl) benzothiazole that gives emission at 460 nm without any metal bonded to it.

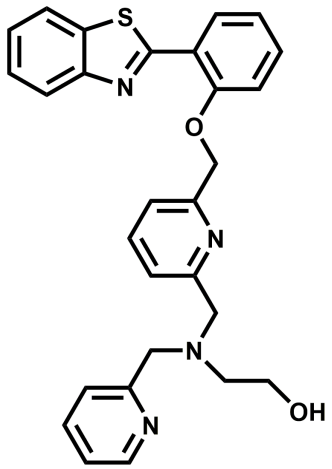

69

The coumarin–quinoline hybrid **70** affords turn-on fluorescence in presence of paramagnetic Co^{2+} and Ni^{2+} ions at 392 nm when excited at 338 nm in methanolic water (9:1, v/v).[105] Heavy metal ions like Ag^{+} also elicit slight fluorescence showing its poor chemoselective nature. The fluorescence appears to be due to binding a metal ion at the site providing NO_2 coordination that stops the deactivation pathway.

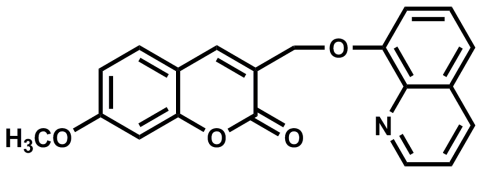

70

2.7. Nickel Chemosensors

Nickel is an essential element in plants and many other biosystems. It is implicated in various enzyme activities[106] that include ureases, hydrogenases, superoxide dismutases, acetyl-coenzyme A synthases, carbon monoxide dehydrogenases, methyl-coenzyme M reductases and frequently used in catalytic processes. However, as an industrial pollutant, nickel is a toxic

element that can cause lung injury, allergy and carcinogenesis. It is, therefore, of importance to have sensors for nickel. A major obstacle is to design receptors selective for Ni^{2+} ion over other biologically relevant metal ions.

In chemosensor **71**, a BODIPY unit is covalently connected to a mixed N/O/S receptor to coordinate the Ni^{2+} cation. The receptor forms a 1:1 complex with Ni^{2+} with an approximate dissociation constant of (195±5) × 10^{-6} M.[107] The probe gives a 25-fold fluorescence enhancement upon Ni^{2+} binding. This turn-on response is reversible as treatment of the Ni^{2+}-loaded **71** with the metal ion chelator TPEN restores the fluorescence back to the free **71** level. Biologically relevant alkali, alkaline earth and transition metal ions except Cu^{2+} do not show any enhancement or interfere with the Ni^{2+} response. Cu^{2+} quenches the enhancement obtained with Ni^{2+} restricting its usefulness. Confocal microscopic studies show that this chemosensor can monitor changes in Ni^{2+} levels within living mammalian cells.

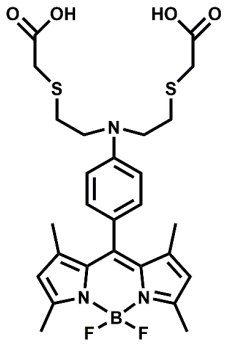

71

Rhodamine derived chemosensor[108] **72** show spiro-ring opened 200-fold fluorescence enhancement in presence of Co^{2+} and Ni^{2+} while other transition metal ions do not interfere in aqueous medium containing 2% DMSO. Both Co^{2+} and Ni^{2+} form 1:1 complexes with the association constants of 2.1 × 10^{4} and 4.5 × 10^{3} M^{-1}, respectively. Binding to both ions is

reversible, as the metal can be extracted with EDTA with concomitant reduction in the fluorescence to the metal-free state. Since Co^{2+} competes fairly well with Ni^{2+}, the detection of Ni^{2+} can be done only if Co^{2+} is not present.

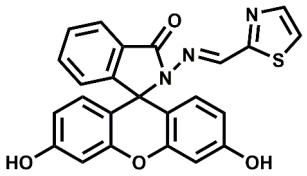

72

The PET chemosensor **73** designed with coumarin attached to a piperazine moiety works in alkaline pH.[109] It affords a 7-fold enhancement in presence of large excess of Ni^{2+} ion. However, Zn^{2+} ion also gives a 10-fold enhancement and therefore, limits its utility.

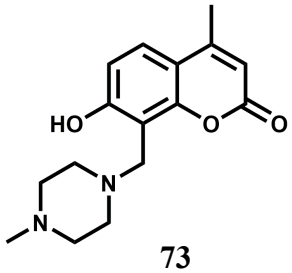

73

The novel Zn^{2+} Schiff base complex **74** bearing acacen^{2-} (dianion of *N,N′*-ethylenebis(acetylacetonylideneaminato)) moieties have been constructed.[110] The crystal structure of its dinickel complex shows that the two Ni^{2+} ions occupy the two metallacycles. In DMF, **74** gives an emission at 361 upon excitation at 293 nm. When Ni^{2+} is added, the structure becomes more rigid blocking its deactivation pathway and hence, a significant increase in the emission quantum yield is observed.

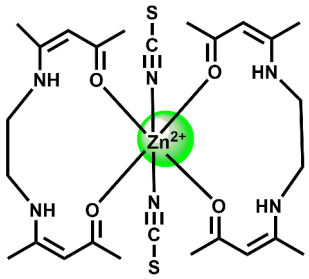

74

The malonohydrazide based PET fluorescent probe **75** forms a 1:1 complex in DMSO-water (1:1, v/v) with Ni^{2+} ion with the association constant of $K_a = 3.3 \times 10^4\ M^{-1}$.[111] The free probe gives an emission peak at 629 nm on excitation at 317 nm which increases significantly and selectively in presence of Ni^{2+} ion (scheme 39). The Ni^{2+} binding at the site is quite selective and strong due to good fitting of the metal ion in the binding pocket. The cause of fluorescence enhancement is not mentioned by the authors but it is more likely to be due to increased rigidity of the system that blocks the deactivation pathway.

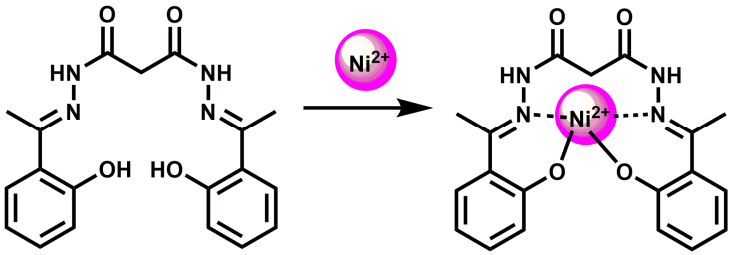

75

Scheme 39 Possible metal ion binding mode of **75**.

2.8. Copper Chemosensors

Copper is the third-most abundant transition metal in the human body. Copper containing proteins are involved in a wide variety of biochemical functions[112] including copper transport (ceruloplasmin), copper storage (metallothionein), protective roles (Cu–Zn superoxide dismutase), terminal oxidase for O_2 respiration (cytochrome *c* oxidase) and so on. Copper ions are mainly metabolized by the liver. Copper in the cytoplasm predominantly binds to metallothionein, and the excess copper is excreted into the bile mainly through a lysosome-to-bile pathway.[113] The level of copper in lysosomes is closely related to a number of neurodegenerative diseases, that include Wilson's disease,[114] Menkes disease[115] and Alzheimer's disease.[116] Copper commonly accumulates in the lysosomes of patients suffering from these diseases. It is therefore, interesting to know the spatial distribution of copper in the biosystems. It follows, therefore, those sensors that can signal the presence of copper ion selectively is of high demand. However, some of the shortcomings for practical applications such as cross-sensitivities toward other metal cations and low fluorescence quantum yields are also to be kept in mind. Also, aqueous medium should be preferred for biological studies. Definitely, development of new Cu^{2+}-selective turn-on fluorescent probes is of utmost importance and necessity.

In the PET chemosensor **76**[117] a N_2O donor receptor has been connected via Schiff base condensation to an electron-withdrawing naphthalimide derivative. It forms a highly stable 1:1 complex with Cu^{2+} ($K_a = 1.1 \times 10^{10}$ M^{-1}) in acetonitrile-water (70:30, v/v). Free **75** shows a weak emission at 519 nm due to an efficient PET from the receptor to the fluorophore (scheme 40). Binding of Cu^{2+} stops the PET giving a 5-fold fluorescence enhancement. The detection limit is calculated to be 1.5×10^{-7} M while changes in fluorescence is observed within 10 s.

Other biologically relevant metal ions show negligible enhancement or do not interfere with the Cu^{2+}-induced emission.

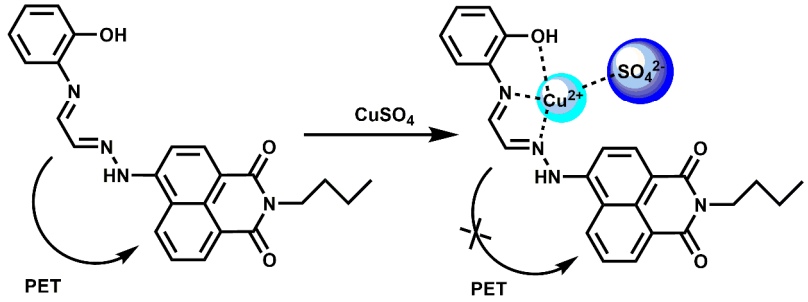

76

Scheme 40 Proposed binding mode of **76** with Cu^{2+}.

The PET chemosensor **77** incorporated with two thioether and three amine units has been designed to detect Cu^{2+} ion in CH_3CN : H_2O (4 : 1) at pH 7.[118] Besides, the larger cavity size of the receptor has lowered the association constant for the 1:1 complex with Cu^{2+} to log K= 4.1 ± 0.1. Ni(II), Cd(II), Zn(II), Ag(I), and Hg(II) (1000 μM) do not interfere in the fluorescence studies. Signification participation of amine nitrogen in binding with Cu^{2+} ion is responsible for the enhancement of fluorescence due to suppression of the PET.

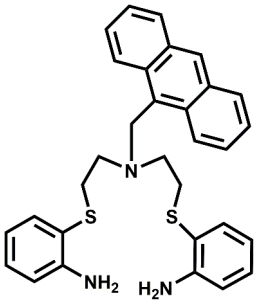

77

In addition to the PET chemosensors mentioned above, intramolecular charge transfer emission has also been used as a mechanism for Cu^{2+} detection. The chemosensor **78** has been synthesized by connecting 2-methoxybenzaldehyde hydrazone with 4-(*N,N*-

dimethylamino)benzamide.[119] The methoxy group rather than a phenolic group has been used to nullify excited-state intramolecular proton transfer (ESIPT) that would have opened another channel of deactivation. The metal ions Cu^{2+}, Zn^{2+}, Hg^{2+} and Pb^{2+} bind to the chemosensor with 1:1 stoichiometry to similar extent in the ground state as the binding constant of comparable value (order, 10^4 M^{-1}) is obtained with each metal ion. In MeCN, **77** emits dual fluorescence, an excited state CT pertaining to the 4-(N,N-dimethylamino)benzamide group at 525 nm and a LE emission at 350 nm. A host of biologically relevant as well as heavy metal ions are used for probing the response of the CT band. These metal ions either quench the fluorescence or have no effect. Only Cu^{2+} exhibits a prominent 30-fold enhancement of the CT band with a substantial blue-shift from 525 to 460 nm. The fluorescence enhancement factor decreased with increasing water content in MeCN, but can still be significant even when the water content is 90% by volume. The low fluorescence quantum yield of **77** in absence of Cu^{2+} can be attributed to radiationless transitions from the nπ* state. Upon addition of Cu^{2+} the metal ion coordinates with the lone pair of the carbonyl O raising the energy level of the nπ* state such that the ππ* state becomes the lowest excited state, leading to a substantial increase in the fluorescence quantum yield. Besides, Cu^{2+} binding can also lead to a conformation restriction which can block a channel of the deactivation pathway.

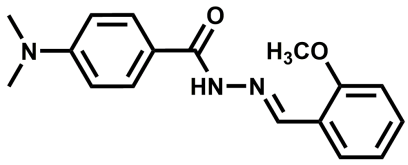

78

The PET chemosensor **79** has been fabricated on a calix[4]arene platform by modifying its upper rim with four iminoquinoline subunits.[120] Metal free **79** shows a very low fluorescence

quantum yield in MeCN due to an efficient PET from the imine N atoms. A Cu^{2+} ion coordinates the four imine N atoms with high association constant (K_a) of 3.67×10^7 M^{-1} to block the PET accompanied by about 1200-fold enhancement of fluorescence. While other transition metal ions do not bind at this site, alkali/alkaline metal ions are expected to bind at the lower rim to the ethereal O atoms without affecting fluorescence. While this is a simple design, its lack of solubility in water restricts its usefulness.

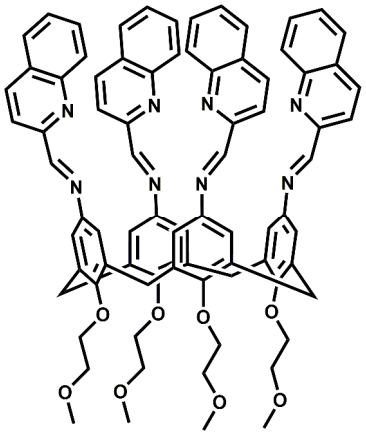

79

Like in the cases of other transition metal sensors, a number of turn-on sensors for Cu^{2+} has been designed based on rhodamine derivatives. The probe **80** has been synthesized by condensing two rhodamine B hydrazides with terephthalaldehyde. In aqueous medium, free **80** shows very weak emission in aqueous medium. Addition of Cu^{2+} ion gives a remarkably high fluorescence at 575 nm due to opening of spirolactam bond while other metal ions do not exhibit any significant emission (scheme 41).[121] Spectroscopic data suggest a 1:1 stoichiometry although no association constant value is provided.

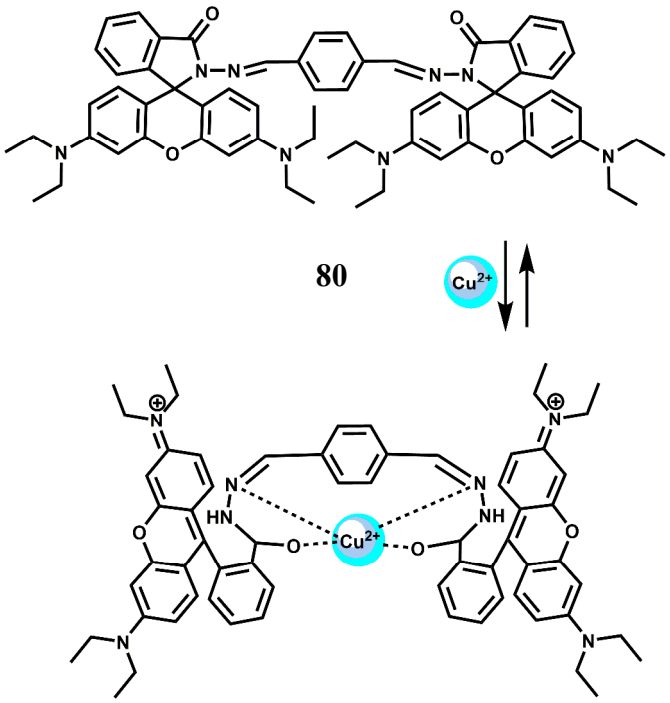

Scheme 41 Proposed binding mode of **80** with Cu^{2+}.

In chemosensor **81,** a Cu^{2+} ion is anchored at the site shown in scheme 42 leading to opening of the spirolactam as well as hydrolytic cleavage of the imine bonds giving high fluorescence.[122] Since it works in aqueous medium, it affords imaging studies of different cell lines with confocal microscopy. However, the hydrolysis step is sluggish and takes at least 1 h and so this probe cannot be used for measuring temporal distribution of Cu^{2+} ion in biological systems.

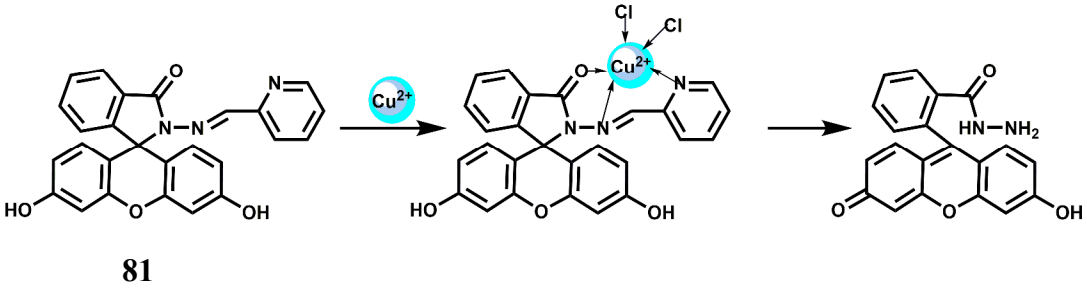

81

Scheme 42 Proposed binding mode of **81** with Cu^{2+}.

The chemosensor **82** is possibly the first example of a boronic acid-linked chemosensor for Cu^{2+} ion (scheme 43).[123] The metal ion is believed to occupy the site as shown giving an association constant value of 2.8×10^3 M^{-1}. When the boronic acid group is replaced by hydrogen, the Cu^{2+} ion does not elicit spiro-ring opened fluorescence enhancement. Thus, boronic acid moiety is important in binding a Cu^{2+} ion at the site. Free **81** forms a colourless solution in 50% aqueous MeCN showing very low emission. Upon addition of Cu^{2+} the colour changes to pink accompanied by spirolactam ring-opened fluorescence enhancement at 585 nm. Other biologically relevant metal ions do not give any fluorescence. Also, metal ion competition experiments show that binding of Cu^{2+} to the chemosensor is unaffected by other metal ions even when used in large excess. When an excess of cyclen is added to the solution containing the Cu^{2+} complex of **82**, the fluorescence disappear and the original structure of the chemosensor is regenerated. Thus, in this case, Cu^{2+}-induced spirolactam ring opening is a reversible process. Confocal microscopic experiments show that **81** can pass through cell membranes and displays a strong fluorescence response to intracellular copper ions in different mammalian cell lines.

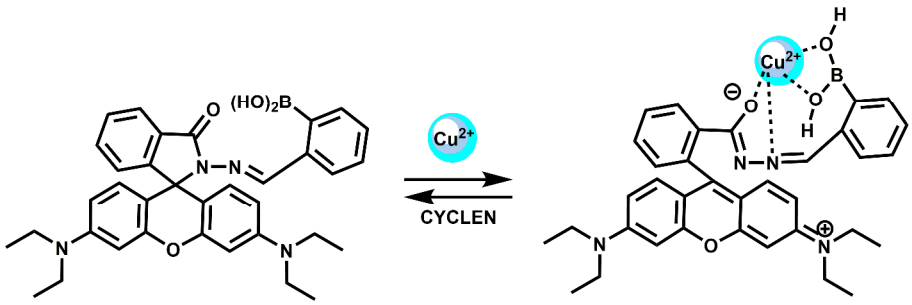

82

Scheme 43 Proposed binding mode of **82** with Cu^{2+}.

The rhodamine B based chemosensor **83** with a six-membered reactive ring was developed by inserting a nitrogen atom in the known fluorescent probe rhodamine B spiro

thiohydrazide.[124] This sensor is shown to be an efficient "turn-on" fluorescent chemodosimeter for Cu^{2+} in a neutral aqueous medium due to opening of the spiro ring (scheme 44). Other biologically relevant or heavy metal ions do not induce ring-opened fluorescence enhancement. Titration experiments reveal that the fluorescence intensity at 597 nm increases linearly with increasing concentrations of Cu^{2+} between 0.10 and 10.0 μM and further smoothly increase until a maximum is reached up to 20.0 μM Cu^{2+}, where an approximately 400-fold enhancement is observed.

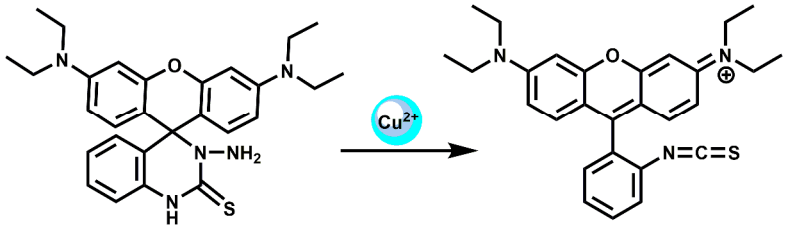

83

Scheme 44 Proposed sensing mechanism of Cu^{2+} by **83**.

The chemosensor **84** has also been found to selectively bind Cu^{2+} ion with the association constant estimated to be 8.9×10^3 M^{-1} in aqueous MeCN (1:1, v/v). Upon binding of Cu^{2+}, strong spiro-ring opened fluorescence enhancement is observed (scheme 45)[125] while other competing metal ions do not bring any discernible fluorescence changes. Also, Cu^{2+} induced fluorescence of **84** is reversible as addition of excess EDTA completely quenches the fluorescence. Experiments with living cells indicate that the chemosensor is cell viable and can detect intracellular Cu^{2+} ion.

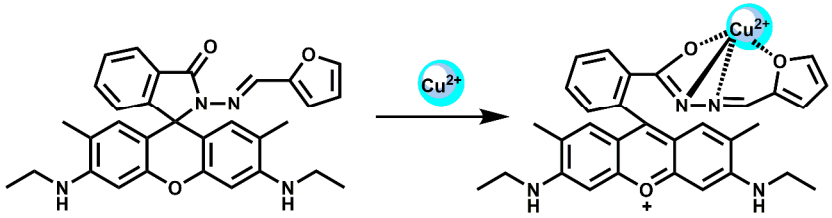

84

Scheme 45 Proposed binding mode of **84** with Cu^{2+}.

Chemosensors **85** and **86** can be easily synthesized using click chemistry.[126] These compounds are non-fluorescent but with increase in pH in presence of Cu^{2+} lead to Fenton reaction promoting ring-opening of triazole linked fluorescein lactone (scheme 46) that leads to strong emission with the detection limit down to 200 nM. Selectivity of this protocol has been evaluated by screening various biologically relevant metal ions that shows none of these metal ions can elicit fluorescence enhancement.

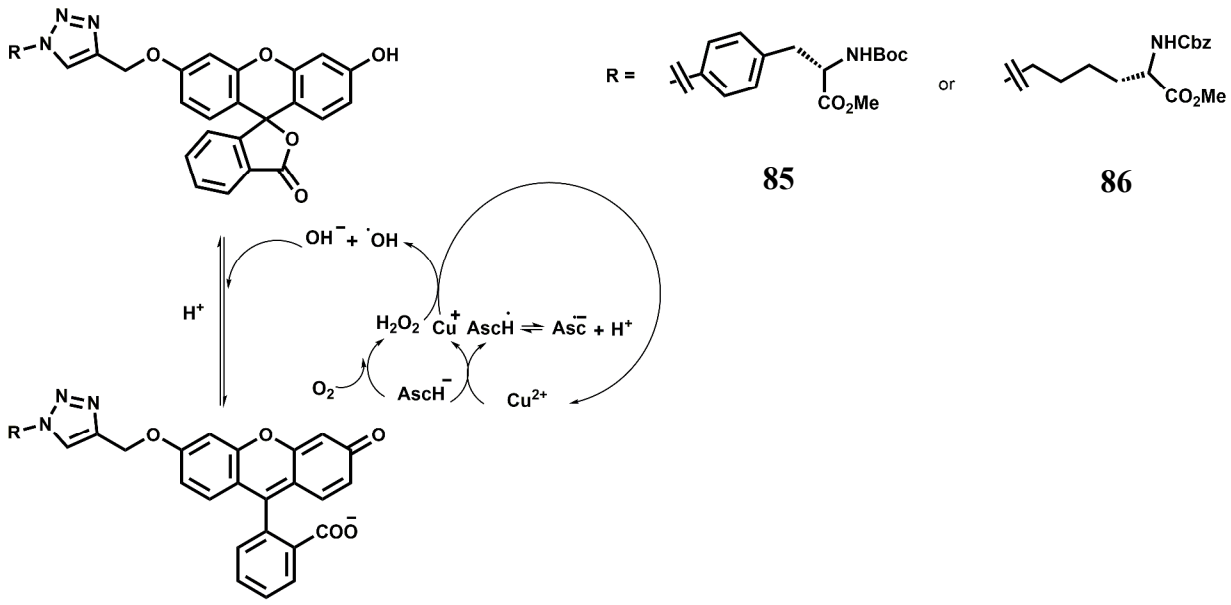

85 **86**

Scheme 46 Proposed mechanism for detection of Cu^{2+} by **85** and **86** based on the Fenton reaction.

The indole derivative of rhodamine **87** specifically binds to Cu^{2+} ion with an association constant of 1.71×10^4 in presence of large excess of other competing ions.[127] The metal-free dye

emits at 490 nm when excited at 340 nm in aqueous MeCN due to the indole moiety. Binding of the Cu^{2+} ion breaks the spiro-bond of the rhodamine moiety (scheme 47). At this stage, excitation at 340 nm results in FRET from the donor indole to the Cu^{2+} bound xanthene acceptor accompanied by a strong emission at 587 nm with concomitant reduction of the emission due to the indole moiety. The detection limit of **87** for Cu^{2+} ion is found to be 3.6 ppb, which is much lower than the U.S. EPA maximum allowable limit for Cu^{2+} ion (1.3 ppm) in drinking water. Besides, fluorescence microscopic studies confirmed that the chemosensor can be used as an imaging probe to study the uptake of Cu^{2+} in HeLa cells.

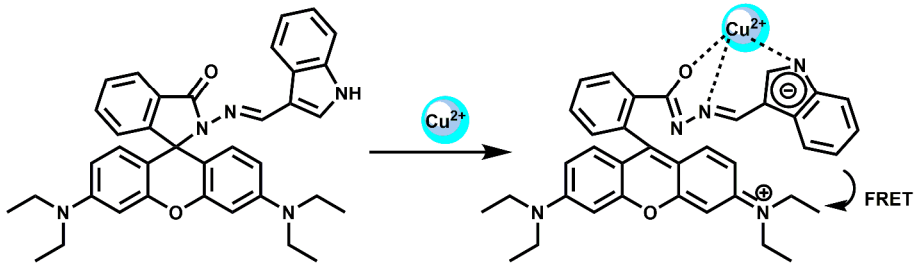

87

Scheme 47 Proposed binding mode of **87** with Cu^{2+}.

The rhodamine B semicarbazide **88** show high spiro-bond opened fluorescence (scheme 48) in aqueous methanol (1:1,v/v), exhibiting a fast response time (in seconds) and a detection limit of 1.6×10^{-7} mol/L at neutral pH.[128] The quick response time allows determination of Cu^{2+} in waste water samples and also monitoring of intracellular Cu^{2+} levels in living cells using confocal fluorescence spectroscopy. The high selectivity of the chemosensor for Cu^{2+} ion might be due to close matching between the Cu^{2+} radius and the size of the binding pocket. However, no association constant value is available.

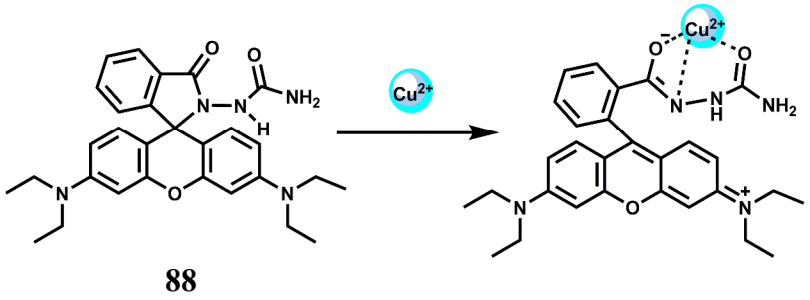

88

Scheme 48 Possible sensing mechanism of **88**.

The strategy of metal induced bond breaking has been adopted for the coumarin-334 derived chemosensor **89**.[129] This compound is non-emissive due to an efficient PET from the imine N atom. Addition of Cu^{2+} catalyzes breaking of the imine linkage to free the coumarin-334. Since the paramagnetic Cu^{2+} is not bound to the coumarin, it offers a strong fluorescence (scheme 49). The detection limit for Cu^{2+} is found to be 8.7×10^{-8} M which is within the EPA (US) acceptable limit in drinking water. Another important property of the chemodosimeter is its high selectivity for Cu^{2+} over other metal ions. The competing metal ions do not catalyze hydrolysis of the imine bond.

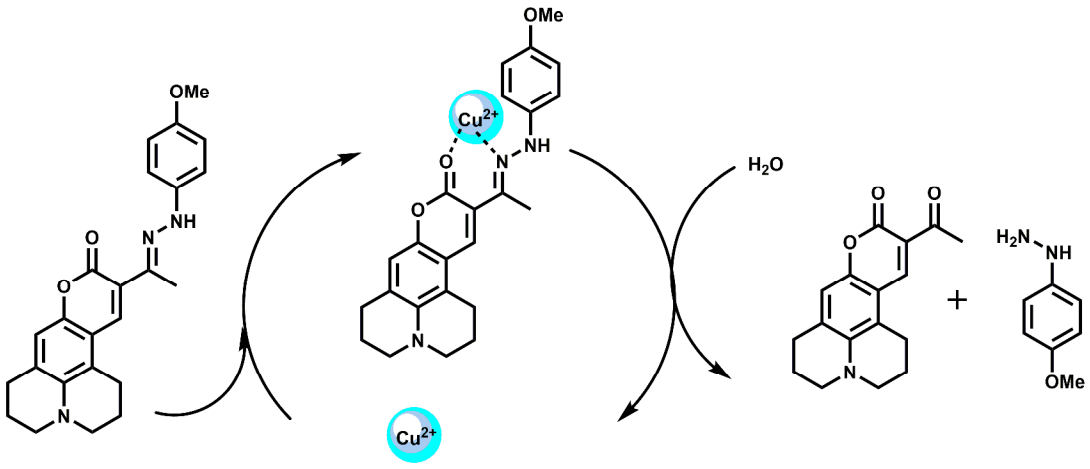

89

Scheme 49 Cu^{2+}-induced catalytic sensing cycle of **89**.

BODIPY is an important fluorophore and has been used for several metal ions because of its visible excitation and emission characteristics. The chemosensor **90** based on BODIPY has been designed to have a receptor specific for Cu^{2+} ion.[130] To one arm of the fluorophore is also attached a *p*-diacetylene benzene moiety to extend conjugation of the system for emission at longer wavelength. Excitation at 620 nm in CH_3CN in presence of Cu^{2+} ion affords an emission with maximum at 651 nm.

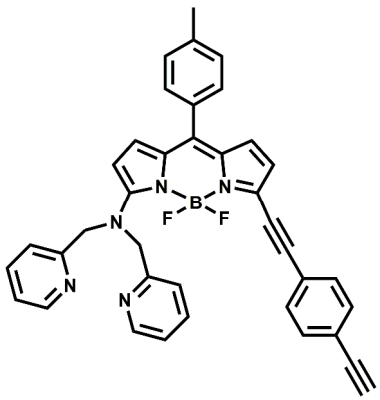

90

Two more BODIPY derived chemosensors **91** and **92** are reported.[131] Compound **91** gives large CHEF enhancement in presence of Pb^{2+} or Cu^{2+} among the metal ions examined. The association constants of **91** with Pb^{2+} and Cu^{2+} are found to be 8.8×10^3 and 5.5×10^4 M^{-1} respectively. On the other hand, **92** exhibits absolute chemoselectivity for Cu^{2+} ion over other competing ions including Pb^{2+} and gives high fluorescence in presence of Cu^{2+} ion through hydrolysis of the acetyl groups (scheme 50).

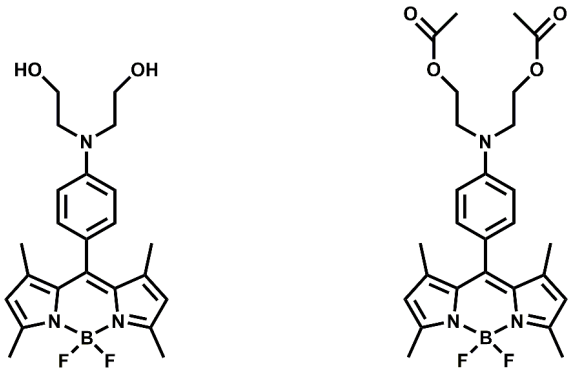

91 **92**

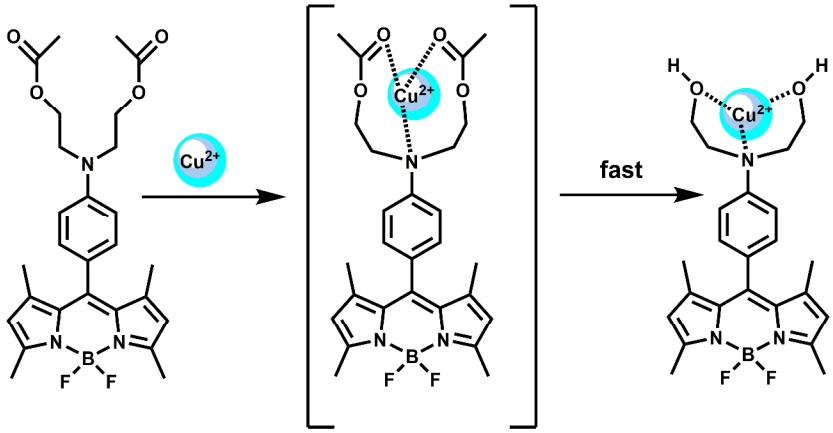

Scheme 50 Proposed sensing mechanism of chemosensor **92**.

When the receptor contains several soft thioether donors as in **93**, the BODIPY based system exhibits excellent selectivity towards the soft Cu^{+} ion[132] giving about 10-fold turn-on

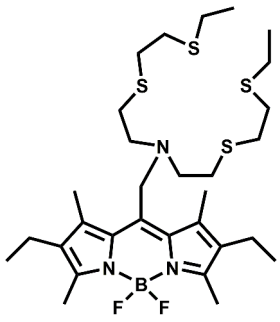

93

response and shows excellent selectivity for Cu^{+} over biologically relevant metal ions, including Cu^{2+}. Confocal microscopic studies indicate that this sensor can be used for detecting Cu^{+} levels within living cells.

A slightly different derivative of a BODIPY reporter with the same thioether-based receptor as above has been constructed to obtain **94** for selective detection of Cu^{+} ion over other biologically relevant metal ions, including Cu^{2+} and Zn^{2+}.[133] Live-cell confocal microscopy experiments show that **94** is membrane-permeable and can sense changes in the levels of labile Cu^{+} pools within living cells by ratiometric imaging, including expansion of endogenous stores of exchangeable intracellular Cu^{+} triggered by ascorbate stimulation in kidney and brain cells. Such knowledge of spatial distribution of Cu^{+} is important to monitor physiology of this important metal.

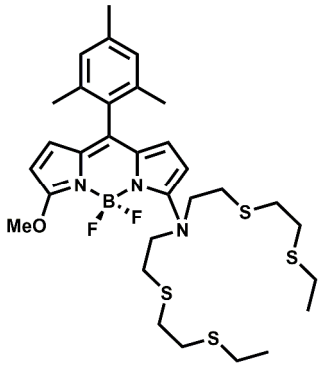

94

The fluorescent probe **95** has been designed as a new type of targetable fluorescent chemosensor for imaging exchangeable mitochondrial copper pools in living cells.[134] The sensor has two distinctive sites: a Cu^{+}-responsive fluorophore and a mitochondrial-targeting triphenylphosphonium moiety for localizing the probe to this organelle. The fluorescence intensity of **95** increases 10-fold with a slight blue shift of the emission maximum to 558 nm with the addition of 1 equiv of Cu^{+}. The observed dissociation constant (K_d) value for Cu^{+} complex is found to be 7.2×10^{-12} M. The fluorescence response of the Cu^{+} bound **95** is not affected by the presence of physiologically relevant concentrations of Ca^{2+}, Mg^{2+}, and Zn^{2+}. Besides, other bioavailable divalent transitionmmetal ions do not induce a change in the emission intensity of **95** or do not interfere with the Cu^{+} response. This PET sensor is found to be very useful in detecting labile Cu^{+} in the mitochondria of living cells.

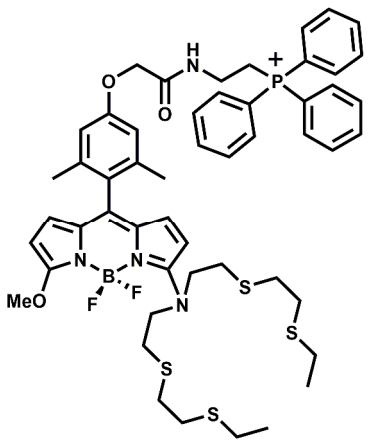

95

Two-photon fluorescence is a preferable technique for imaging live cells. Two-photon microscopy has a number of advantages over one photon microscopy including increased penetration depth (4500 mm), localized excitation and reduced photodamage and photobleaching effects, thereby allowing tissue imaging for a longer period of time. Besides, no interference from natural amino acid fluorophores occurs which allows for sharp images. The chemosensor

96 has been designed with the same receptor as above for binding a Cu^{+} ion inside. The Cu^{+} complex of **96** affords a TPA (two-photon absorption) value of 67 GM at 750 nm.[135]

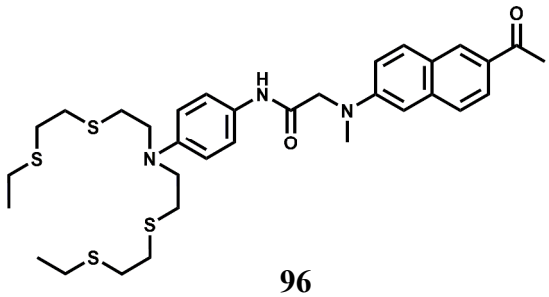

96

The chemosensor **97** is based on coumarin fluorophore that displays high selectivity for Cu^{2+} in aqueous medium[136] with high emission quantum yield due to blocking of PET from the imine N atom to the fluorophore with association constant $K_a = 3.34 \times 10^4\ M^{-1}$. The association constant with Cu^{2+} is calculated to be $3.34\times10^4\ M^{-1}$. Its operation in aqueous medium allows for microscopic imaging in LLC-MK2 cells (*in vitro*) and several living organs (*in vivo*).

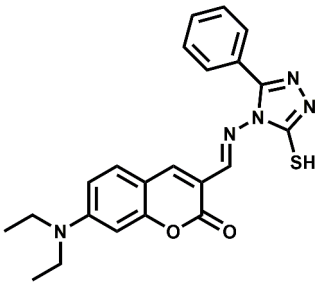

97

The weakly fluorescent thiosemicarbazone derivative **98** was found to be a selective optical and "turn-on" fluorescent chemodosimeter for Cu^{2+} ion in aqueous ethanolic medium.[137] It is argued that Cu^{2+} selectivity results from an oxidative cyclization of **98** into the highly fluorescent rigid 4,5-dihydro-5,5-dimethyl-4-(naphthalen-5-yl)-1,2,4-triazole-3-thione (scheme 51). The chemodosimetric reaction, in combination with selective metal ion-induced catalysis, can be a promising approach to develop selective detection methods for different metal ions.

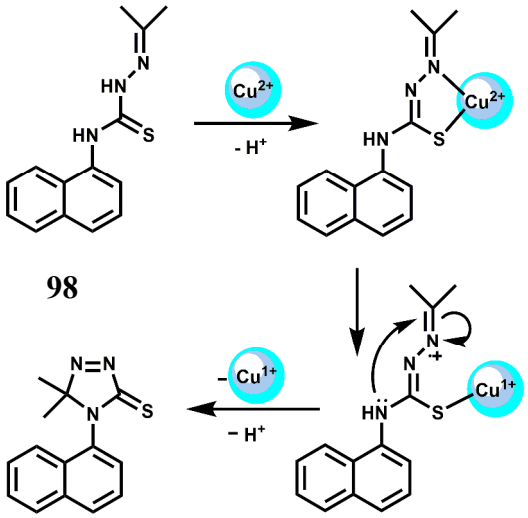

Scheme 51 Proposed oxidative cyclization mechanism of **98** by Cu^{2+}.

A coumarin moiety is covalently attached on either side of benzyl dihydrazone to have the sensor **99**.[138] Upon excitation at 468 nm, the aqueous solution of the metal-free sensor gives an emission at 534 nm with very low quantum yield due to efficient PET from the hydrazone moiety to the coumarin fluorophore association constant (K_a) 3.67×10^6 M^{-1}. Upon addition of Cu^{2+} it undergoes conformational change as shown (scheme 52) and at the same time, blocks both the PET pathways to afford a strong fluorescence. This system functions in aqueous medium and therefore, is suitable for use in live cell imaging studies.

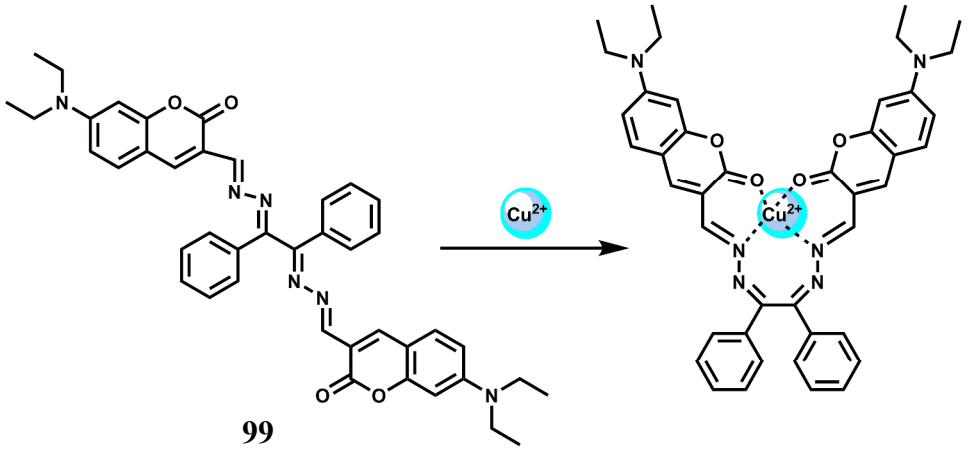

99

Scheme 52 Proposed binding mode of **99** with Cu^{2+}.

In designing the PET sensor **100**, a tricarbocyanine dye is used as the NIR fluorophore and *2,2'*-azanediyl bis(*N*-hydroxyacetamide) as the Cu^{2+} receptor.[139] The specificity of Cu^{2+} binding at the receptor is accomplished due to matching of the cavity of the binding site with radius of Cu^{2+} ion (scheme 53). The metal-free system shows very weak fluorescence, however, in presence of Cu^{2+} ion, the PET is blocked giving high fluorescence at 800 nm in aqueous medium with a dissociation constant of 2.7×10^4 μM in in buffered aqueous medium. The emission maximum lies within the biological window and more importantly, aqueous medium can be used both of which make this chemosensor quite important.

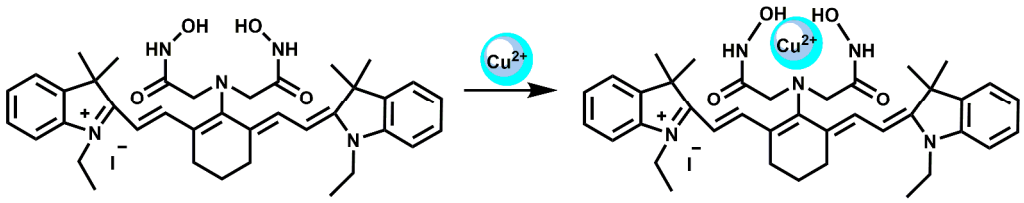

100

Scheme 53 Proposed binding mode of **100** with Cu^{2+}.

The chemosensor **101** obtained by derivatizing the upper rim of a thiacalix[4]arene by a crown ether and the lower rim by two pyrene moieties.[140] Upon addition of Cu^{2+} in aqueous organic medium, two Cu^{2+} ions are believed to occupy the sites as shown (scheme 54) with the binding constant $>10^{11}$. This makes the two pyrene moieties well-separated and offering only monomer emission due to blocking of PET. However, addition of Li^{+} ion which occupies the crown ether cavity leads to ejection of the Cu^{2+} ions. This brings the two pyrene moieties closer for π-stacking giving an excimer emission.

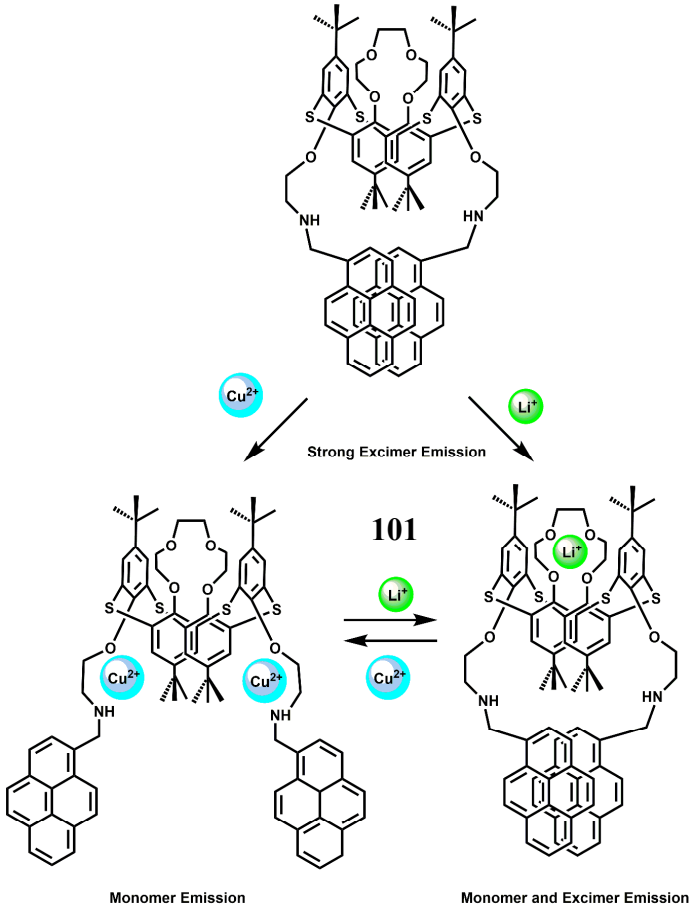

Scheme 54 Proposed binding mode of **101**.

The electron-withdrawing fluorophore 7-nitrobenz-2-oxa-1,3-diazole (NBD) derived chemosensor **102** binds a Cu^{2+} ion at the pocket shown (scheme 55).[141] This mode of binding by the Cu^{2+} ion blocks the PET recovering fluorescence in aqueous MeCN.

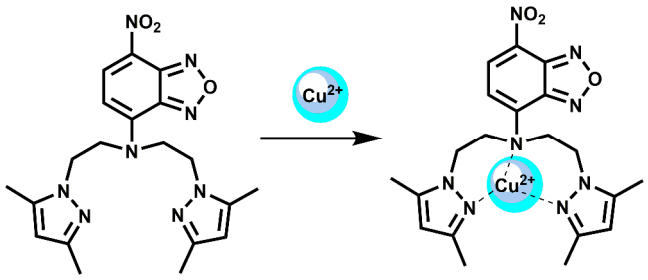

102

Scheme 55 Proposed binding mode of **102**.

In an elegant approach, a sensor system that separates the sensing and the signaling events have been designed. Two different fluorogenic ligands **103** and **104** are capable of metal chelation.[142] The system functions as illustrated below (scheme 56).

103 **104**

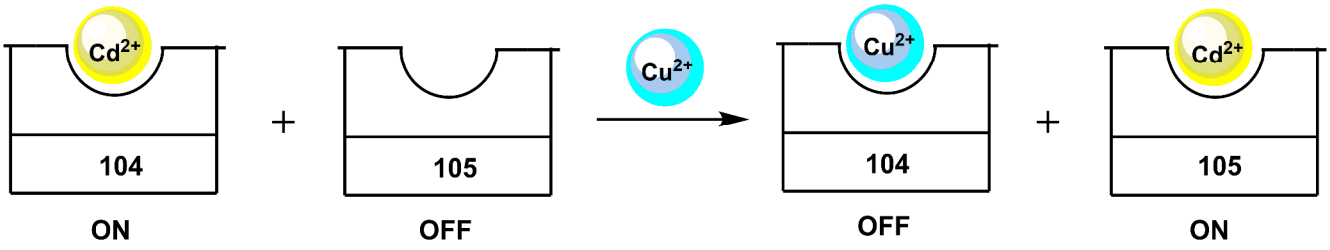

Scheme 56 Schematic representation of a ratiometric Cu^{2+} sensor system.

In presence of 1 equivalent of Cd^{2+}, it preferably chelates with **103** giving strong emission centering at 435 nm due to stoppage of PET. When an equivalent amount of Cu^{2+} is added it displaces Cd^{2+} from **103** leading to fluorescence quenching from the paramagnetic ion. However, Cd^{2+} is now bonded to **104** giving strong emission at 518 nm again due to blocking of PET. The entire operation can be performed in aqueous media in HEPES ((4-(2-hydroxyethyl)-1-piperazineethanesulfonic acid) buffer at pH 7.2. This way, detection of Cu^{2+} is indirect.

The chemosensor **105** acts as an ICT based ratiometric and colourimetric fluorescent chemosensor selective for Cu^{2+} ion (scheme 57).[143] A Cu^{2+} ion binds fairly strongly at the site shown with an association constant estimated to be $2.58x10^4$ M^{-1}. Upon addition of Cu^{2+}, the metal free absorption band shifts from 328 nm to about 540 nm due to deprotonation as shown with the disappearance of the ICT band centering at 496 nm and the appearance of a new band at 620 nm.

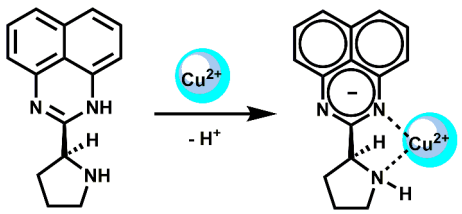

105

Scheme 57 Proposed binding mode of **105** with Cu^{2+}.

The quinoline-indene derived PET chemosensor **106** was found to be sensitive towards Cu^{2+} ion in 1:1 aqueous MeCN giving a 5-fold enhancement of fluorescence (scheme 58).[144] The receptor cavity binds a Cu^{2+} ion with an association constant estimated to be (log *K*) 6.48±0.48.

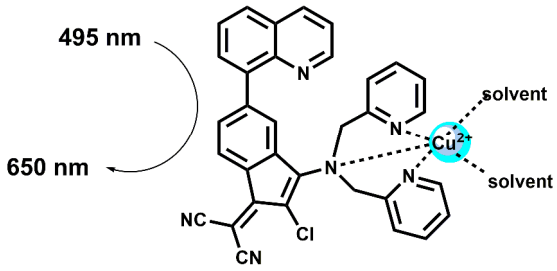

106

Scheme 58 Proposed binding mode of **106** with Cu^{2+}.

Two 4,5-disubstituted-1,8-naphthalimide derivatives **107** and **108** have been synthesized as Cu^{2+} ion sensors.[145] The free sensor **107** displays a broad emission centering at 534 nm in aqueous medium. Upon addition of Cu^{2+} this band reduces in intensity with the appearance of a new band centered at 478 nm due to complex formation with the probe. Compound **108** on the other hand, quenches emission of the free probe although colour of the solution changes sharply from yellow to pink.

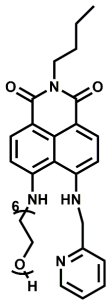

107

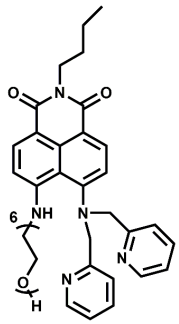

108

The compound **109** is non-emissive although in presence of Cu^{2+} ion,[146] it undergoes oxidative cyclization (scheme 59) to form a highly fluorescent benzotriazole. This cyclization reaction can be triggered by μM level concentration of Cu^{2+} in water at pH = 6-8, at room temperature. The cyclic product exhibits a green emission at 530 nm.

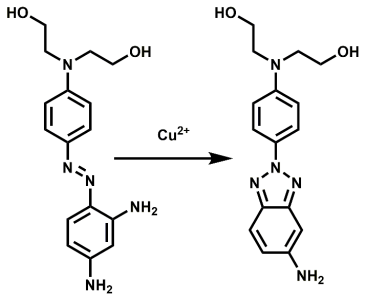

109

Scheme 59 Cu^{2+} ion induced oxidative cyclization of **109**.

The receptor in the fluorescent probe **110** can accommodate a Cu^{2+} ion with a high association constant of 2.95 × 10^5 M^{-1}. Once the metal ion occupies the site, the two naphthalimide moieties come closer to each other. Upon addition of 1 equiv of Cu^{2+} ion, the two naphthalimide moieties come closer giving an excimer emission at 558 nm. Further addition of another equiv of Cu^{2+}, triggers a change in the conformation of the chemosensors where the two naphthalimide groups are move far apart from each other giving a naphthalimide monomer emission at 461 nm (scheme 60).[147]

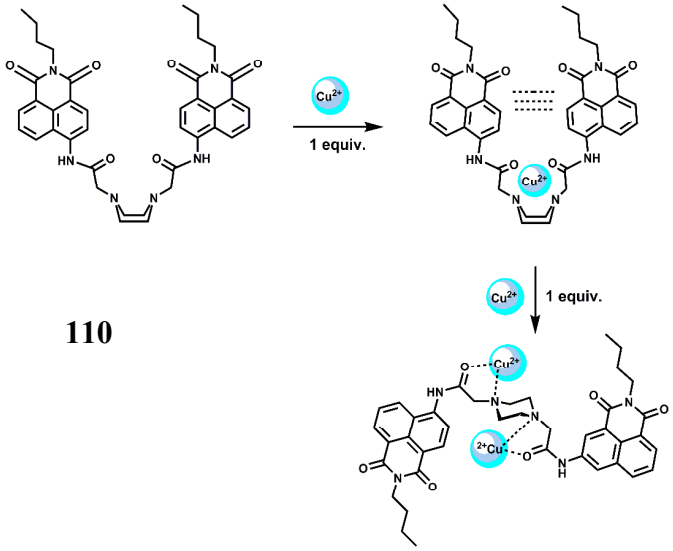

110

Scheme 60 Proposed binding mode of **110** with Cu^{2+}.

The chemosensor **111** has been designed based on the strong tendency of the pyrene moiety to form intermolecular dimers.[148] The free sensor exhibits pyrene monomer emission at 388 nm upon excitation in acetonitrile solution. Upon addition of Cu^{2+} ion, the monomer emission is partially quenched but a strong excimer emission at 460 nm is observed. It is argued that interaction of the quinolinylamide group with the Cu^{2+} ion induces an intermolecular π-π* interaction which is responsible for the fluorescence changes. With increasing the length between the pyrene and quinolinylamide moieties, excimer formation is hindered.

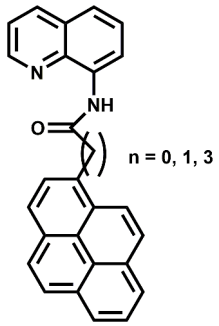

111

The thiophene based Schiff base **112** was found to be highly selective fluorescence turn-on PET chemosensor for Cu^{2+} in aqueous medium.[149] It affords a high binding constant of 4.23×10^5 in aqueous medium with the detection limit of 0.418 nM. The sensor gives a 35-fold enhancement at 430 nm in presence of Cu^{2+} when excited at 370 nm. In presence of Cr^{3+} and Sn^{2+} the enhancement maximum is obtained at 465 nm while other metal ions do not interfere. This probe can be used for studying Cu^{2+} ion in the living cell by confocal microscopy.

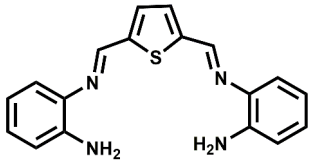

112

The fluorescent probe **113** was easily synthesized via Schiff base condensation as a chemosensor for Cu^{2+}.[150] The free probe does not give any emission when excited at 400 nm in acetonitrile due to an efficient PET. Upon addition of Cu^{2+} it affords 120-fold fluorescence enhancement at 468 nm as the PET process is blocked. The N and S atoms provide a binding scaffold for recognition of Cu^{2+} (scheme 61) with fairly high affinity (K_a = 4.35 × 10^4 M^{-1}). Other competing metal ions do not interfere. The simplicity and elegance of the probe design should spur further research for water soluble signaling systems for biological applications.

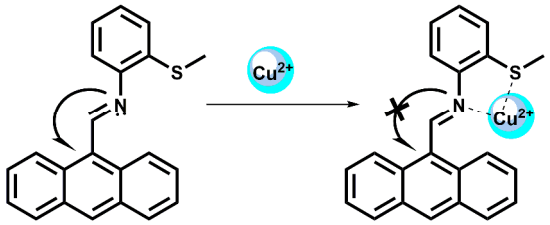

113

Scheme 61 Possible sensing mechanism of **113**.

The coumarin derived fluorescent probe **114** is found to be highly selective for Cu^{+} ion.[151] The benzylic ether bond of the probe can be cleaved selectively in presence of Cu^{+} under a physiological condition to release the coumarin derivative that is highly fluorescent (scheme 62). Other competing metal ions do not give any fluorescence as they cannot cleave the benzylic ether bond.

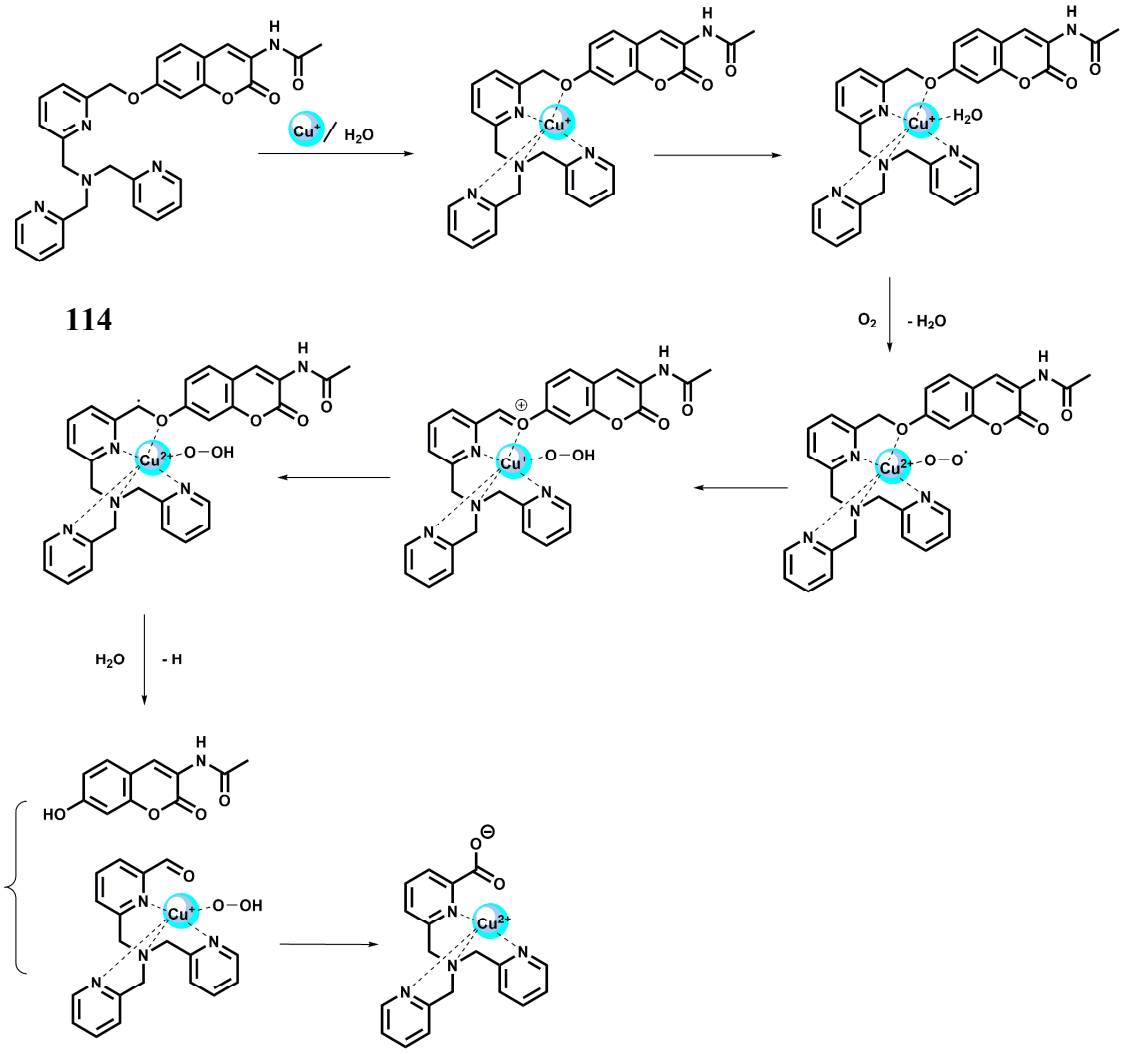

Scheme 62 Possible sensing mechanism of **114**.

For monitoring real-time copper fluxes in living animals and thus offers an opportunity to examine copper physiology, the chemosensor **115** is designed.[152] It consists of a near-infrared emitting cyanine dye with a sulfur-rich receptor to provide a selective and sensitive turn-on response to Cu^{+}. This probe with negligible cytotoxicity is capable of monitoring fluctuations in exchangeable copper stores in living cells and mice under basal conditions, as well as in situations of copper overload or deficiency. This new generation sensor is definitely expected to spur research on sensors for monitoring fluctuations in exchangeable metal ions in biosystems.

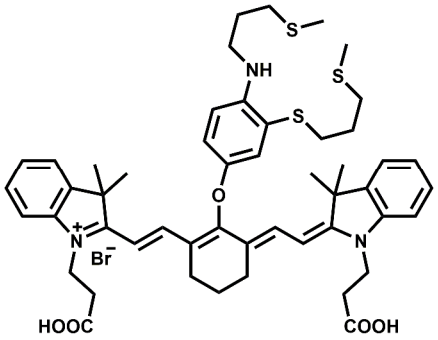

115

3. Conclusions

It is now clear that several design principles have been adopted for signalling the presence of first-row transition metal ions through turn-on fluorescence. The nature of the fluorophore assumes great significance. It is often found that PET/PCT based sensors often lead to quenching of fluorescence. Of all the designs, rhodamine derived sensors are particularly attractive as they are capable of overcoming fluorescence quenching by paramagnetic transition metal ions. Several key issues still remain in the fluorescence detection of biologically relevant first-row transition metal ions. Most important being aqueous solubility of the probe and a very quick response with high selectivity and sensitivity for temporal distribution with high fidelity of the metals in live cells. Of course, cell viability of the sensor is an important parameter that should always be kept in mind. For live cell imaging studies, systems that show two-photon fluorescence are of crucial importance as they can nullify the background effect of natural fluorophores. Finally, availability of variable oxidations states of transition metals have not been exploited in designing chemosensors. Thus, despite considerable advances, this subject still requires a lot of attention from chemists to purposely build fluorescence signalling probes.

Acknowledgments

Financial support for this work is provided by the DST, New Delhi, India and DRDO, New Delhi, India. SP and NC wish to thank CSIR for the senior research fellowship. PKB wishes to thank all his students who made significant contributions in the area of fluorescence signalling and fluorescence based logic gates over the years.

Notes and references

1 (*a*) W. Kaim and B. Schwedeski, in *Bioinorganic Chemistry*: *Inorganic Elements in the Chemistry of Life*, John Wiley and Sons, New York, 1994; (*b*) R. W. Hay, J. R. Dilworth and K. B. Nolan, eds., *Perspectives on Bioinorganic Chemistry*, JAI Press, London, 1991; (*c*) H. Sigel, Eds., *Metal Ions in Biological Systems*, Marcel Dekker, New York, 1973; (d) R. Wever and K. Kustin, *Adv. Inorg. Chem*., 53, **81**, 1990.

2 (*a*) P. S. Dobbin and R. C. Hider, *Chem. Brit*., 1990, **26**, 565; (*b*) W. Mertz, *Science*, 1981, **213**, 1332; (*c*) A. Butler and C. J. Carrano, *Coord. Chem. Rev*., 109, **61**, 1991.

3 (*a*) J. R. Lakowicz, *Principles of Fluorescence Spectroscopy*, 3rd Edition, Springer, 2006; (*b*) B. Valeur and I. Leray, *Coord. Chem. Rev*., 2000, **205**, 3.

4 (*a*) L. Fabbrizzi, M. Licchelli, P. Pallavicini, L. Parodi, A. Taglietti, in *Transition Metals in Supramolecular Chemistry*, ed. J. P. Sauvage, John Wiley & Sons Ltd., New York, 1999, vol. 5.; (*b*) L. Fabbrizzi and A. Poggi, *Chem. Soc. Rev*., 1995, **24**, 197.

5 G. Das, P. K. Bharadwaj, M. Basu-Roy and S. Ghosh, *Chem. Phys*., 2002, **277**, 145.

6 (*a*) A. P. de Silva, H, Q. N. Gunaratne and C. P. McCoy, *Nature*, 1993, **42**, 364; (*b*) A. P. de Silva, N. D. McClenaghan and C. P. McCoy, in *Electron Transfer in Chemistry*, ed. V. balzani, Wiley-VCH, Weinheim, 2001, Vol. 5. (*c*) A. P. de Silva and S. Uchiyama, *Top. Curr. Chem.,* 2011, **300**, 1.

7 (*a*) Z. Xu, J. Yoon and D. R. Spring, *Chem. Soc. Rev*., 2010, **39**, 1996; (*b*) E. L. Que, D. W. Domaille and C. J. Chang, *Chem. Rev.* 2008**, 108***,* 1517; (*c*) E. Tomat and S. J. Lippard, *Curr. Opin. Chem. Biol.*, 2010, **14** , 225; (*d*) E. M. Nolan and S. J. Lippard, *Acc. Chem. Res*., 2009, **42**, 193; (*e*) K. Kikuchi, K. Komatsu and T. Nagano, *Curr. Opin. Chem. Biol.*, 2004, **8**, 182; (*f*) P. Jiang and Z. Guo, *Coord. Chem. Rev*., 2004, **248**, 205.

8 *(a)* Z. Liu, W. He and Z. Guo, *Chem. Soc. Rev*., 2013, **42**, 1568; (*b*) H. N. Kim, Z. Guo, W. Zhu, J. Yoon and H. Tian, *Chem. Soc. Rev*., 2011, **40**, 79; (*c*) J. Wu, W. Liu, J. Ge, H. Zhang and P.

Wang, *Chem. Soc. Rev*., 2011, **40**, 3483; (*d*) D.T. Quang and J. S. Kim, *Chem. Rev*., 2010, **110**, 6280; (*e*) Y. Yang, Q. Zhao, W. Feng and F. Li, *Chem. Rev*., 2013, **113**, 192; (*f*) M. Formica, V. Fusi, L. Giorgi, M. Micheloni, *Coord. Chem. Rev*., 2010, **256,** 170; (*g*) A. P. de Silva, T. S. Moody and G. D. Wright, *Analyst*, 2009, **134**, 2385; (*h*) X. Li, X. Gao, W. Shi and H. Ma, *Chem. Rev*., 2014, **114**, 590; (*i*) K. P. Carter, A. M. Young and A. E. Palmer, *Chem. Rev*., 2014, **114**, 4564; (*j*) P. K. Bharadwaj, *Prog. Inorg. Chem*., 2003, **51**, 251.

9 (a) S. Liu, J. P. C. Pestano and C. Wolf, *J. Org. Chem*., 2008, **73**, 4267; (b) D. P. Iwaniuk, K. Yearick-Spangler and C. Wolf, *J. Org. Chem*. 2012, **77**, 5203.

10 J. Yuasa and S. Fukuzumi, *J. Am. Chem. Soc.*, 2006, **128**, 15976.

11 K. H. Thompson, J. H. McNeill and C. Orvig, *Chem. Rev*., 1999, **99**, 2561.

12 (*a*) D. C. Crans, J. J. Smee, E. Gaidamauskas, L. Yang, *Chem. Re*v., 2004, **104**, 849; (*b*) R. L. VanEtten, P. P. Waymack, D. M. Rehkop, *J. Am. Chem. Soc.,* 1974, **96**, 6782; (*c*) W. Plass, *Angew. Chem., Int. Ed.,* 1999, **38**, 909; (*d*) D. R. Davies, W. G. J. Hol, *FEBS Lett.,* 2004, **577**, 315.

13 H. Vilter, *Phytochemistry,* 1984, **23**, 1387.

14 A. Butler, J. N. Carter-Franklin, *Nat. Prod. Rep.,* 2004, **21**, 180.

15 M. Mracova, D. Jirova, H. Janci and J. Lener, *Sci. Total Environ. Part 1*, 1993, 16.

16 F.-J. Huo, J. Su, Y.-Q. Sun, C.-X. Yin, H.-B. Tong, Z.-X. Nie, *Dyes Pigm*., 2010, **86**, 50.

17 M. J. R. Rama, A. R. Medina and A. M. Díaz, *Talanta*, 2005, **66**, 1333.

18 A. M. García Campaña, F. Alés Barrero and M. Román Ceba, *Anal. Sci*., 1996, **12**, 647.

19 Y. Zhou, J. Y. Jung, H. R. Jeon, Y. Kim, S.-J. Kim, and J. Yoon, *Org. Lett.*, 2011, **13**, 2742.

20 X. Zhang and W.-D. Woggon, *J. Am. Chem. Soc.*, 2005, **127**, 14138.

21 (a) Z. Xu, N. J. Singh, J. Lim, J. Pan, H. N. Kim, S. Park, K. S. Kim, J. Yoon, *J. Am. Chem. Soc.* 2009, **131**, 15528; (b) F. Wang, R. Nandhakumar, J. H. Moon, K. M. Kim, J. Y. Lee, J. Yoon, *Inorg. Chem*., 2011, **50**, 2240.

22 (*a*) W. Mertz and K. Schwarz, *Arch. Biochem. Biophys*., 1955, **58**, 504; (*b*) H. Arakawa, *J. Biol. Chem*., 2000, **275**, 10150; (*c*) R. Anderson, R. A. Chromium, *Trace Elements in Human and Animal Nutrition*, Academic Press, New York, 1987.

23 J. B. Vincent, *Nutr. Rev*., 2000, **58**, 67.

24 (*a*) C. Núñez, R. Bastida, A. Macías, E. Bértolo, L. Fernandes, J. L. Capelo, C. Lodeiro, *Tetrahedron*, 2009, **65**, 6179; (*b*) M. J. E. Resendiz, J. C. Noveron, H. Disteldorf, S. Fischer and P. J. Stang, *Org. Lett*., 2004, **6**, 651.

25 (*a*) M. Sarkar, S. Banthia and A. Samanta, *Tetrahedron Lett*., 2006, **47**, 7575; (*b*) J. Mao, L. N. Wang, W. Dou, X. L. Tang, Y. Yan and W. S. Liu, *Org. Lett*., 2007, **9**, 3188.

26 K. Huang, H. Yang, Z. Zhou, M. Yu, F. Li, X. Gao, T. Yi and C. Huang, *Org. Lett.*, 2008, **10**, 2557.

27 J. Mao, L. Wang, W. Dou, X. Tang, Y. Yan and W. Liu, *Org. Lett.*, 2007, **9**, 4567.

28 M. Li, D. Zhang, Y. Liu, P. Ding, Y. Ye and Y. Zhao, *J Fluoresc*., 2014, **24**, 119.

29 Y. Zhou, J. Zhang, L. Zhang, Q. Zhang, T. Ma and J. Niu, *Dyes and Pigments*, 2013, **148**, 97.

30 A. J. Weerasinghe, C. Schmiesing and E. Sinn, *Tetrahedron Lett*., 2009, **50**, 6407.

31 P. Mahato, S. Saha, E. Suresh, R. D. Liddo, P. P. Parnigotto, M. T. Conconi, M. K. Kesharwani, B. Ganguly and A. Das, *Inorg. Chem*., 2012, **51**, 1769.

32 Z. Zhou, M. Yu, H. Yang, K. Huang, F. Li, T. Yi and C. Huang, *Chem. Commun*., 2008, 3387.

33 R. H. Lipson, Y. J. Shi, and D. Lacey, in *An Introduction to Laser Spectroscopy*, ed. D. L. Andrews and A. A. Demidov, Kluwer Academic / Plenum Publishers, New York, 2nd edn., 2002, pp. 257-309.

34 Z. Xiaolin, X. Yi and Q. Xuhong, *Angewandte Chem. Int. Ed.*, 2008, **47**, 8025.

35 Y. Wan, Q. Guo, X. Wang and A. Xia, *Analytica Chimica Acta*,. 2010, **665**, 215.

36 M. Sarkar, S. Banthia and A. Samanta, *Tetrahedron Lett*., 2006, **47**, 7575.

37 J. -N. Wang, Q. Qi, L. Zhang and S. -H. Li, *Inorg. Chem*., 2012, **51**, 13103.

38 H. Wu, P. Zhou, J. Wang, L. Zhao and C. Duan, *New J. Chem*., 2009, **33**, 653.

39 D. Wang, Y. Shiraishi and T. Hirai, *Tetrahedron Lett*., 2010, **51**, 2545.

40 X. Hu, X. Zhang, G. He, C. He and C. Duan, *Tettrahedron*, 2011, **67**, 1091.

41 A. E. Albers, V. S. Okreglak and C. J. Chang, *J. Am. Chem. Soc.*, 2006, **128**, 9640.

42 S. Panda, P. B. Pati and S. S. Zade, *Chem. Commun.,* 2011, **47**, 4174.

43 V. Bravo, S. Gil, A. M. Costero, M. N. Kneeteman, U. Llaosa, P. M. E. Mancini, L. E. Ochando and M. Parra, *Tetrahedron*, 2012, **68**, 4882.

44 S. Wu, K. Zhang, Y. Wang, D. Mao, X. Liu, J. Yu and L. Wang, *Tetrahedron Lett*., 2014, **55**, 351.

45 L. –J. Ma, W. Cao, J. Liu, M. Zhang and L. Yang, *Sensors and Actuators B*, 2013, **181,** 782.

46 S. Goswami, A. K. Das, A. K. Maity, A. Manna, K. Aich, S. Maity, P. Sahab and T. K. Mandal, *Dalton Trans*., 2014, **43**, 231.

47 S. Guha, S. Lohar, A. Banerjee, A. Sahana, I. Hauli, S. K. Mukherjee, J. S. Matalobos and D. Das, *Talanta*, 2012, **91**, 18.

48 J. Emsley in *Nature's Building Blocks: An A-Z Guide to the Elements,* Oxford University Press, Oxford,, 2001, pp. 249 – 253.

49 J. H. Lee and A. P. Koretsky, *Curr. Pharm. Biotechnol*., 2004, **5**, 529.

50 J. A. Roth, *Biol. Res*. 2006, **39**, 45.

51 X.i Mao, H. Su, D. Tian, H. Li and R. Yang, *ACS Appl. Mater. Interfaces*., 2013, **5**, 592.

52 J. Liang and J. W. Canary, *Angew. Chem. Int. Ed*., 2010, **49**, 7710.

53 Z. D. Dai, K. N. Khosla,, J. W. Canary, *Supramol. Chem*. 2009, **21**, 296.

54 R. G. Pearson, *J. Chem Educ*. 1968, **45**, 581.

55 F. Gruppi, J. Liang, B. B. Bartelle, M. Royzen, D. H. Turnbullb and J. W. Canary, *Chem. Commun*., 2012, **48**, 10778.

56 K. Dutta, R. C. Deka and D. K. Das, *J Fluoresc*., 2013, **23**, 1173.

57 (*a*) R. Baliga, N. Ueda and S. V. Shah, *Biochem. J.* 1993, **291**, 901; (*b*) G. Balla, G. M. Vercellotti, J. W. Eaton and H. S. Jacob, *J. Lab. Clin. Med*., 1990, **116**, 546; (*c*) K. Ŏllinger and K. Roberg, *J. Biol. Chem*., 1997, **272**, 23707; (*d*) O. Sergent, I. Morel, P. Cogrel, M. Chevanne, N. Pasdeloup, P. Brissot, G. Lescoat, P. Cillard and J. Cillard, *Biol. Trace Elem. Res.*, 1995, **47**, 185; (*e*) A. Voogd, W. Sluiter, H. G. van Eijk and J. F. Koster, *J. Clin. Invest*., 1992, **90**, 2050.

58 J. Fandrey, S. Frede, W. Ehleben, T. Porwol, H. Acker and W. Jelkmann, *Kidney Int.*, 1997, **51**, 492.

59 (*a*) W. Breuer, S. Epsztejn and Z. I. Cabantchik, *J. Biol. Chem.*, 1995, **270**, 24209; (*b*) S. Epsztejn, O. Kakhlon, H. Glickstein, W. Breuer and Z. I. Cabantchik, *Anal. Biochem.*, 1997, **248**, 31; (*c*) S. P. Young and P. Aisen, in *The Liver: Biology and Pathobiology*, ed. I. M. Arias,J. L. Boyler and N. Fausto, Raven Press, Ltd., New York, 3rd edn., 1994, pp. 597–617.

60 (*a*) M. B. Delatycki, R. Williamson and S. M. Forrest, *J. Med. Genet*., 2000, **37**, 1; (*b*) H. Puccio and M. Koenig, *Hum. Mol. Genet*., 2000, **9**, 887; (*c*) M. F. Beal, *Biochim. Biophys. Acta.*, 1998, **1366**, 211.

61 M. Zhang, Y. Gao, M. Li, M. Yu, F. Li, L. Li, M. Zhu, J. Zhang, T. Yia and C. Huang, *Tetrahedron Lett.*, 2007, **48**, 3709.

62 S. Bae and J. Tae, *Tetrahedron Lett*., 2007, **48**, 5389.

63 M. H. Lee, T. V. Giap, S. H. Kim, Y. H. Lee, C. Kang and J. S. Kim, *Chem. Commun*., 2010, **46**, 1407.

64 Z. -Q. Hu, X. -M. Wang, Y. -C. Feng, L. Ding, M. Li and C. -S. Lin, *Chem. Commun*., 2011, **47**, 1622.

65 L. Huang, F. Hou, J. Cheng, P. Xi, F. Chen, D. Baib and Z. Zeng, *Org. Biomol. Chem*., 2012, **10**, 9634.

66 S. Goswami, S. Das, K. Aich, D. Sarkar, T. K. Mondal, C. K. Quah and H. K. Fun, *Dalton Trans*., 2013, **42**, 15113.

67 S. Ji, X. Meng, W. Ye, Y. Feng, H. Sheng, Y. Cai, J. Liu, X. Zhu and Q. Guo, *Dalton Trans*., 2014, **43** 1583.

68 H. Sheng, X. Meng, W. Ye, Y. Feng, H. Sheng, X. Wang, Q. Guo, *Sensors and Actuators B*, 2014, **195**, 534.

69 G. Sivaraman, V. Sathiyaraja and D. Chellappa, *J. Lumin.*, 2014, **145**, 1837.

70 J. Arden-Jacob, K. –H. Drexhage, R. Herrmann, H. –P. Josel, Pentacyclic compounds and their use as absorption or fluorescent dyes, *US Pat*., 5 750 409, 1998.

71 J. Wang, D. Zhang, Y. Liu, P. Ding, C. Wang, Y. Ye and Y. Zhao, *Sensors and Actuators B*, 2014, **191**, 344.

72 P. Xie, F. Guo, R. Xia, Y. Wang, D. Yao, G. Yang and L. Xie, *J. Lumin.*, 2014, **145**, 849.

73 L. Tolosa, K. Nowaczyk and J. Lakowicz, in *An Introduction to Laser Spectroscopy,* ed. D.L. Andrews and A. A. Demidov, Kluwer Academic/Plenum Publishers, New York, 2nd ed., 2002.

74 S. Wang, X. Meng and M. Zhu, *Tetrahedron Lett*., 2011, **52**, 2840.

75 F. Ge, H. Ye, H. Zhang and B.-X. Zhao, *Dyes Pigm*., 2013, **99**, 661.

76 B. Wang, J. Hai, Z. Liu, Q. Wang, Z. Yang and S. Sun, *Angew. Chem. Int. Ed*., 2010, **49**, 4576.

77 Y. Xiang and A. Tong, *Org. Lett*., 2006, **8**, 1549.

78 A. J. Weerasinghe, F. A. Abebe, E. Sinn, *Tetrahedron Lett*., 2011, **52**, 5648.

79 X. Chen, H. Hong, R. Han, D. Zhang, Y. Ye and Y. -F. Zhao, *J. Fluoresc.,* 2012, **22**, 789.

80 C.-Y. Li, C.-X. Zou, Y.-F. Li, J.-L. Tang and C. Weng, *Dyes Pigm*., 2014, **104**, 110.

81 J. L. Bricks, A. Kovalchuk, C. Trieflinger, M. Nofz, M. Büschel, A. I. Tolmachev, Jörg Daub, and K. Rurack, *J. Am. Chem. Soc*., 2005, **127**, 13522.

82 H. Wang, D. Wang, Q. Wang, X. Li and C. A. Schalley, *Org. Biomol. Chem.*, 2010, **8**, 1017.

83 (*a*) M. R. Wasielewski, *J. Org. Chem.*, 2006, **71**, 5051; (*b*) J. A. A. W. Elemans, R. van Hameren, R. J. M. Nolte and A. E. Rowan, *Adv. Mater.*, 2006, **18**, 1251; (*c*) H. Langhals, *Helv. Chim. Acta*, 2005, **88**, 1309; (*d*) F. Würthner, *Chem. Commun.*, 2004, 1564.

84 W. Lin, L. Yuan, J. Feng and X. Cao, *Eur. J. Org. Chem.*, 2008, 2689.

85 (*a*) A. S. Chauvin, Y. M. Frapart, J. Vaissermann, B. Donnadieu, J. P. Tuchagues, J. C. Chottard and Y. Li, *Inorg. Chem.*, 2003, **42**, 1895; (*b*) H. Ohta, Y. Sunatsuki, M. Kojima, Y. Ikuta, Y. Goto, N. Matsumoto, S. Iijima, H. Akashi, S. Kaizaki, F. Dahan and J. -P. Tuchagues, *Inorg. Chem*., 2004, **43**, 4154; (*c*) L. L. Bénisvy, S. Halut, B. Donnadieu, J. -P. Tuchagues, J. -C. Chottard and Y. Li, *Inorg. Chem*., 2006, **45**, 2403.

86 H. J. Jung, N. Singh and D. O. Jang, *Tetrahedron Lett*., 2008, **49,** 2960.

87 N. C. Lim, M. D. Morton, H. A. Jenkins and C. Brückner, *J. Org. Chem*., 2003, **68**, 9233.

88 N. C. Lim, S. V. Pavlova and C. Brückner, *Inorg. Chem*., 2009, **48**, 1173.

89 Z. Li, Y. Zhou, K. Yin, Z. Yu, Y. Li and J. Ren, *Dyes Pigm*., 2014, **105**, 7.

90 K. Ghosh, S. Rathi and R. Kushwaha, *Tetrahedron Lett*., 2013, **54**, 6460.

91 P. K. Chung, S.-R. Liu, H.-F. Wang and S.-P. Wu, *J. Fluoresc.,* 2013, **23**, 1139.

92 Y. Chen, L. Wan, X. Yu, W. Li, Y. Bian and J. Jiang, *Org. Lett*., 2011, **13,** 5774.

93 (*a*) C. Little, S. E. Aakre, M. G. Rumsby and K. Gwarsha, *Biochem. J.*, 1982, **207**, 117; (*b*) M. Dennis and P. E. Kolattukudy, *Proc. Natl. Acad. Sci. U.S.A.*, 1992, **89**, 5306; (*c*) W. Maret and B. L. Vallee, *Methods Enzymol.*, 1993, **226**, 52; (*d*) K. W. Walker and R. A. Bradshaw, *Protein Sci.*, 1998, **7**, 2684.

94 (*a*) A. Leonard and R. Lauwerys, *Mutat. Res.*, 1990, **239**, 17; (*b*) A. I. Seldén, C. Norberg, C. Karlson-Stiber and E. Hellström-Lindberg, *Environ. Toxicol. Pharmacol.*, 2007, **23**, 129.

95 H. Irving and R. J. P. Williams, *J. Chem. Soc.*, 1953, 3192.

96 H. Y. Au-Yeung, E. J. New and C. J. Chang, *Chem. Commun*., 2012, **48**, 5268.

97 Q. Maa, Q. -E. Cao, Y. Zhao, S. Wu, Z. Hu and Q. Xu, *Food Chemistry*, 2000, **71**, 123.

98 (*a*) O. Warburg, *Hoppe-Seyler's Z. Physiol. Chem.*, 1911, **76**, 331; (*b*) D. Kellin, *Proc. R. Soc. London, Ser. B*, 1929, **104**, 206; (*c*) B.Vennesland, E. E. Comm, C. J. Knownles, J. Westly and F. Wissing, *Cyanide in Biology*, Academic Press: London, 1981, pp. 487–494.

99 (*a*) J. D. Johnson, T. L. Meisenheimer; G. E. Isom, *Toxicol. Appl. Pharmacol.*, 1986, **84**, 464; (*b*) B. K. Ardelt; J. L. Borowitz; G. E. Isom, *Toxicology*, 1989, **56**, 146.

100 J. H. Lee, A. R. Jeong, I. -S. Shin, H. -J. Kim and J. -I. Hong, *Org. Lett*., 2010, **12**, 764.

101 M. Shamsipur, M. Sadeghi, K. Alizadeh, H. Sharghi and R. Khalifeh, *Anal. Chim. Acta*., 2008, **57**, 630.

102 S. H. Mashraqui, M. Chandiramani, R. Betkar and K. Poonia, *Tetrahedron Lett*., 2010, **51**, 1306.

103 S. -P. Wu, K. -J. Du and Y. -M. Sung, *Dalton Trans.,* 2010, **39**, 4363.

104 D. Maity, V. Kumar and T. Govindaraju, Org. Lett., 2012, **14**, 6008.

105 W. Lin, L. Yuan, Z. Cao, J. Feng and Y. Feng, *Dyes Pigm*., 2009, **83**, 14.

106 H. Küpper and P. M. H. Kroneck ,in *Nickel and Its Surprising Impact in Nature,* ed. A. Sigel, H. Sigel, R. K. O. Sigel, John Wiley & Sons Ltd., U. K., 2007, vol. 2, pp. 31-62.

107 S. C. Dodani, Q. He and C. J. Chang, *J. Am. Chem. Soc*., 2009, **131**, 18020.

108 F. A. Abebe, C. S. Eribal, G. Ramakrishna and E. Sinn, *Tetrahedron Lett*., 2011, **52**, 5554.

109 N. Chattopadhyay, A. Mallick, S. Sengupta, *J. Photochem. Photobiol., A*, 2006, **177**, 55.

110 G. -B. Li, H. -C. Fang, Y. -P. Cai, Z. -Y. Zhou, P. K. Thallapally and J. Tian, *Inorg. Chem*., 2010, **49**, 7241.

111 U. Fegade, J. Marek, R. Patil, S. Attarde and A. Kuwar, *J. Lumin.*, 2014, **146**, 234.

112 *Copper Proteins*, ed. T. G. Spiro, John Wiley, New York, 1981.

113 R. S. Britton, *Semin. Liver Dis*., 1996, **16**, 3.

114 (*a*) S. C. Leary, P. A. Cobine, B. A. Kaufman, G. H. Guercin, A. Mattman, J. Palaty, G. Lockitch, D. R. Winge, P. Rustin, R. Horvath and E. A. Shoubridge, *Cell Metab*., 2007, **5**, 9; (*b*) S. Lutsenko, A. Gupta, J. L. Burkhead and V. Zuzel, *Arch. Biochem. Biophys*., 2008, **476**, 22.

115 (*a*) S. G. Kaler, *Nat. Rev. Neurol*., 2011, **7**, 15; (*b*) I. Bertini and A. Rosato, *Cell. Mol. Life Sci*., 2008, **65**, 89.

116 (*a*) K. J. Barnham, C. L. Masters and A. I. Bush, *Nat. Rev. Drug Discovery*, 2004, **3**, 205; (*b*) E. Gaggelli, H. Kozlowski, D. Valensin and G. Valensin, *Chem. Rev*., 2006, **106**, 1995; (*c*) D. R. Brown and H. Kozlowski, *Dalton Trans*., 2004, 1907.

117 Z. Chen, L. Wang, G. Zou , J. Tang, X. Cai, M. Teng and L. Chen, *Spectrochim. Acta Part A*., 2013, **105**, 57.

118 S. Kaur and S. Kumar, *Chem. Commun*., 2002, 2840.

119 Z. -C. Wen, R. Yang, H. Hea and Y. -B. Jiang, *Chem. Commun*., 2006, 106.

120 G. -K. Li, Z. -X. Xu, C. -F. Chen and Z. -T. Huang, *Chem. Commun*., 2008, 1774.

121 Y. Zhou, J. Zhang, H. Zhou, Q. Zhang,T. Ma and J. Niu, *J. Lumin.*, 2012, **132**, 1837.

122 F. -J. Huo, C. -X. Yin, Y. -T. Yang, J. Su, J. -B. Chao and D. -S. Liu, *Anal. Chem.*, 2012, **84**, 2219.

123 K. M. K. Swamy, S. -K. Ko, S. K. Kwon, H. N. Lee, C. Mao, J. -M. Kim, K. -H. Lee, J. Kim, I. Shin and J. Yoon, *Chem. Commun.,* 2008, 5915.

124 C. Wu, Q. -N. Bian, B. -G. Zhang, X. Cai, S. -D. Zhang, H. Zheng, S. -Y. Yang and Y. -B. Jiang, *Org.Lett*., 2012, **14**, 4198.

125 L. Huang, X. Wang, G. Xie, P. Xi, Z. Li, M. Xu, Y. Wu, D. Bai and Z. Zeng, *Dalton Trans*., 2010, **39**, 7894.

126 Y. -B. Ruan, C. Li, J. Tangb and J. Xie, *Chem. Commun*., 2010, **46**, 9220.

127 C. Kar, M. D. Adhikari, A. Ramesh and G. Das, *Inorg. Chem*., 2013, **52**, 743.

128 M. Saleem and K. -H. Lee, *J. Lumin.*, 2014, **145**, 843.

129 M. H. Kim, H. H. Jang, S. Yi, S. -K. Chang and M. S. Han, *Chem. Commun.,* 2009, 4838.

130 S. Yin, V. Leen, S. V. Snick, N. Boensa and W. Dehaen, *Chem. Commun*., 2010, **46**, 6329.

131 X. Qi, E. J. Jun, L. Xu, S. -J. Kim, J. S. J. Hong, Y. J. Yoon and J. Yoon*, J. Org. Chem*., 2006, **71**, 2881.

132 L. Zeng, E. W. Miller, A. Pralle, E. Y. Isacoff and C. J. Chang, *J. Am. Chem. Soc.*, 2006, **128**, 10.

133 D. W. Domaille, L. Zeng and C. J. Chang, *J. Am. Chem. Soc*., 2010, **132** , 1194.

134 S. C. Dodani, S. C. Leary, P. A. Cobine,| D. R. Winge and C. J. Chang, *J. Am. Chem. Soc*., 2011, **133**, 8606.

135 C. S. Lim, J. H. Han, C. W. Kim, M. Y. Kang, D. W. Kang and B. R. Cho, *Chem. Commun*., 2011, **47**, 7146.

136 K. C. Ko, J. -S. Wu, H. J. Kim, P. S. Kwon, J. W. Kim, R. A. Bartsch, J. Y. Lee and J. S. Kim, *Chem. Commun*., 2011, **47**, 3165.

137 A. Basu and G. Das, *Dalton Trans*., 2011, **40**, 2837.

138 G. He, X. Zhao, X. Zhang, H. Fan, S. Wu, H. Li, C. He and C. Duan, New *J. Chem*., 2010, **34**, 1055.

139 P. Li, X. Duan, Z. Chen, Y. Liu, T. Xie, L. Fang, X. Li, M. Yin and B. Tang, *Chem. Commun*., 2011, **47**, 7755.

140 M. Kumar, N. Kumar and V. Bhalla, *Dalton Trans*., 2012, **41**, 10189.

141 T. Mistri, R. Alam, M. Dolai, S. K. Mandal, A. R. Khuda-Bukhsh and M. Ali, *Org. Biomol. Chem*., 2013, **11**, 1563.

142 M. Royzen, Z. Dai and J. W. Canary, *J. Am. Chem. Soc*., 2005, **127**, 1612.

143 S. Goswami, D. Sen and N. K. Das, *Org. Lett*., 2010, **12**, 856.

144 E. Ballesteros, D. Moreno, T. Gómez, T. Rodríguez, J. Rojo, M. Gracía-Valverde and T. Torroba, *Org. Lett*., 2009, **11**, 1269.

145 Z. Xu, J. Pan, D. R. Spring, J. Cui and J. Yoon, *Tetrahedron*, 2010, **66**, 1678.

146 J. Jo, H. Y. Lee, W. Liu, A. Olasz, C. -H. Chen and D. Lee, *J. Am. Chem. Soc*., 2012, **134**, 16000.

147 Z. Xu, J. Yoon and D. R. Spring, *Chem. Commun.,* 2010, **46**, 2563.

148 H. S. Jung, M. Park, D. Y. Han, E. Kim, C. Lee, S. Ham and J. S. Kim, *Org. Lett*., 2009, **11**, 3378.

149 S. Suganya, S. Velmathi and D. MubarakAli, *Dyes Pigm*., 2014, **114**, 116.

150 L. Yang, Q. Song, K. Damit-Og and H. Cao*, Sensors and Actuators B,* 2013, **176**, 181.

151 K. –K. Yu, K. Li , J. –T. Hou and X. –Q. Yu, *Tetrahedron Lett*., 2013, **54**, 5771.

152 T. Hirayama, G. C. Van de Bittner, L. W. Gray, S. Lutsenko and C. J. Chang, *Proc. Natl. Acad. Sci. U.S.A.,* 2012, **109**, 2228.